

INVESTIGATION OF FLY ASH CHARACTERISTICS ON ZEOLITE 4A
SYNTHESIS

A THESIS SUBMITTED TO
THE GRADUATE SCHOOL OF NATURAL AND APPLIED SCIENCES
OF
MIDDLE EAST TECHNICAL UNIVERSITY

BY

SÜLEYMAN ŞENER AKIN

IN PARTIAL FULFILLMENT OF THE REQUIREMENTS
FOR
THE DEGREE OF MASTER OF SCIENCE
IN
MICRO AND NANOTECHNOLOGY

SEPTEMBER 2019

Approval of the thesis:

**INVESTIGATION OF FLY ASH CHARACTERISTICS ON ZEOLITE 4A
SYNTHESIS**

submitted by **SÜLEYMAN ŞENER AKIN** in partial fulfillment of the requirements
for the degree of **Master of Science in Micro and Nanotechnology Department,**
Middle East Technical University by,

Prof. Dr. Halil Kalıpçılar
Dean, Graduate School of **Natural and Applied Sciences**

Prof. Dr. Almıla Güvenç Yazıcıoğlu
Head of Department, **Micro and Nanotechnology**

Assist. Prof. Dr. Feyza Kazanç Özerinç
Supervisor, **Mechanical Engineering, METU**

Prof. Dr. Burcu Akata Kurç
Co-Supervisor, **Micro and Nanotechnology, METU**

Examining Committee Members:

Prof. Dr. Almıla Güvenç Yazıcıoğlu
Mechanical Engineering, METU

Assist. Prof. Dr. Feyza Kazanç Özerinç
Mechanical Engineering, METU

Prof. Dr. Burcu Akata Kurç
Micro and Nanotechnology, METU

Assist. Prof. Dr. Fatma Toksoy Köksal
Geological Engineering, METU

Assoc. Prof. Dr. Selis Önel
Chemical Engineering, Hacettepe University

Date: 09.09.2019

I hereby declare that all information in this document has been obtained and presented in accordance with academic rules and ethical conduct. I also declare that, as required by these rules and conduct, I have fully cited and referenced all material and results that are not original to this work.

Name, Surname: Süleyman Şener Akın

Signature:

ABSTRACT

INVESTIGATION OF FLY ASH CHARACTERISTICS ON ZEOLITE 4A SYNTHESIS

Akın, Süleyman Şener
Master of Science, Micro and Nanotechnology
Supervisor: Assist. Prof. Dr. Feyza Kazanç Özerinç
Co-Supervisor: Prof.Dr. Burcu Akata Kurç

September 2019, 110 pages

There is lack of information about the relation between the candidate raw material fly ash and end product, Zeolite 4A. This study aims to fill the gap in the literature through controlled ash production experiments, characterization studies and Zeolite 4A synthesis. As a result of studies, the nucleation behaviour of the alkali fusion product obtained from fly ash was demonstrated and the most crystalline Zeolite 4A with cubic morphology were obtained from Seyitömer fly ash with alkali fusion product of Si/Al mol ratio 1,17 at the conditions, 47 °C, 12 hour aging and 90°C, 4 hour crystallization with the least sodalite impurity. It was observed that hematite and mullite content of fly ash caused differences in the alkali fusion product and Zeolite 4A. In addition, it has been observed that the hematite, mullite content and crystallinity of ash could be tuned by combustion parameters. From the Tunçbilek ash obtained from the drop tube furnace at 1000 °C, which is the poorest in mullite and hematite because of the conditions (high cooling rate and low combustion temperature), Zeolite 4A with 64,1 % crystallinity and cubic structure and minimum sodalite content was achieved under optimal synthesis conditions. Sodalite phase impurity content increased in parallel with hematite and mullite mineral content. In the synthesis product of Soma ash, katoite was obtained because of high level of calcium impurity. Finally, the ash from combustion experiments of the blend of sodium carbonate-coal-aluminum hydroxide,

the synthesis of zeolite 4A was carried out under optimized conditions without the need for a fusion step and zeolite 4A was obtained with low crystallinity.

Keywords: Fly Ash, Zeolite 4A Synthesis, Alkali Fusion, Combustion, Hydrothermal Treatment

ÖZ

KÜL ÖZELLİKLERİNİN ZEOLİT 4A SENTEZİ ÜZERİNDEKİ ETKİSİNİN İNCELENMESİ

Akın, Süleyman Şener
Yüksek Lisans, Mikro ve Nanoteknoloji
Tez Danışmanı: Dr. Öğr. Üyesi Feyza Kazanç Özerinç
Ortak Tez Danışmanı: Prof.Dr. Burcu Akata Kurç

Eylül 2019, 110 sayfa

Aday bir hammadde olarak uçucu kül ile son ürün olan Zeolit 4A arasındaki ilişki açısından bir bilgi eksikliği mevcuttur. Bu çalışma, literatürdeki bu boşluğu kontrollü kül üretim deneyleri, karakterizasyon çalışmaları ve zeolit 4A sentezi ile doldurmayı amaçlamaktadır. Yapılan çalışmalar sonucunda, uçucu külden elde edilen alkali füzyon ürününün çekirdeklenme davranışı ortaya konmuş ve en az sodalit safsızlığına ve kubik morfolojiye sahip Zeolit 4A 47° C 12 saat yaşlandırma koşulları ve 90°C 4 saat kristalizasyon koşullarında Seyitömer külünün 1,17 Si/Al mol oranına sahip olan jelinden elde edilmiştir. Class F küllerinin sahip olduğu demir içeriği ve özellikle minerolojik açıdan hematit ve mullit içeriğinin alkali füzyon ürünü ve zeolite 4A kristal fazları üzerinde farklılığa neden olduğu gözlenmiştir. Bunun yanı sıra, külün sahip olduğu hematit, mullit içeriği ve kristalinitesinin yanma parametreleriyle değiştirilebildiği gözlenmiştir. Bu duruma bağlı olarak, yüksek soğutma hızı ve düşük yanma sıcaklığı gibi koşullarla mullit ve hematite açısından fakir olan, düşey borulu fırından 1000° C’de elde edilen Tunçbilek külünden,optimal koşullarda yürütülen sentez sonucunda en az sodalit içeriğine sahip %64,1 kristallikte ve istenilen kübik morfolojide Zeolit 4A elde edilmiştir. Sodalit faz safsızlığı içeriğinin, hematit, mullit mineral bileşimiyle paralel olarak artış gösterdiği gözlenmiştir. Soma külünden elde edilen sentez ürününde, yüksek kalsiyum safsızlığından ötürü katoit elde edilmiştir.

Son olarak, sodyum karbonat-kömür-aluminyum hidroksit karışımından elde edilen yanma deneyi sonucunda elde edilen küllerden füzyon adımına ihtiyaç duymaksızın, optimize edilmiş koşullarda Zeolit 4A sentezi gerçekleştirilmiş ve düşük kristalinite ile Zeolit 4A elde edilmiştir.

Anahtar Kelimeler: Uçucu Kül,Zeolit 4A sentezi, Alkali Füzyon, Yanma, Hidrotermal İşlem

To my family

ACKNOWLEDGEMENTS

First of all, I would like to express my sincere gratitude to my dear advisor Feyza Kazanç Özerinç and Burcu Akata Kurç for providing such a work and always supporting me with their understanding and guiding attitude.

I would also like to take this opportunity to thank both TUBITAK and my professors for making me a part of the TUBITAK 1001 project as a scholarship student.

I would like to express my gratitude to PhD students, Duarte Magalhaes and Salih Kaan Kirdeciler, for their valuable support, and for their valuable friends, at every point I have stuck.

I would like to give my appreciation to have my sister, Assoc. Prof. Gülşen Akın Evingür as to be my role model and guide to be part of academic world and my motivation for research.

In addition to this, I would like to thank my friends Burak Özer, Kaan Gürel and Mehmet Baghizrade, who have made important contributions to the direction of my research and made this process easier for me by sharing their observations with me in experimental studies and sharing their observations with me

I would like to thank you to my dear family and of course my friends, who are part of my lifelong friendship, Cemal Madanoğlu, Mehmet Satılmış, Abdullah Furkan Terzi, Gökçe Oruç, Zeynep Aktosun, İlkay İloğlu and Fatma Çambay are always by my side for helping me through even the most difficult times and many other things.

During this research, I would like to thank all METU MERLAB employees for their analysis. I also extend my thanks to my colleague Şeyma Bozkurt for providing Tunçbilek ashes as soon as possible and indirectly contributing to my research.

TABLE OF CONTENTS

ABSTRACT.....	v
ÖZ	vii
ACKNOWLEDGEMENTS	x
TABLE OF CONTENTS.....	xi
LIST OF TABLES	xiv
LIST OF FIGURES	xv
LIST OF ABBREVIATIONS	xviii
CHAPTERS	
1. INTRODUCTION	1
1.1. Background Information	1
1.2. Motivation	2
1.3. Research Questions and Objectives	3
2. LITERATURE REVIEW	9
2.1. Origin of Coal Mineral Matter and Fly Ash Chemical Composition.....	9
2.2. Classification of Coal Fly Ashes	11
2.3. Formation of Fly Ash and Mineral Transformations of Coal during Combustion Process.....	12
2.4. Utilization of Fly Ashes	18
2.5. Zeolite Structure, Composition and Classification, Applications	18
2.6. Synthesis and Formation Mechanism of Zeolites	21
2.6.1. Ostwald’s Rule of Successive Transformations.....	23
2.6.2. Effect of Parameters on Zeolite 4A Synthesis	24
2.7. Hydrothermal Synthesis of Zeolite 4A From Fly Ashes with Alkali Fusion ..	25

2.7.1. Pretreatment of Fly Ashes with Alkali Fusion Process	25
2.7.2. Hydrothermal Synthesis of Zeolite 4A after Alkali Fusion Process	26
3. MATERIALS AND EXPERIMENTAL METHODOLOGY	31
3.1. Methods of obtaining fly ash from reactors with different heating rates.....	31
3.1.1. Coal selection, analysis and preparation for combustion experiments	31
3.1.2. Combustion Experiments for Tunçbilek Lignite.....	33
3.1.3. Characterization of Fly Ashes	40
3.2. Zeolite 4A Synthesis Experiments with Alkali Fusion.....	41
3.2.1. Investigation of Nucleation Behaviour with Aging Experiments	43
3.2.2. Optimization of Crystallization Conditions	45
3.3. Zeolite 4A Synthesis Experiments with other Fly Ash Sources	47
3.4. Zeolite 4A Synthesis Experiments with Fly ashes from Combustion Blends	48
3.5. Analysis Techniques	49
3.5.1. X Ray Fluorescence (XRF)	49
3.5.2. X Ray Diffraction (XRD).....	50
3.5.3. Scanning Electron Microscopy (SEM).....	50
4. RESULTS AND DISCUSSION	51
4.1. Effect of the Fuel Type on Fly Ash Characteristics.....	51
4.1.1. Chemical Composition	51
4.1.2. Mineral Content.....	52
4.2. Effect of Combustion Parameters on Fly Ash Characteristics.....	54
4.2.1. Effect of Combustion Temperature	55
4.2.2. Effect of Heating Rate	58
4.2.3. Effect of Cooling Rate.....	60

4.3. Optimization of Zeolite 4A synthesis.....	61
4.3.1. Optimization of Si/Al ratio	63
4.3.2. Optimization of Crystallization Temperature	65
4.3.3. Optimization of the Aging Temperature.....	69
4.3.4. Optimization of the Alkalinity	71
4.3.5. Optimization of Crystallization Time and Aging Time.....	72
4.4. Zeolite 4A Synthesis for Different Fly Ashes with the Optimized Parameters	75
4.4.1. Effect of Chemical Composition on the Zeolite 4A	76
4.4.2. Effect of Combustion Parameters on Zeolite 4A.....	79
4.5. Zeolite 4A Synthesis with Fly Ashes from Combustion Blends.....	84
5. CONCLUSION AND FUTURE RESEARCH	89
5.1. Conclusion.....	89
5.2. Future Research.....	94
REFERENCES.....	97
APPENDICES	107

|

LIST OF TABLES

TABLES

Table 2.1. Summary of Synthesis Conditions from the Studies of Alkali Fusion assisted Zeolite 4A Synthesis from fly ash.....	29
Table 3.1. Ultimate and Proximate Analysis of Tunçbilek Coal.....	31
Table 3.2. Summary of Experimental Conditions of Combustion	33
Table 3.3. Cooling Rate Experiments on WMR at 1200°C.....	38
Table 3.4. Si/Al mass ratio and mol ratios of prepared fusion mixture in this study	44
Table 3.5. Experimental Conditions of Optimization of Zeolite 4A Synthesis.....	47
Table 3.6. Combustion Experiments with Coal-inorganic Blends	49
Table 4.1. Chemical Composition of Power Plant Ashes.....	52
Table 4.2. Main Components of Tunçbilek Fly Ashes	55
Table 4.3. Mineral Content and Crystallinity of Class F Fly Ashes in this study	59
Table 4.4. Effect of Cooling Rate on mineral composition and crystallinity of WMR Ashes at 1200°C	60
Table 4.5. Chemical Composition of Fusion Product with different Si/Al mixing ratio	63
Table 4.6. Chemical Composition of Fusion Product from different fly ash sources with mixing ratio of Si/Al:0,72.....	76
Table 4.7. Relation of Mineral Composition and Ash Crystallinity on Zeolite Crystallinity	82

LIST OF FIGURES

FIGURES

Figure 2.1. Schematic of the coal fly ash formation	14
Figure 2.2. Mineral Transformation Mechanism during combustion [43]	15
Figure 2.3. Tetrahedras of SiO_4 and AlO_4 and negative zeolite charge and counter-balancing metal cation M^+	19
Figure 2.4. Framework of zeolite A	20
Figure 2.5. SEM Image of Zeolite 4A obtained from lab chemicals[62]	21
Figure 2.6. Overview of Synthesis Mechanism of Zeolites	23
Figure 3.1. Retsch Sieve Set in CCTL	32
Figure 3.2. Schematic Diagram of Drop Tube Furnace in CCTL.....	34
Figure 3.3. a) Tecora Impactor b) Overview of Drop Tube Furnace in CCTL.....	35
Figure 3.4. Wire mesh reactor (WMR) in Clean Combustion Technologies Laboratory (CCTL).....	37
Figure 3.5. Protherm ashing furnace	39
Figure 3.6. Heating Profile of Muffle Furnace for 800 °C, 900 °C and 1000 °C	39
Figure 3.7. Influence of Si/Al mass ratio on the Si/Al mol ratio of fusion product...45	
Figure 3.8. Process Flowchart for Zeolite 4A Synthesis from fly ash source.....	46
Figure 4.1. XRD Patterns of Seyitömer and Soma Power Plant Ashes Q:Quartz, M: Mullite, H: Hematite, An:Anorthite, Anh:Anhydrite, Lm: Lime, Me: Melilite.....	53
Figure 4.2. XRD Patterns of Seyitömer and Tunçbilek Power Plant Ashes	53
Figure 4.3. XRD patterns of Tunçbilek Fly Ashes at 800, 900 and 1000 °C from MF experiments Q: Quartz; M; Mullite; K: Kaolinite; H: Hematite, Cr: Corundum, Msc: Muscovite.....	56
Figure 4.4. XRD patterns of Tunçbilek Fly Ashes at at 800, 900 and 1000 °C from Wire Mesh Reactor combustion experiments, Q: Quartz; M; Mullite; K: Kaolinite; H: Hematite, Mag: Magnetite, Cr: Corundum	57
Figure 4.5. XRD Patterns of Tunçbilek Fly Ashes at 800, 900 and 1000 °C from DTF experiments Q: Quartz; M; Mullite; K: Kaolinite; H: Hematite, Cr: Corundum.....	58

Figure 4.6. XRD Patterns of effect of cooling rate on Tunçbilek Ash from WMR combustion experiments at 1200 ° C, Q: Quartz; M; Mullite; , H: Hematite, Mag: Magnetite	61
Figure 4.7. SEM Images of synthesized Zeolite 4A with sodium aluminate and sodium silicate in Nanodev Research Lab.....	62
Figure 4.8. XRD pattern of commercial Zeolite 4A	63
Figure 4.9. XRD patterns of zeolite 4A synthesized with different Si / Al ratios using Seyitömer Fly ash aged during 16 h at 47 ° C and crystallized during 7 h at 100 ° C, S: sodalite, 4A: zeolite 4A	64
Figure 4.10. SEM Analysis of Zeolite 4A obtained from the gel with Si/Al mol ratio 1,04	65
Figure 4.11. XRD pattern of zeolite 4A synthesized with different crystallization temperatures (85, 90, and 100 °C) for 7 h , and 16 h aging at 47 °C for a gel with Si/Al ratio of 1,17 S: sodalite, 4A: zeolite 4A	66
Figure 4.12. XRD pattern of zeolite 4A synthesized with different Si/Al mol ratio of 1,17(S6) and 1,35(S8) for 16 h aging at 47 °C and 7 h crystallization at 90°C , S: sodalite, 4A: zeolite 4A	67
Figure 4.13. XRD pattern of zeolite 4A Synthesized with different crystallization temperatures (90 and 100 °C) for 7 h , and 16 h aging at 47 °C for a gel with Si/Al mol ratio of 1,35, S: sodalite, 4A: zeolite 4A	68
Figure 4.14. SEM Analysis of Zeolite 4A obtained from the gel with Si/Al mol ratio a) 1,35 and b) 1,17 for crystallazition at 90°C.....	69
Figure 4.15. XRD pattern of Zeolite 4A synthesized with different aging temperatures (25, 37, and 47 °C), crystallized at 90 °C during 16 h for Si/Al: 1,17 S: sodalite, 4A: zeolite 4A.....	70
Figure 4.16. XRD pattern of Zeolite 4A synthesized with different alkalinity ratios (1,35 and 1,10), aged at 47 °C during 16 h, crystallized at 90 °C during 7 h for mol ratio of Si/Al, 1.17, S: sodalite, 4A: zeolite 4A	72

Figure 4.17. XRD Pattern of Zeolite 4A Synthesized with different crystallization times (4 and 7 h), aged at 47 °C during 16 h, crystallized at 90 °C, for Si/Al of 1.17 S: sodalite, 4A: zeolite 4A.....	73
Figure 4.18. XRD Pattern of Zeolite 4A Synthesized with different aging times(4,8,12 and 16 h) aged at 47 °C , crystallized at 90 °C for 4 h, for Si/Al of 1.17 S: sodalite, 4A: zeolite 4A, N: Nepheline.....	74
Figure 4.19. XRD pattern of Zeolite 4A synthesis of Seyitömer Fly Ashes at 90°C crystallization , for 47°C aging for 12 h for 4h and 7 h crystallization S: sodalite, 4A: zeolite 4A	75
Figure 4.20. XRD Pattern of Zeolite 4A Synthesis of Seyitömer and Soma Fly Ashes at 90°C crystallization , for 47 °C aging for 16 h and 7 h crystallization, Kt: Katoite ($\text{Ca}_3\text{Al}_2(\text{SiO}_4)_{1,5}(\text{OH})_6$, 4A: Zeolite 4A.....	77
Figure 4.21. XRD Pattern of Alkali Fusion of Tunçbilek PP, Seyitömer PP ashes for same Si/Al mass ratio (0,72), N: nepheline (NaAlSiO_4), SS: Sodium disilicate (NaSi_2O_5) , SA: sodium aluminate(NaAlO_2)	78
Figure 4.22. XRD Pattern of Alkali Fusion of Tunçbilek PP, DTF1000 and MF1000 ashes for same Si/Al mass ratio (0,72), N: nepheline (NaAlSiO_4), SS: Sodium disilicate (NaSi_2O_5) , SA: sodium aluminate(NaAlO_2).....	79
Figure 4.23. XRD Pattern of Synthesized Zeolites from different Class F Ashes at optimal conditions, S: Sodalite, 4A: Zeolite 4A	81
Figure 4.24. SEM Analysis of Zeolite 4A obtained from the fusion product of a) Seyitömer PP b) Tunçbilek PP, c) MF100 d) DTF1000, ashes	83
Figure 4.25. XRD Patterns of Tunçbilek Fly Ashes ;from combustion experiments with sodium carbonate in Ashing Furnace at 1000 °C.....	85
Figure 4.26. XRD Patterns of Zeolite 4A Synthesis Tunçbilek Fly Ashes from combustion experiments with sodium carbonate in Ashing Furnace at 1000 °C with 12 h Aging at 47°C and 4 h crystallization at 90°C, 4A: Zeolite 4A, S: Sodalite.....	86
Figure 4.27. Smoothed XRD Patterns of Zeolite 4A synthesis from the combustion blends with mass ratio 7,57 Coal: 1,25 Na_2CO_3 :1 $\text{Al}(\text{OH})_3$ in Ashing Furnace at 1000 °C with 12 h Aging at 47°C and 4 h crystallization at 90°C.....	87

LIST OF ABBREVIATIONS

ABBREVIATIONS

MF, Muffle Furnace

WMR, Wire Mesh Reactor

DTF, Drop Tube Furnace

PP, Power Plant

FA, Fly Ash

XRD, X Ray Diffraction

XRF, X Ray Fluorescence

SEM, Scanning Electron Microscopy

TUIK, Türkiye İstatistik Kurumu

TEIAS, Türkiye Elektrik İşletmeleri Anonim Şirketi

CHAPTER 1

INTRODUCTION

1.1. Background Information

Energy demand and environmental impact are quickly becoming the most important and prominent problems to tackle in this century. Coal is one of the primary energy sources, accounting for 30% of the world energy demand [1], [2], [3]. Turkey is a very rich country in terms of lignite reserves (number of million tonnes) and as of the end of 2016 the share of coal use in energy production had risen to the first place and it is predicted that it will increase TEIAS (2016). However, the low calorific value of Turkish lignite along with its high moisture and ash content prompts the import of higher grade coal. According to the current data, [4] around 50 million tons of ash from 14 thermal power plants in Turkey are exposed, and the failure to recycle these ashes creates major economic and environmental problems. According to TUIK (2016) data, 87,8 % of the fly ash produced from thermal power plants and the 83,3% of produced fly ashes stored in ash dams. The rest of them were disposed or used in construction [1], [2], [3], [5], [6]. Environmental concerns allied with the surge of emergent technologies have allowed the utilization of fly ashes as a value-added product. Recent studies have shown that fly ash can be transformed to value-added products such as zeolites, geopolymers, activated carbons, nanoporous silicates, and catalysts for carbon nanotube production [1], [2], [3], [7].

The production of zeolites from fly ash presents several advantages. Fly ash contains active phases such as mullite, quartz and other aluminosilicate glassy phases; zeolites are also aluminosilicate crystals, meaning that fly ash presents itself as a very good candidate for raw material for zeolite production [1], [3], [8]. Zeolites are typically

proper for a wide range of environmental applications such as water treatment and reduction and adsorption of emission gases, owing to their unique crystal structures and porous surfaces [1], [2], [3]. Synthetic zeolite production in the world is around 1.4 million tons per year. Although there are many advantages over natural zeolites, such as better channel structures, no impurities and higher ion exchange capacities, the high production costs of synthetic zeolites have caused some limitations in their industrial use. In order to reduce the production costs of zeolites, the use of various natural resources and industrial wastes, such as kaolin, feldspar, iron ore tailing, and fly ash has been accelerated in recent years [9], [10], [11]. The preponderant factor to be considered is the amount of silicon and aluminum measured in the natural sources. Accordingly, it is safe to say that fly ashes from Turkish lignites are the suitable candidates for the study of zeolite synthesis [6], [12]. If this is not the case, it is possible to produce zeolite after the required silicon and aluminum content is obtained by using various laboratory level chemicals as in traditional methods [13].

1.2. Motivation

The burning of lignite coal results in the formation of large quantities of fly ash which can be used for the production of value added products such as zeolites. The production of zeolite from fly ash offers great opportunities in terms of cost reduction, increase in supply security due to lower dependence on imported zeolite, and mitigation of the impact on the environment.

There is, however, a deficit of studies that focuses not only on the synthesis of zeolite using fly ash at a fundamental level, but also on the establishment of a reproducible route for industrial scale production which guarantees sustainability and subsequent application area(s) of the end product.

This thesis aims to fill this gap in the literature through controlled ash production experiments, characterization studies and zeolite synthesis. At the end of this thesis, information on zeolite synthesis from fly ash obtained from controlled combustion

experiments will be obtained, allowing a deep understanding between fly ash properties and zeolite synthesis. This information will contribute to the existing literature, as well as to the industry players in Turkey that will benefit from this information to reduce production costs.

1.3. Research Questions and Objectives

- **What is the effect of the combustion conditions on fly ash characteristics?**

To better understand the effect of fly ash properties on zeolite synthesis, it is important to fully characterize it and investigate the effect of combustion conditions on properties such as ash crystallinity, mineral composition, and ratio of glassy silicate and aluminosilicate phases. In this thesis, relevant combustion conditions such as the heating and cooling rates, as well as the combustion temperature were varied to assess the subsequent effect on the fly ash properties.

To investigate the effect of heating rate on the fly ash characteristics, a drop tube furnace (DTF) and a wire mesh reactor (WMR) were used since these set ups can reach conditions deemed similar to industrial boilers [14], [15]. For comparison with low heating rates, a muffle furnace was used. The effect of the combustion temperature, experiments were carried out at 800, 900, and 1000°C in DTF, WMR and muffle furnace.

A separate set of experiments was conducted to observe the effect of the cooling rate. For this purpose, fly ash was obtained from a WMR at 1200 °C. The cooling rate was varied by selection of the nitrogen flow injected into the chamber following combustion of the sample.

Chemical and physical properties of the obtained ash were characterized by methods such as XRF, XRD and SEM.

- **What is the effect of coal source on the mineral composition and crystallinity of fly ash?**

The chemical composition of the ash of coals varies depending on the geographical region from which they are extracted. Thus, it is obvious that there is an effect of coal on the mineral composition and crystallinity of the ash to be obtained as a result of the combustion process [16]. Particularly for zeolite synthesis, fly ash from Turkish lignites will be used as a source material. It is therefore important to determine the content of fly ash, alumina and silica as well as the impurity content. Within the scope of the thesis, fly ashes were obtained from Tunçbilek, Seyitömer and Soma Thermal Power Plants and the parameters such as morphology and surface area, chemical content and physical properties were done by methods such as SEM, XRF, XRD.

- **How do the combustion parameters affect the fusion product?**

One of the other objectives of this thesis is to observe the possible effect of fly ash properties, on the Zeolite 4A product. In order to achieve the synthesis of Zeolite 4A by hydrothermal process, alkali fusion process is needed to obtain the required water-soluble sodium aluminate, sodium silicate, and sodium aluminosilicate compounds [17]. As compared to the high purity traditional laboratory chemicals used in synthetic zeolite synthesis, fly ash has a highly complex structure that includes both amorphous structures and crystal structures, as well as undesired impurities. Especially the ash crystallinity and ash mineral composition, which depend on the combustion parameters, directly affect the crystal structure and the mineral form of the sodium compounds to be formed as a result of the alkali fusion process [18], [19], [20]. Therefore, in order to understand the possible effect of fly ashes on the zeolite 4A synthesis, the alkali fusion step should first be examined.

In order to achieve this objective, the fusion products obtained using Tunçbilek lignite ash obtained under different conditions (i.e. muffle furnace, drop tube furnace, and thermal power plant) were analyzed by XRD method.

- **What is the nucleation behavior of fusion product for Zeolite 4A synthesis?**

The nucleation behavior influences the phase impurity and crystal size of the zeolite [13]. Even though fly ash is used as an aluminum and silicon source during zeolite synthesis, a cation source such as sodium with silicon and aluminum is required. As mentioned before, the actual starting product for zeolite synthesis is from the alkali fusion process. In this case, an alkali agent such as sodium hydroxide or sodium carbonate is preferred [21], [22]. Moreover, since zeolite 4A has a low Si / Al ratio, an additional source of aluminum are often used [19], [21]. In this thesis, unlike the studies in the literature, aluminum hydroxide was added to the fly ash along with the alkali agent sodium carbonate before the fusion step [10]. Thus resulting in a fusion product with differences in both mineral composition and crystallinity. Accordingly, aging experiments were carried out for the fusion product to understand the nucleation behavior. The effect of parameters such as Si / Al ratio, alkalinity(Na_2CO_3 /fly ash (by mass)), aging temperature, and aging time was studied. Ash from Seyitömer thermal power plant was chosen as fly ash source for this experimental set.

- **Which condition is optimal for the crystal growth of Zeolite 4A?**

The formation of zeolite crystals takes place at higher temperature during the crystallization step – the last step of the hydrothermal treatment [13]. Therefore, it is necessary to determine the optimal temperature and optimal crystallization time that ensures crystal growth as well as nucleation behavior. In this thesis, synthesis experiments were carried out at three different temperatures and for two different crystallization times for the fusion product obtained from Seyitömer Thermal Power Plant ash.

- **Is there a direct relation between combustion conditions and zeolite 4A synthesis?**

The greatest difficulty in producing zeolite from fly ash arises from the fact that the quality and characteristics of the fly ash obtained from different thermal plants vary widely [1], [6], [9]. This greatly impairs parametric studies since oftentimes several parameters change simultaneously. To address this issue, ashes from a single coal (Tunçbilek lignite) were obtained under different combustion conditions. In addition, the determination of optimal conditions for the synthesis of zeolite 4A was carried out using Class F Seyitömer thermal power plant ash, a source of ash with a chemical composition similar to Class F Tunçbilek lignite ash except only iron content [6]. Therefore, the findings presented by these two experimental matrices need to be combined in order to answer the proposed research question. Within this scope, zeolite 4A was synthesized using Tunçbilek ashes obtained from muffle furnace, drop tube furnace, and thermal power plant at optimal aging and crystallization conditions. Under the light of these experiments, explanation of the effect of combustion parameters (heating rate, and combustion temperature) on zeolite crystallinity and zeolite yield was attempted.

Moreover, the zeolite obtained from fly ash was compared with a commercial Zeolite 4A sample in terms of percentage of crystallinity and morphology.

- **What is the effect of impurities of fly ash on the zeolite synthesis?**

Coals contain clay minerals, carbonate group minerals, phosphate group minerals and at the trace level, almost all of the elements in the periodic table, but CaO and Fe₂O₃ are higher except from the alumina and silica content in coals in terms of percentage content. Furthermore, these compounds are important as impurities compared to other components because they have a more dominant effect in the nucleation and crystallization step in zeolite synthesis [16]. However, these compounds can be considered impurities in zeolite 4A [1]. In order to observe the effects of these impurities, Tunçbilek and Seyitömer thermal power plant ash with different iron content as well as fly ash obtained from 5-6 units of Soma Thermal Power Plant

containing different degree of calcium impurities were used to synthesize zeolite. Synthesis experiments were carried out for the aforementioned ashes based on the optimal experimental conditions determined using Seyitömer thermal power plant ash.

- **Is it possible to eliminate alkali fusion step during zeolite 4A synthesis with the help of the combustion process?**

In the studies carried out in the literature, as an alternative solution to the problems such as PM emission and SO_x emission, it is seen that coal is burned together with sodium carbonate [23], [24], [25]. In these studies, the presence of sodium aluminate, sodium silicate and sodium-aluminosilicate minerals were determined on the obtained fly ashes. In addition, there have been studies [26], [27] in which aluminum source was used together with coal in order to prevent the formation of slag and fouling. Based on this information, the sodium carbonate and aluminum hydroxide compounds used in the alkali fusion step were mixed with Tunçbilek lignite before combustion. In this context, the ashes of Tunçbilek lignite blends with respective additives were obtained from combustion in the muffle furnace. Synthesis was carried out after aging and crystallization steps without the need for an alkali fusion step from the ashes obtained from the combustion of these blends. Synthesis experiments were carried out under the determined optimal aging and crystallization conditions.

CHAPTER 2

[LITERATURE REVIEW]

[Through this literature review, it was focused on mostly characteristics and classification of fly ash , zeolite synthesis from fly ashes with alkali fusion process and briefly theoretical background related to mineral transformations during combustion process and also the formation mechanism of zeolites.

2.1. Origin of Coal Mineral Matter and Fly Ash Chemical Composition

Coal could be defined as rocks of solid organic origin formed in result of natural geological process and contains 55-95% combustible carbon in the form of volatiles and chars and inorganic components, respectively. Inorganic components of coal are either bound organically or as a mineral matter of true minerals [28]. Chemical and physical properties of coal depends on the nature of coal matrix. The nature of coal matrix varies according to its geographical location and affects the overall behavior of a given coal sample [2]. Consequently, systematic classification of coal is important. Classification of coal are made up based on coal rank, coal grade, petrographic composition. ASTM standard D388 divided type of coals ranked according to following main classes: Anthracite, bituminous, subbituminous and lignite. Anthracite coals are mostly carbon with averaging 90% percent; bituminous coals with %45-86 carbon content; subbituminous coals averaging 40% carbon content and latter is lignite within the range of 25% to 35% percent of carbon content [2], [29]. In Turkey, reserves are rich in lignites which contains high sulfur, moisture, ash and only small percentage of the reserves are high rank coals. These are Soma, Afşin-Albistan, Seyitömer, Tunçbilek and other lignites and bituminous coal in Çatalağzı region (TEIAS, 2016).

Coal mineral matter is divided in two parts as inherent minerals and extraneous minerals. The source of inherent minerals is from the inorganic parts of the plant that transforms into peat and then to coal. Inherent minerals represent less than 10% of organic particles that couldn't be removed by coal enrichment methods. Extraneous mineral matter could be said the separable inorganic part as the impurity associated after coal formation. It represents 90% of the mineral matter of the coal [30]. Most of the coal mineral matter transforms into fly ash in result of combustion process. Fly ash contains very complex mixture of crystal and amorphous compounds as irregular or angular particles within the range of 0.2 μm - 200 μm intimately associated and finely dispersed solid, liquid, and gaseous components since dependency on the combustion conditions and basically the type of coal [16], [31].

Fly ash mineral materials could be divided into three main groups, namely major, minor and trace mineral substances. Major minerals are compounds that comprise more than 10% of the total mineral material in coal; concentrations of minor minerals are 1-2%; the trace minerals are below 1%. Clays, carbonates, sulfides, sulfurous and silicate minerals are in the major group. Silicates are the 20% of the total mineral matter. Minor substances are sulfates, feldspars and sulphides. The mineral impurities contained in the coal reflect the geological environment of the region in which they are formed. More than 95% of the minerals contained in coal are major components. Minor components and trace minerals contain many of the elements in the periodic table [16], [30],[31].

There are some studies that investigate the coal mineral matter of Turkish Lignites. Karayiğit et al.(2000) determined in their study, Tunçbilek, Seyitömer and Soma coal contain montmorillonite and clay minerals such as illite, kaolinite, chlorite and feldspat, calcite, dolomite, pyrite. Moreover, siderite was detected in these coals besides from the other coals in the study.(other coals: Orhaneli, Çayırhan,Elbistan, Kangal, Çatalağzı, Yeniköy, Yatağan) [32],[33],[34].

2.2. Classification of Coal Fly Ashes

The well known classification method for the fly ashes is according to their bulk chemical composition which divided fly ashes into two main class. By this classification method, fly ashes could be classified according to their chemical content as Class C with CaO content with higher than 10% percent, and class F ashes has $\text{SiO}_2 + \text{Al}_2\text{O}_3 + \text{Fe}_2\text{O}_3$ higher than 70% with lower than 10% CaO content[35]. Class C fly ash contains less than 1% unburned carbon and typical crystal phases of these ashes could be listed as; anhydrite (CaSO_4), tricalcium aluminate ($\text{Ca}_3\text{Al}_2\text{O}_6$), anorthite ($\text{CaAl}_2\text{Si}_2\text{O}_8$), lime (CaO), quartz (SiO_2), mullite ($\text{Al}_6\text{Si}_2\text{O}_{13}$). In the case of Class F, fly ash contains more than 2% unburned carbon and the main phases are quartz, mullite, hematite and magnetite [36].

However, this classification might give some idea about the fly ash characteristics, fuel processing also effect indirectly the coal characteristics. Vassileva et al. (2007) studied fly ash characterization and tried to explain systematically in detail according to their origin, composition and behavior and properties of fly ashes. Fly ashes were obtained from 41 power plants from Bulgaria, Spain, Greece and Turkey. Fly ashes were analyzed according to water soluble fractions, mineral phases, particle size, chemical content, ash fusion temperature, density, pH determination and their magnetic fractions with respected analysis method. Mineral phases and chemical content were determined by XRF and XRD techniques [31]. They classified ashes according to their chemical content and crystal phases with some subgroups according to their acid tendencies. Their results suggested that the fly ash with sialic or high sialic with high acid tendencies characteristics as well as pozzolanic or high pozzolanic characteristics are good candidate for zeolite synthesis [31].

The minerals and phases in fly ashes can be classified as original (primary) or newly formed (secondary and tertiary) in terms of their formations. Primary species are original coal minerals and phases in which no phase transformations occur during combustion [16], [37]. These species are generally materials with relatively high

melting temperatures such as some stable silicates, oxides, sulfates, phosphates and carbonates. Secondary species are new phases formed during combustion. These are various silicates, oxides, sulfates, carbonates, sulfides, glass and char [16], [37].

Different coals and combustion conditions result in the formation of various minerals or mineral groups. To date approximately 188 minerals or mineral groups have been identified in various coal fly ashes alumina, but content varies depending on coal type and combustion conditions [16], [37].

In addition to these studies, in terms of the potential recycling of fly ash, the glassy and crystalline content and mineral percentages is also important for classification of ash. In this context, various groups have recommended the ash obtained from different thermal power plants to be characterized by the Rietveld analysis method in addition to the XRD analysis. These studies are important in terms of comparing the ratio of quartz, mullite and alumina silicate and silicate glassy phases [38], [39].

2.3. Formation of Fly Ash and Mineral Transformations of Coal during Combustion Process

Coal combustion is an exothermal chemical reaction of coal and oxygen with sufficient heat at certain conditions and simply defined as three stage process, namely release of moisture, devolatilization and char combustion. In result of complete combustion, CO₂ and water released, and remains inorganic part ash, but it could be SO_x, NO_x and other exhaust gases produced depend on the combustion conditions [2], [29],[40].

Beyond the fuel chemical (inorganic)content, char combustion is also dependent on the boiler type which is decided the particle size [2], [29]. Because of the complex and multiphase reactions, heat and mass transfer processes also affected by fuel size and it has a major effect on the combustion and relatively potential emissions. Char combustion could be classified as thermal thick and thermal thin regimes which is related with particle size and porosity [29], [40]. This determines heat and mass transfer rate and chemical kinetics which occurs as a heterogenous reactions at the gas- solid boundary layer [29], [40].

Pulverize combustion boilers are generally used for coal combustion process. That's why it is known as Pulverized coal-fired boiler (PCC) in literature. Pulverized coal has a size less than 100 μm [2], [29], [40]. There are two main reason behind the grinding (pulverizing) coal. As coal particle gets larger, oxygen in the air has less chance to have contact with the carbon at the center of coal particle. Therefore, there was unburned carbon at the outlet of the furnace. Another reason is to minimize the residence time of the particle in furnace by increasing the surface area of the particle. Therefore, in a certain (fixed) time interval, more amount of coal can be burned. It's working temperature is generally 1200-1700 $^{\circ}\text{C}$ [2], [29], [40].

During pulverized coal combustion, the coal particles form particles which become gaseous when heated, and the formed parts burn like charred particles. They eventually reach a higher temperature than the outer mineral particles containing less than 10% organic matter [41]. Natural minerals (0.1 μm) change in carbonized particles and carbonization they are released during the process of fragmentation [29], [30]. During the dissolution of the minerals and the solid phase, gas is released. These gases cause homogenous and heterogeneous concentrations by entering homogeneous chemical reaction. The size of ashes with dimensions of 0.02-0.2 μm is the homogenous condensation and the decomposition of minerals. The recombination of the disintegrated mineral particles causes the ash to form 0.2-10 μm . The largest ash particles (10-90 μm) are composed of transformed outer mineral particles [29], [30]. In Figure 2.1, schematic of the formation of fly ash mechanism during combustion was represented [41].

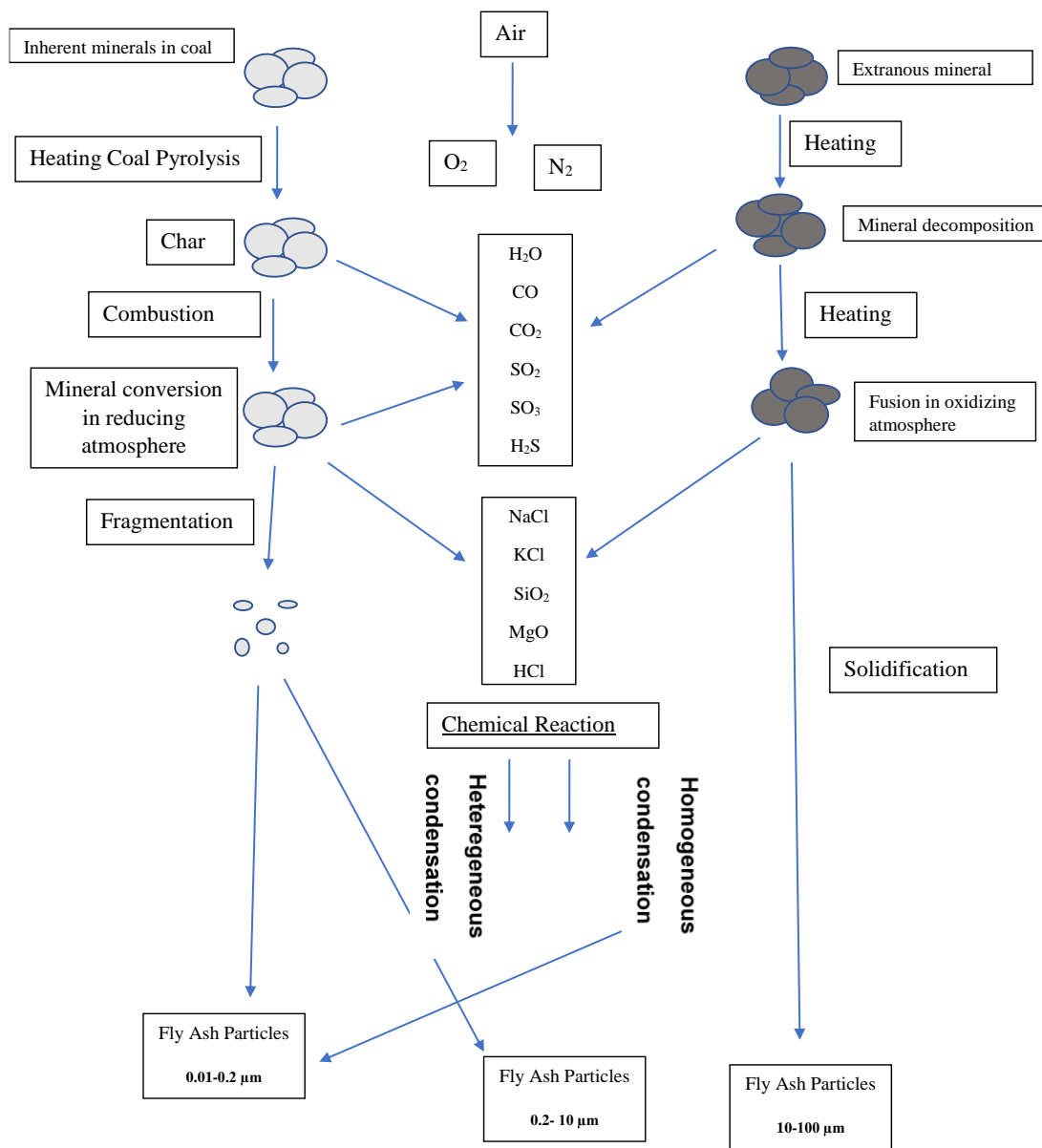


Figure 2.1. Schematic of the coal fly ash formation mechanism from pulverized fuel combustion [41]

Despite of detailed classification of fly ashes according to their characteristics, the explanation of effect of combustion parameters is another issue. Because, these studies were carried out by obtaining ashes from some power plants. As mentioned before, boiler type and combustion conditions are also key parameters on the fly ash

characteristics [1], [2], [42]. In Figure 2.2, the transformation of minerals from the McLennan study were shown.

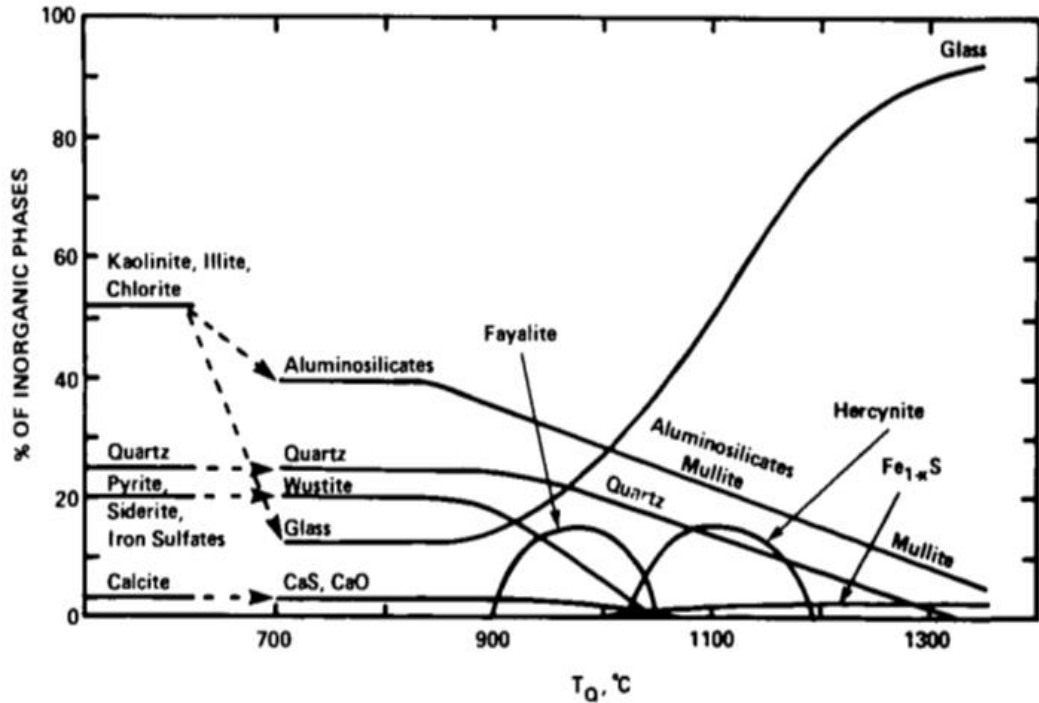


Figure 2.2. Mineral Transformation Mechanism during combustion [43]

Classification of ashes according to their crystalline phases would be a guide for selection of ash types. In particular, the mullite phase ratio, which is important for zeolite synthesis, has been observed to vary depending on the cooling rate of the thermal power plants [38].

New quartz phases and mullite phases have gone formed during combustion process according to combustion conditions [16]. Quartz could transform its polymorphs during the combustion such as α -quartz, β quartz, tridymite or cristobalite. Especially, quartz and mullite crystal phases are very important for zeolite synthesis, because these phases determines cation exchange capabilities of the fly ashes [16].

In scope of this, Vassileva et al. (2005) investigated behavior of inorganic matter transformation of low grade Lignites that has Class C ashes by gradually heating up

to 1300 °C in DTA-TGA analyser which are their ash fusion temperature. Formation of mineral phases was correlated with combustion temperature. It was discovered that silicate phases (i.e quartz, mullite) occurred above 800°C and up to 1300 °C [44]. It was mentioned on this study that kaolinite is stable up to max 1000°C, but transformation of kaolinite into mullite depends on the residence time of the combustion in real condition, residence time is very short, so heating rate could affect mineral transformation, in addition to combustion temperature [44]. The authors studied also mineral transformation of the subbituminous and bituminous coal in their other study [37]. Compared to lignites, they observed that the behavior of corundum and mullite phases, which are Al₂O₃ minerals, differed in the ash of higher quality coals because of having less calcium content and higher silica and alumina content. In particular, they found that mullite was the dominant phase at elevated temperatures of 1200-1600 °C due to the high content of alumina and silica. On the other hand, Ca-silicate minerals such as anorthite, which have calcium content, have been observed at a very low rate. They also reported that due to the low Ca content, the corundum phase occurred at a higher temperature (800°C -1000°C) than lignites[37]. In another study, Tomeczek et al.(2002) studied kinetics of mineral matter transformation by carrying out experiments with TGA up to 1700 K [41]. It was obtained reaction mechanism to determine how phases are competing with each other. They identified mineral transformation of iron related minerals. They observed both iron oxide mineral form occurs, but they indicated free Fe atoms tends to transform magnetite in lesser oxygen presence[41], [45] These findings also explain the reduction of hematite to magnetite due to the diffusion limitation mentioned in previous studies [37], [45].

Inorganics and amounts of inorganics in solid fuels are generally obtained by standard methods [46] (Lignite: ASTM D3174-12). These methods are based on obtaining the chemical content of the ash which is burned under standard conditions. However, as the combustion conditions used in these methods (low heating rate, low temperature) and the physical phenomena such as convective heat transfer, mass transfer due to

flow feed, are very different from those in the actual combustion system, the ash compositions may differ from those obtained from real boilers [2].

Although the aforementioned studies described the conversion of ashes to the mineral material due to the combustion temperature, the reactors used in these studies are far from the actual combustion conditions and have a very low heating rate. It should be mentioned the studies which consider the ash characteristic with the help of the drop tube furnace, which is a widely used experimental setup with high heating rate (10^4 °C / s). Meng et al. (2012) examined the combustion kinetics and ash characteristics by burning low grade lignite, O₂ / N₂ and O₂ / CO₂ atmospheres, with the help of drop tube furnace, in the 800-1200 °C range. As a result of the results obtained, it was observed that the crystallinity of mullite phase in proportion to the temperature was proportional to the temperature range. Also, kaolinite phases were reported at 1200° C [14]. Zhao et al.(2011) investigated aluminum mineral transformations during combustion with aluminum rich coal by drop tube furnace [47]. They observed, the mullite content is higher than kaolinite content at 900°C which shows the liberation of aluminum oxide from the kaolinite. They also mentioned, due to the slow nucleation of corundum phase, liberated aluminum oxide tends to form aluminosilicate mineral, mullite. This is the important findings for heating rate effect on the aluminum minerals. Yu et al.(2012) studied iron mineral transformation on drop tube furnace under oxy-fuel and air combustion conditions[48]. Their findings was the same with the low heating rate conditions [37]. Iron oxide tends to form hematite under rich oxygen condition instead of magnetite.

Although there are studies about the characteristic of ash, there is no study investigated the both the low heating-cooling rate, the temperature range. There is also no systematic study for for Class F Turkish fly ashes which is a proper raw material for zeolite synthesis with higher silica and alumina content with low calcium content.

2.4. Utilization of Fly Ashes

Several approaches have been proposed for the recycling and industrial applicability of fly ash. One of the approaches put forward as a premise is soil improvement practices [49], [50]. Furthermore, the use of fly ashes as an adjunct to reduce the cost of cement production is the longest recognized and typical method of industrial applicability [1], [12], [5], [51]. In addition, as Class F characteristic ashes have pozzolan properties, they can be employed individually as a cement alternative in building materials [12], [5]. However, these uses are far from being widespread. With the increasing demand for coal-borne energy and the tightening of regulations on fly ash in terms of waste management, efforts to minimize fly ash as waste and to work on innovative and sustainable application areas have gained momentum again. [3], [9].

There are many recent studies about the utilization of fly ashes. The innovative approach was suggested for the use of fly ash as a catalyst in the production of carbon nanotubes with the help of iron content [52], the separation of heavy metals from waste water, as well as the use of alkaline activation method in the production of lightweight construction materials such as geopolymer [53], [54]. In addition to this, the idea that fly ash is used as a raw material for zeolite production with its rich alumina silica content has come to the fore [1], [8]. However, although it offers quite innovative approaches in terms of environmental applications, these studies have not been carried to the industrial scale. There are many comprehensive studies on the characterization and classification of fly ash [31], [55], [56]. However, the properties of fly ashes vary widely depending on the source from which they are obtained. Therefore, regardless of the source, for the intended application, fly ash should be treated as a raw material and classified within the relevant field of application according to its required properties.

2.5. Zeolite Structure, Composition and Classification, Applications

Zeolites are aluminosilicate crystals in the class of porous materials. Structurally, zeolites consists of primary and secondary building units. Primary building unit is

made up from AlO_4 and SiO_4 tetrahedra arranged at the center with silicon or aluminum ions that is surrounded by shared oxygen atoms [13], [57], [58],[59]. Tetrahedrons are linked to each other as a periodically repeating unit to form more complex secondary building units(SBU). These SBU's connected to establish pores and channels of zeolites. Polyhedras are result of the combination of the SBU's and polyhedras forms zeolites. Even based on the same secondary building unit, different and unique structure of polyhedra could form with combinations of secondary building unit. The interesting properties of zeolites are brought about by the pore system which penetrates the zeolite in one, two or three directions and the pores vary in size and shape [13], [57], [58]. The primary building of zeolites, AlO_4 and SiO_4 tetrahedra were shown in Figure 2.3.

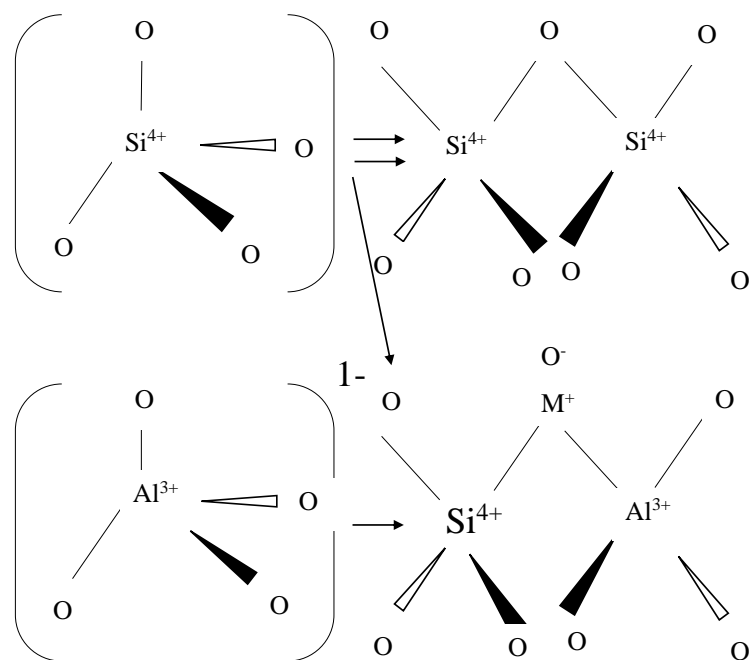


Figure 2.3. Tetrahedras of SiO_4 and AlO_4 and negative zeolite charge and counter-balancing metal cation M^+

Aluminosilicate framework requires cations as extra framework species (i.e. sodium) to provide electronic neutrality due to charge imbalance of tetravalent silicon atoms and trivalent aluminum atoms. Cations are introduced as extra framework species in

to voids. The cations introduced are usually readily exchangeable and are not part of the lattice framework structure [13], [57], [58].

By helping of their three dimensional framework and uniform pore structure, zeolites are known as molecular sieves [60]. Additionally, zeolites has some unique features such as pore sizes in the range of nanometer to micrometer scales, ion-exchange properties, high thermal stability and reversible hydration ability and acidity. Within these characteristic properties, zeolites are used in various applications [1],[5], [13], [57], [58].

The arrangement of structural units in the zeolite framework results in the generation of pores and cavities of different dimensions. Zeolites have channels that can be characterized by channel direction. Zeolites are classified according to their channel direction and type of the cages and named with the first three letter of cages (FAU, SOD, CHA) [61]. The framework of Zeolite 4A were shown in Figure 2.4

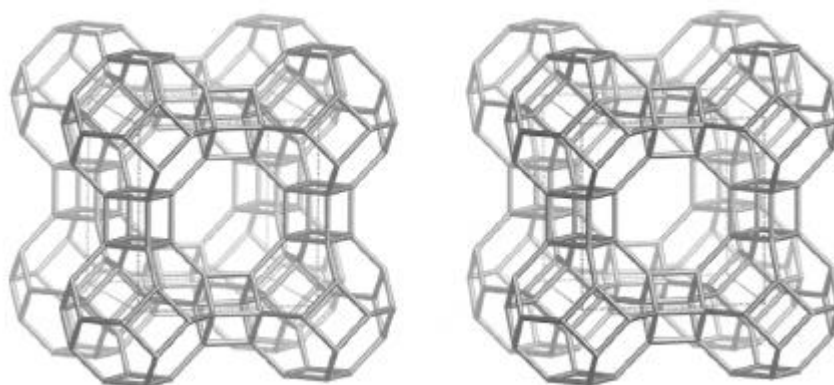


Figure 2.4. Framework of zeolite A

The low silica zeolite 4A was the most manufactured zeolite over the world. Zeolite 4A was named because of pore size of 4 Å [60]. The other names LTA or Na-A is also common for this type of zeolite. The usage of these zeolite 4A in the newly developed white goods (washing machine, dishwasher, dryer, refrigerator, etc.), except for long-known and benefited from these materials such as petrochemical, gas purification, flue gas cleaning (CO₂ capture) and glass industry, is also accelerating. Although the use

of zeolites in drying and heat applications is very new, it has become widespread in industrial area. The SEM image of Zeolite 4A synthesized from lab chemicals were given in Figure 2.5[62].

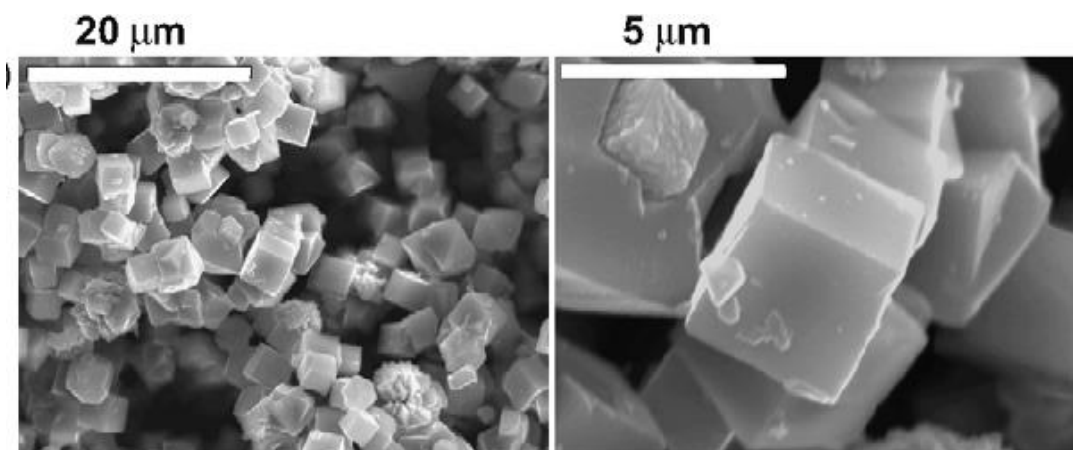


Figure 2.5. SEM Image of Zeolite 4A obtained from lab chemicals[62]

2.6. Synthesis and Formation Mechanism of Zeolites

Zeolite synthesis research started after understanding of the formation mechanism of natural zeolites through geological process [63]. During the 1940s, scientists began to produce successfully synthetic zeolites from sodium aluminasilicate gels that was prepared by pure sodium aluminate, sodium silicate and sodium hydroxide solutions in the laboratory by mimicking natural conditions of the hydrothermal processes [13], [60]. Since these pionerring research, hydrothermal synthesis method has become most widely used procedure on zeolite production industry and research. Due to the high reactivity of reactants and the easy control of the solution and environmentally friendly nature of the hydrothermal process is favorable [13], [57], [58], [59]. Synthetic zeolites are generally obtained by mixing the aluminate and silicate aqueous solutions with mineralizers (generally hydroxides and fluorites of alkali metals) and obtaining the gel by heat treatment of the mixture at a temperature of 100 °C and above.

The formation mechanism of zeolites has a complexity involving many different chemical reactions such as polymerization equilibrium reactions, nucleation and crystal growth of aluminum and silicon sources in alkali solution medium[58] . Polymerization equilibrium reactions can be said as the precursor step of the nucleation step required for the formation of zeolite. At this stage, Si-OH and Al-OH bonds are formed by hydrolysis, the generally accepted approach, for nucleation to begin. After this, condensation occurs and Si-O-Al bonds are formed [64]. In order to achieve the formation of zeolite, after forming the precursor Si-OH and Al-OH bonds, conditions must be provided to dictate nucleation while maintaining the presence of Si-O-Al bonds. In the nucleation step, small structures are formed to assure the growth of the targeted zeolite crystal by assimilating the amorphous aluminosilicate gel formed in the precursor step from the solution phase [13].

Crystal growth refers to the macroscopic evolution of the targeted zeolite atomic structure from nuclei, which were previously formed small structures, by hydrothermal treatment at a temperature higher than the nucleation step [60]. Zeolite crystal growth is solution-mediated and occurs at the crystal-solution interface by condensing dissolved species (secondary structural units) to the crystal surface . Generalized mechanism for formation of zeolites that developed by Cundy and Cox(2005) were shown in Figure 2.6.

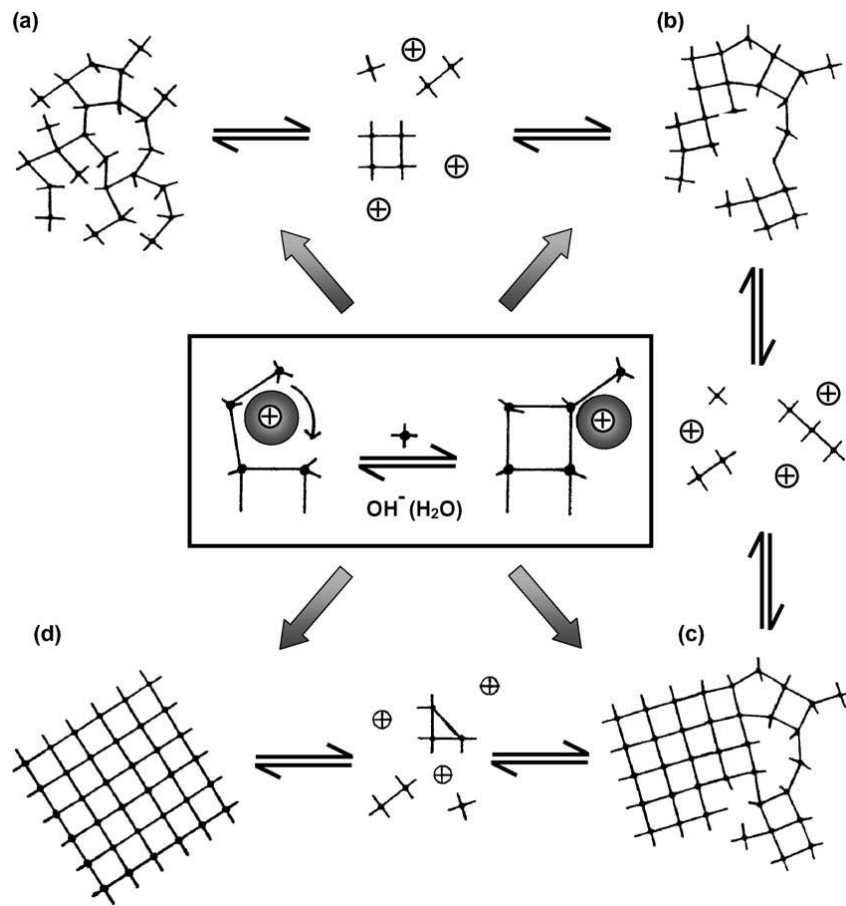


Figure 2.6. Overview of Synthesis Mechanism of Zeolites a) Depolymerization b) Nucleation c) Crystal Growth d) Coordination and Construction of Frameworks [13]

2.6.1. Ostwald's Rule of Successive Transformations

The mechanism of zeolite formation takes place as described above when the desired conditions for the targeted zeolite formation are met. However, it may vary depending on the parameters that determine the thermodynamic behavior of the system. In general, this is explained by Ostwald's rule of successive transformations [58], [65]. Accordingly, "If a system is far from equilibrium, intermediate metastable phases crystallize generally before the thermodynamically stable phase" [58]. In terms of zeolite synthesis, the targeted zeolite structure is generally not the most thermodynamically stable phases.

2.6.2. Effect of Parameters on Zeolite 4A Synthesis

The achievement of zeolite 4A synthesis depends on multiple parameters such as Si / Al molar ratio, alkalinity level, aging time and temperature, and crystallization time and temperature[58]. Si/Al mole ratios affect the behavior and mechanism of polymerization reactions. Alkalinity affects the pH of the solution media and also formation of framework. The temperature and time affect kinetic and thermodynamic behavior, particularly nucleation and crystal growth steps. As mentioned in the previous subsection, the optimization of the synthesis process can be explained in relation to the Ostwald's rule.

Previous research has indicated the excess level of Al have a positive impact on crystallization of Zeolite 4A, in other words, Al is the limiting reactant of the reaction mechanism [17], [19], [66], [67]. The level of alkalinity has a predominant effect on nucleation behavior. A high level of alkalinity encourages the formation of more nuclei, but the excess level of alkalinity results in formation of more thermodynamically stable sodalite phase [22], [58].

Crystal growth follows nucleation, but the conditions of crystal growth are far more tolerant to variation than the nucleation process. While the nucleation rate is inversely proportional to temperature [68], the temperature has an increasing effect on the crystal growth rate [69]. However, if the crystallization temperature is too high, the system tends to form sodalite.

A number of studies have found that the number of formed nuclei is increased by the extension of aging period [13]. This provides the acceleration of crystal growth and decrease the crystal size [70]. Due to high crystallization rate of Zeolite 4A, the aging time is an sensitive parameter in terms of end product properties.

Regardless of the aging time effect, the duration of the hydrothermal process is crucial in terms of crystallization kinetics [13]. The crystallization time has two distinct determining effects on the final product. One of these is to achieve phase impurity. When the crystallization time exceeds the optimal time, the zeolite 4A crystals formed

dissolve and trigger the formation of phase impurities such as sodalite [20], [66], [71]. In the absence of sufficient time for crystal growth, amorphous aluminasilicate hydrate is formed instead of crystalline Zeolite 4A.

In summary, it has been found that sodalite formation, which is a thermodynamically more stable phase instead of zeolite 4A, occurs when optimal conditions for any parameter are not provided. In the studies on the synthesis of zeolite 4A from fly ashes, many studies have been carried out on the optimization of related parameters depending on the content of the ash source used. In the following section, these studies will be mentioned.

2.7. Hydrothermal Synthesis of Zeolite 4A From Fly Ashes with Alkali Fusion

Since the pionerring study of Höller and Wirsching, research were focused on elimination of drawbacks the alkali digestion hydrothermal method. A large amount of literature exists on the formation of zeolites from coal fly ash and other aluminosilicates, however much of the information is contradictory with regard to which zeolites form under which conditions [17], [22], [72]. Repeatability and zeolite quality and zeolite yield are the main drawbacks of the alkali digestion hydrothermal method. In this context, it has been found that alkali fusion method is more advantageous in terms of zeolite yield and quality compared to direct hydrothermal synthesis method based on treatment of ash with an alkaline aqueous solution [1].

2.7.1. Pretreatment of Fly Ashes with Alkali Fusion Process

The introduction of the alkaline fusion step is a prior to hydrothermal treatment. In this method, the fly ash is mixed with NaOH or Na₂CO₃ as fusion chemicals and the product of the mixture is fused at temperatures above 500°C [73], [74]. In general, the fusion results in the conversion of fly ash into soluble sodium aluminate, sodialumunosilicate or sodium silicate, which is further dissolved in water. The dissolved mixture is then reacted under hydrothermal conditions. Introduction of this fusion step is characterised by high fly ash conversion and a high energy demand because of the fusion temperatures [17], [75].

Researches have reached a common finding that quartz and mullite are converted to minerals such as nepheline, sodiumdisilicate, sodiualuminate, regardless of the source of ash, with the alkali fusion step [19], [22], [66], [76]. The findings overcome the problem of water solubility of these minerals which was mentioned in the studies of alkali digestion method [8]. However, the fact that the mineral content of ash on the fusion product is not addressed clearly leads to the failure of a sustainable synthesis method by the alkali fusion process.

To better understand the effect of mineral composition, chemistry of alkali fusion should be considered. Jesse J. Brown et al. (1995) reviewed the literature about the reactions of sodium carbonate and aluminosilicate refractories to predict corrosion level. The study offered use of triple phase diagram of $\text{Na}_2\text{O}:\text{SiO}_2:\text{Al}_2\text{O}_3$ to distinguish real effect of respected compounds on the formation of corrosive alkali minerals. The study covered the laboratory studies and industrial scale observations. They found that the silica minerals could easily melt and form sodiumsilicate minerals around 800-850 °C, they indicated mullite is more resistive than silicate minerals. The lower crystallinity level of mullite provides to form beta-alumina (sodium aluminate) or direct conversion of nepheline depends on the aluminum content [18]. This findings could be applicable for the fly ashes to explain the ash crystallinity and mineral composition on the fusion product composition and later the nucleation behavior could be predicted.

2.7.2. Hydrothermal Synthesis of Zeolite 4A after Alkali Fusion Process

The general consideration about the aging step is to conduct at room temperature. Moreover, optimization of Si/Al mol ratio is provided with addition of aluminum solution after fusion process and filtration steps for desilification of fusion products. Although the synthesis step includes these laborious steps, valuable findings on the level of alkalinity, crystallization time, aging time and temperature have been reported in the literature.

The very first study about the Zeolite 4A synthesis with alkali fusion step was conducted by Shigemeto et al.(1993) [73]. They introduced fusion step to the hydrothermal treatment to obtain water soluble sodium aluminate, sodium silicate and sodialuminasilicate phases within the fusion product by adding NaOH powder into fly ashes. They concluded, alkali fusion step provides phase pure zeolite A and X, seperately.

Chang et al. (2000) studied Zeolite A and Zeolite X synthesis with alkali fusion step. They concluded proper Si/ Al ratio for phase pure Zeolite A was provided by addition of $\text{Al}(\text{OH})_3 \cdot \text{H}_2\text{O}$ into gel solution before hydrothermal treatment and Zeolite A was obtained at 60 °C crystallization temperature in 4 days. They also discovered that Al species in the solution controls synthesis process [17], [77]. Similary, Ameh et al. (2017) investigated the addition of different source of aluminum solution(aluminum hydroxide and sodium aluminate) and crystallized the solution at 100°C for 3 h. They observed that the decreasing crystallinity of zeolite 4A by increasing of Si/Al mol ratio of the aging mixture. Alternatively, some research conducted by addition of NaAlO_2 after fusion process to gel solution during aging step. Izidoro et. al (2013) studied Zeolite A and X synthesis from Class F Brazilian coal fly ash for heavy metal removal from water and Zeolite A was successfully synthesized by addition of NaAlO_2 after 16h aging at room temperature and crystallization at 100 °C for 7 h [21]. In the other study, Musyoka et al. (2012) studied Zeolite A, X and P synthesis from Class F South African fly ash and it was suggested addition of sodium aluminate solution into the gel solution before hydrothermal treatment and Zeolite A was obtained after 2 h treatment at 100°C [78]. Similary, Soe et al. (2016) studied CO_2 adsorption performance and Ca ion exchange capacity of Zeolite A and Zeolite X synthesized from high silica fly ash with 63% and high iron oxide impurity with 17% percent and applied addition of NaAlO_2 into the gel solution and phase pure Zeolite A was succesfully synthesized after hydrothermal treatment at 100°C for 4 h [76].

There is a few study that using Class C fly ash for Zeolite A synthesis with alkali fusion step because of high calcium impurity. Kunecki et al. (2017) suggested

filtration of gel solution to eliminate calcium impurity and addition of aluminum foil into the solution to produce Zeolite A and it was obtained after 4h at 80°C hydrothermal treatment [79].

On aforementioned studies, sodium hydroxide was used as an alkali fusion agent. Recent studies focused on cheaper alternative alkali agent such as sodium carbonate. Jiang et al. (2016) studied possibility of using sodium carbonate as an alkali agent, but as a different approach, sodium hydroxide solution for aging step was added onto fusion product. Zeolite NaA was obtained with aging step at room temperature for 1 h with 3 M NaOH solution and followed by hydrothermal treatment at 80°C and for 3 or 4 h [80]. Monzon et al. (2017) studied Zeolite A synthesis with sodium carbonate as an alkali agent for fusion step, but Zeolite A was synthesized with sodalite phase impurities by 64% yield with steps with addition of NaOH- NaAlO₂ solution for aging step at room temperature and followed by hydrothermal treatment at 100 °C for 5 h.[81] Interestingly, Hu et al. (2017) studied silica and aluminum rich fly ash for Na-X and Na-A synthesis. It was suggested tablet compression for better contact of Na₂CO₃ with fly ashes. Phase pure Zeolite A was obtained with aging step at room temperature for 1 h and hydrothermal treatment at 80°C and 6 h without adding aluminum source [82].

There is a large volume of published studies describing the role of the crystallization temperature and crystallization time. Previous studies have been reported that, the extended crystallization time and the higher temperature results in formation of sodalite, that is parallel with Ostwald's Rule of Successive Transformation. However, much uncertainty still exists about the relation between the nucleation behavior of fusion product and zeolite crystallinity. The most of the researchers mentioned the differences of fly ash characteristics and still unclarified the aging conditions for nucleation according to temperature and duration. The summary of the synthesis conditions from the literature studies were given in Table 2.1.

Table 2.1. Summary of Synthesis Conditions from the Studies of Alkali Fusion assisted Zeolite 4A Synthesis from fly ash

Reference	Alkali Fusion	Si/Al optimization method	Aging Conditions	Crystallization Conditions
Chang and Shih(2000)	1:1.2 NaOH, 550 °C, 1 h	Addition of Al(OH) ₃ , H ₂ O solution	25°C, 24 h	72 h, 60°C
Soe et al.(2016)	1:1.2 NaOH, 550 °C, 1 h	Addition of NaAlO ₂ solution	25°C, 24 h	4 h, 100°C
Monzon et al.(2017)	1:1 Na ₂ CO ₃ , 800°C, 2h	Addition of NaAlO ₂ -NaOH solution	25°C, 48 h	48 h, 100°C
Hu et al.(2017)	1:1 Na ₂ CO ₃ , 800°C, 2h	-	25°C, 1 h	6 h, 80°C
Ren et al.(2018)	1:1.5 NaOH, 750 °C, 2 h	Addition of NaAlO ₂ before fusion	25°C, 12 h	18 h, 75°C
Panitchakarn et al.(2014)	1:2.25 NaOH, 550 °C, 1 h	Addition of Al ₂ O ₃ before fusion	25°C, 12h	4 h, 80°C
Yang et al.(2019)	NaOH+Na ₂ CO ₃ , 760°C	Addition of diatomite before fusion	25°C, 2 h	4 h, 90°C
Ameah et al.(2017)	1:1.2 NaOH, 550 °C, 1 h	Addition of NaAlO ₂ or Al(OH) ₃ solution	25°C, 15 min	3 h, 100°C
Izidoro et al.(2013)	1:1.2 NaOH, 550 °C, 1 h	Addition of NaAlO ₂ solution	25°C, 16h	7 h, 100°C
Guozhi et al.(2019)	1:1.2 NaOH 850°C, 1 h	Addition of NaAl(OH) ₄ solution	25°C, 6 h	18 h, 90°C
Jiang et al.(2016)	1:1.5 Na ₂ CO ₃ 800 °C, 2 h	-	25°C, 1 h	3 h, 100°C

Considering the impurities, such as iron content, it is remarkable that a separate study is necessary for fly ash obtained from Turkish lignites. Considering the difference in terms of inorganic content, it was found that there is no study for the synthesis of hydrothermal zeolite 4A by alkali fusion for Tunçbilek, Seyitömer and Soma thermal power plant ashes. In this respect, hydrothermal zeolite 4A synthesis parameters will be studied for the first time by using sodium carbonate, including thermal power plant ashes.

CHAPTER 3

MATERIALS AND EXPERIMENTAL METHODOLOGY

3.1. Methods of obtaining fly ash from reactors with different heating rates

3.1.1. Coal selection, analysis and preparation for combustion experiments

The lignite coal was selected to yield desirable silicon and aluminum contents for zeolite 4A synthesis. Based on this information, the coal ash should be selected from Class F ashes or more specifically sialic or high sialic ashes are proper candidate for zeolite synthesis [31]. Due to this reason, Tunçbilek lignite (TL) was selected for the combustion experiments. In addition, Tunçbilek lignite is a widely burned lignite in Turkey, representing 0,38 % of the total installed capacity (TEIAS, 2016). Moreover, the previous studies on Tunçbilek lignite combustion carried out in the Clean Combustion Technologies laboratory provide important data and experimental procedures to be used in this study. The coal characteristics was presented with ultimate and proximate analysis in Table 3.1.

Table 3.1. Ultimate and Proximate Analysis of Tunçbilek Coal

	Parameter	Tunçbilek
Proximate analysis (weight%, as received)	Moisture at 105 °C	2,8
	Volatile matter, at 950 °C	31,1
	Fixed Carbon*	52,1
	Ash Content	14,0
Ultimate Analysis (wt.%, ash free, dry basis)	C	61,8
	H	5,6
	N	2,7
	S	1,5
	O	28,5
Ash Analysis (weight%, dry basis)	Al ₂ O ₃	15,3
	CaO	1,19
	Fe ₂ O ₃	12,5
	SiO ₂	40,5
	SO ₃	23,4
	Other oxides	7,1
	LHW (MJ/kg)	27,8
	HHW (MJ/kg)	25,7

The Tunçbilek Lignite was obtained from Turkey Coal Enterprises (TKI) and analyzed for its chemical composition and heating value. As visible in Table 3.1, Tunçbilek lignite has low heating value, high ash content, and high sulfur content. Preparation of Tunçbilek lignite was carried out in METU Mining Engineering Mineral Processing Laboratory. As a first step, Tunçbilek lignite was ground to micron level with the help of a roll crusher and a ring mill. Following grinding, a Retsch sieve set (75, 106, 125, 250, 500 μm) shown in Figure 3.1 was used to sieve to the desired particle size range of 106-125 μm . Even though some of the size cuts were not used for this study, the large number of sieves was used to prevent saturation. Sieving was performed with a Retsch sieve Shaker for the duration of 10 min and this process was repeated until the mass of the $>106 \mu\text{m}$ sieve did not vary more than 1 %. Finally, these collected samples sieved for a final time, dried overnight at 105 °C in a muffle furnace and stored for use in combustion experiments. Some studies in the literature have argued that particle size distribution affects the combustion behavior of fuels [2], [14].



Figure 3.1. Retsch Sieve Set in CCTL

In order to avoid these effects, a narrow particle size range of 106-125 μm , was preferred. This size range was also in line with previous studies conducted in the CCTL[83].

3.1.2. Combustion Experiments for Tunçbilek Lignite

The prepared TL fuel was burned using different setups in order to analyze the influence of the combustion conditions on the fly ash. Specifically, a drop tube furnace (DTF), a wire mesh reactor (WMR), and a muffle furnace were used to analyze the effect of heating rate and temperature. Moreover, WMR was also used to observe the effect of the cooling rate.

The temperature values were chosen as 800, 900, and 1000 $^{\circ}\text{C}$ for all reactors to observe the effect of the combustion temperature on fly ash characteristics. The lower limit is selected as 800 $^{\circ}\text{C}$ because the secondary quartz phase and the mullite phase, which are important for zeolite synthesis, begin to form at 800 $^{\circ}\text{C}$ [37], [44]. Furthermore, the indicated temperature is well beyond the burnout temperature for the respective coal, which ensures complete burnout of the sample. The upper limit temperature is also the maximum comparable temperature for all the reactors used. Each experimental setup differs greatly in the maximum heating rate to which the fuel is subjected to. The DTF achieves rates of $\sim 10^4$ $^{\circ}\text{C s}^{-1}$, the WMR $\sim 10^3$ $^{\circ}\text{C s}^{-1}$, and the muffle furnace < 1 $^{\circ}\text{C s}^{-1}$. The conditions of the conducted experiments for ash collection were given in Table 3.2.

Table 3.2. Summary of Experimental Conditions of Combustion

Reactor	Heating Rate	Combustion Temperature ($^{\circ}\text{C}$)	Amount of Coal(g)
Muffle Furnace	0,17 $^{\circ}\text{C /s}$	800, 900, 1000	3
Wire Mesh	10^3 $^{\circ}\text{C /s}$	800, 900, 1000	0,15
Drop Tube Furnace	10^4 $^{\circ}\text{C /s}$	800, 900, 1000	2,8

Drop Tube Furnace Experiments

The drop tube furnace consists of an alumina reactor, a feeding unit and a collection unit. The DTF setup is shown in Figure 3.2.

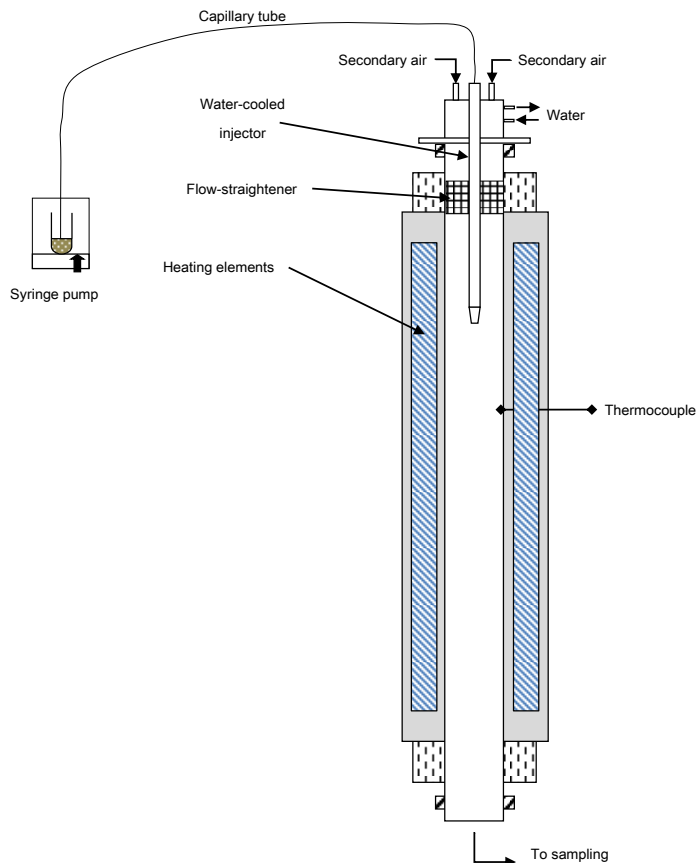


Figure 3.2. Schematic Diagram of Drop Tube Furnace in CCTL

The DTF is an electrically heated furnace with silicon carbide and molybdenosilicate thermal elements capable of reaching a maximum power of 7.5 kW. The alumina reactor limits the maximum operating temperature to 1100 °C. The vertical reactor consists of a ceramic (60% Al_2O_3) tube with length of 1500 mm and inner radius of 75 mm. The temperature control is carried out with the aid of an S-type thermocouple to ensure a constant temperature throughout the reaction zone which is 1000 mm

length. The mixture of oxidizer gases in the reactor can be measured and defined by means of mass flow controllers.

The feeding unit consists of a water-cooled injector, syringe pump and a capillary tube. The water-cooled injector is designed to feed solid fuels and combustible gases downwards into the constant temperature (1000 °C) zone of the vertical tube furnace at room temperature. A test tube was fitted into the syringe pump that was coupled with a vibrating motor. The combination of the linear movement of the syringe pump, the vibration, and the injection of transport air into the test tube forced a constant flow of particles into the capillary tube and therefrom to the reaction zone.

Ashes are collected by the collection unit that consisted of an ash impactor (Tecora MSSI) and a vacuum pump. The Tecora Impactor was shown in Figure 3.3a. The overview of Drop Tube Furnace was given in Figure 3.3b. Collection was done at the outlet of the furnace. More details on the experimental setup can be found elsewhere.

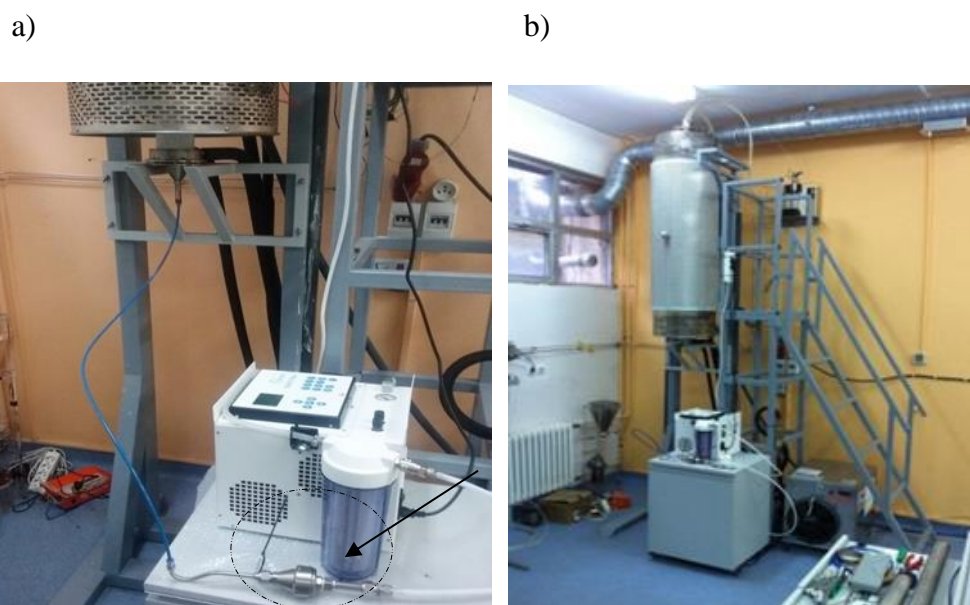


Figure 3.3. a) Tecora Impactor b) Overview of Drop Tube Furnace in CCTL

The experimental procedure during DTF experiments was as follows: (i) the processed fuel is placed in a test tube and weighed; (ii) the test tube is placed in the syringe pump unit; (iii) the primary air (4 L/min) used to transport the fuel and the secondary air (16

L/min) are sent directly into the furnace; (iv) the vacuum pump is switched on and a waiting time of 5 min is respected to reach steady flow conditions in the reaction zone; (v) the vibration motor is started respectively and the linear movement of the syringe is initiated. (vi) fuel is fed during 10 minutes (vii) in order, the vibration motor, syringe pump, flows, and vacuum pump are terminated; (viii) at the end of the test, the test tube containing the fuel is separated from the system and its mass is measured and the mass of the fuel supplied to the system is determined; (ix) the ashes are collected from the paper filter. The constant mass flow rate proved by the weight difference in the test tube for the consecutive experiments.

Wire Mesh Reactor Experiments

The wire mesh reactor comprises a wire mesh onto which the fuel sample is placed and heated, conductive electrodes to conduct high current, a thermocouple to measure the wire mesh temperature, and the atmosphere inside the chamber is defined as atmospheric air. The high temperature ($> 1200\text{ }^{\circ}\text{C}$), high heating rate ($\sim 10^3\text{ }^{\circ}\text{C s}^{-1}$) of the reactor is ensured by the supply of high current and low voltage. The temperature of the reactor is measured with an R-type $125\text{ }\mu\text{m}$ thermocouple, which is welded onto the wire mesh. The whole setup of wire mesh reactor was shown in Figure 3.4. More information on the wire mesh reactor (WMR) used herein can be found elsewhere. For this thesis experiments, the amount of coal for ash collection was optimized as 150 mg and the residence time setted as 50 s to complete burnout of the coal.

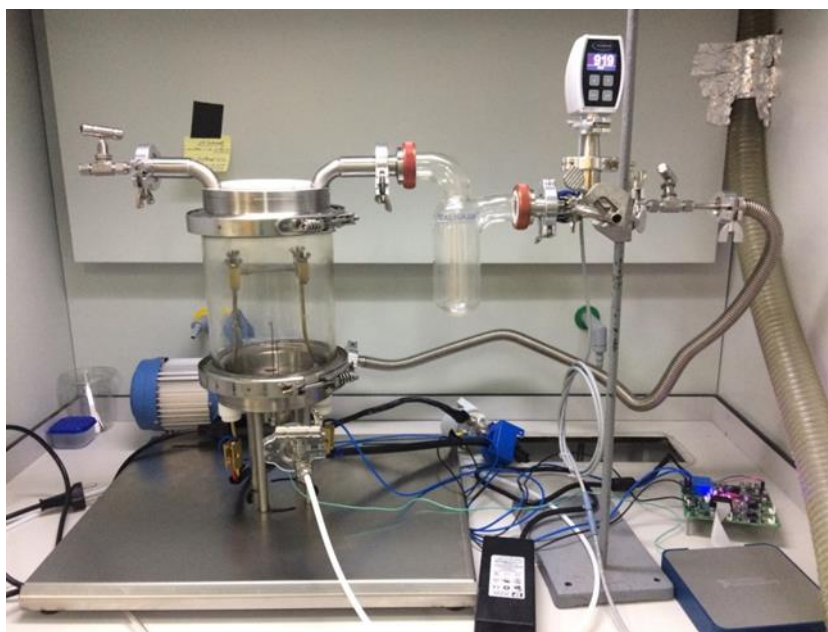


Figure 3.4. Wire mesh reactor (WMR) in Clean Combustion Technologies Laboratory (CCTL).

The experimental procedure was as follows: (i) a thin layer of fuel is placed in between two wire meshes; (ii) these wire meshes are clamped using the copper plates ; (iii) the glass chamber is placed ; (iv) the power supply is switched on and the wire mesh plates are kept at the prescribed temperature value for the duration of the test; (vi) following completion of the combustion process, the reaction chamber is cooled using nitrogen under atmospheric conditions; (vii) upon reaching room temperature the fly ash sample is carefully removed from the wire mesh for further analysis.

The cooling rate particularly affects the percentage of mullite, the aluminosilicate mineral in fly ash. In order to observe this effect, the cooling rate was measured after the power supply was switched off and the temperature-time profile recorded with the LabView™ software as $260\text{ }^{\circ}\text{C} / \text{s}$ for $1200\text{ }^{\circ}\text{C}$. In order to observe the possible decrease in mullite percentage, it was aimed to increase the cooling rate by feeding nitrogen gas at two different flow rates after the power supply was cut off in order to roughly increase the cooling rate measured. Since the glass lantern was placed open top, the additional cooling provided by the feed nitrogen flow but it could not be accurately recorded. Therefore, the cooling rate was expressed as the nitrogen flow

rate. The nitrogen gas was provided at rates of 4 L/min and 8 L/min for 10 s after switch-off. The conditions were shown in detail below on Table 3.3 for the experiments.

Table 3.3. Cooling Rate Experiments on WMR at 1200°C

Experimental Rig	Combustion in WMR
Cooling Rate	
Without N ₂ (260°C/s)	
4L/min N ₂ quench	
8L/min N ₂ quench	1200°C

Muffle Furnace Experiments

Muffle furnaces are widely used laboratory furnaces to determine the ash yield of a material. Herein, it is used to investigate the mineral conversion during combustion, i.e. the mineral chemistry, at different temperatures and low heating rate. In order to observe the mineral transformations and compare the ash with that from other experimental apparatuses with higher heating rates, the heating rate was set to 10°C/min for each of the three different temperatures (800, 900 and 1000°C). For ash extraction experiments, 3 g of coal was used for each sample. In order to avoid agglomeration during combustion, the weighed sample was dispersed homogeneously in the crucible. Concurrently with the start of the heating program, dry air inflow was set to 3 L/min with the help of a flowmeter. After the end of the program, the samples were to cooled to room temperature. The crucible was removed from the furnace and the mass of ash was measured, and the ash conserved for further analysis. Ash yield was observed to be 15% for all samples. For the experiments, Protherm Muffle

Furnace was used and represented in Figure 3.5. The heating ramps applied in the tests are shown in Figure 3.6.



Figure 3.5. Protherm ashing furnace at Clean Combustion Technologies Laboratory (CCTL)

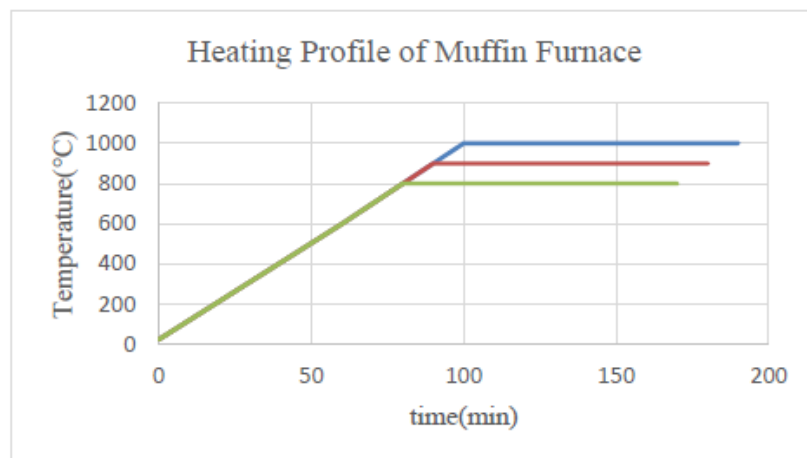


Figure 3.6. Heating Profile of Muffle Furnace for 800 °C, 900 °C and 1000 °C

3.1.3. Characterization of Fly Ashes

The ashes obtained from three different thermal power plants (Seyitömer Thermal Power Plant, Tunçbilek Thermal Power Plant and Soma Thermal Power Plant 5-6 units), as well as those obtained from the three aforementioned setups (DTF, WMR, and muffle furnace) were analyzed for their chemical composition. Characterization techniques included X-Ray Fluorescence (XRF) and X-Ray Diffraction (XRD). To investigate the effect of chemical composition on fly ash characteristics, two different Class F fly ash and a Class C fly ash were selected.

Tunçbilek lignite ash, also used in the lab scale experiments, was selected as one of the thermal power plant ashes. Seyitömer thermal power plant ash was selected due to its different iron content. As a comparison, it was planned to use a Class C fly ash source and it was selected Soma Power Plant Fly ash from the 5-6 Unit of the respected Power Plant.

Especially, the mineral composition of the Power Plant fly ashes were detected by XRD and examined to observe the differences which was related with chemical composition. Percentages of crystallinity and mineral composition distribution was calculated from the obtained diffraction patterns. Active phases for zeolite synthesis (quartz and mullite) and impurities (hematite and anorthite) were particularly observed. The method used to calculate percentages is shown in Equation 3.1.

$$\%crystallinity\ of\ product = \frac{\text{sum of the area under the peaks of the product}}{\text{total area}} \times \%100 \text{ Equation (3.1)}$$

In addition, the chemical content of the supplied thermal power plant ashes was determined by XRF and observed morphologically using Scanning Electron Microscopy (SEM).

As a result of the combustion experiments, the fly ashes obtained from the three different reactors were compared one by one over the phases which are active in zeolite synthesis (quartz and mullite), and the so-called impurity for zeolite synthesis

(hematite and magnetite). In addition, the ash obtained from the experiments carried out in three different cooling rates in the WMR was compared in terms of mullite ratio. Finally, Tunçbilek ashes obtained from three different reactors were compared separately with the Tunçbilek thermal power plant ashes for their XRD patterns.

The muffle furnace ashes and the drop tube furnace ashes (both obtained at 1000°C) and the Tunçbilek Power Plant ashes were also compared in terms of chemical composition using XRF. The low amounts of ash obtained from WMR prevented the use of the ash from this setup for XRF analysis and zeolite 4A synthesis. More details about the analysis methods will be given in Section 3.5.

3.2. Zeolite 4A Synthesis Experiments with Alkali Fusion

Alkali fusion is a frequently used as a pretreatment method for the production of high yield and high crystallinity Zeolite 4A from fly ash [9]. In this study, Zeolite 4A synthesis experiments were carried out by the hydrothermal method following the alkali fusion step.

Class F Seyitömer thermal power plant fly ash was used as the ash source. Here, unlike the studies in the literature, the extra aluminum source required for the synthesis of zeolite 4A was not added in the aging step. Instead, the aluminum hydroxide powder was subjected to the fusion step by mixing with fly ash with sodium carbonate which was used as an alkali agent prior to the fusion step. In this study, for all alkali fusion processes, heating rate was 10 ° C / min, fusion temperature was 900 °C and duration was 1 hour. Alkali fusion process was carried out in the Muffle Furnace.

Zeolite 4A is a thermodynamically metastable phase relative to the sodalite phase [13]. However, sodalite is a phase impurity for the Zeolite 4A crystal. Thus, it can be observed in the XRD diffraction pattern depending on the synthesis conditions in the experiments. Chronologically, the conditions were determined with the help of this information. By other words, the elimination of phase impurities has been a priority for the conducted synthesis experiments in the experimental matrix. In parallel, the

determination of nucleation behavior and optimal crystal growth conditions of alkali fusion product obtained from Seyitömer thermal power plant fly ash were studied.

For the starting point, experience and knowledge of Nanodev Research Group's Lab were provided for the alkali fusion process and synthesis procedures. In the synthesis experiments carried out using Seyitomer fly ash, the experimental steps followed independently of the conditions can be listed as follows. 1) Fly ash, sodium carbonate and aluminum hydroxide are mechanically mixed and placed into the ceramic vessel homogenously and then appointed to fusion at 900°C. 2) After the oven temperature is allowed to cool to room temperature, the sample is ground with mortar. 3) The intermediate products obtained as a result of the alkali fusion are mixed with distilled water with the ratio of 1,6 by mass (DI water/fusion product) and placed in HDPE bottles. 4) Aging with the help of magnetic fish and magnetic stirrer is carried out at 500 rpm at the specified temperature for the specified time. 5) After the aging process is finished, the stirrer is stopped and the sample temperature is measured. 6) The HDPE bottle is allowed to react in the oven at the previously determined temperatures. 7) The reaction products are separated from the liquid by centrifugation, washed several times using ultra-pure water and dried in the oven at 70 ° C overnight.

The conditions in the outlined experimental steps were carried out depending on parameters such as reaction temperature and time, aging time, aging temperature, Si / Al molar ratio and also Na / Si mass ratio which determines the alkalinity level (Na_2CO_3 /fly ash) [1].

The products obtained as a result of zeolite synthesis were characterized by SEM for the morphology and XRD for the analysis of the crystal phases. The obtained Zeolite 4A samples were compared according to morphology with the Zeolite 4A that was synthesized with laboratory chemicals and provided from Nanodev Research Group's previous work.

3.2.1. Investigation of Nucleation Behaviour with Aging Experiments

Aging studies are one of the methods frequently used in hydrothermal synthesis studies to investigate the nucleation behavior of silicon and aluminum sources in solution medium [13]. In the literature, the appropriate Si / Al molar ratio range for Zeolite 4A has been reported as 1-1,5 [84]. Accordingly, Si / Al optimization was studied with fusion product having 4 different Si / Al molar ratios on this range. The product obtained with the aid of alkali fusion should have a reproducible Si / Al molar ratio. Based on the analysis results obtained after the preliminary studies, the relationship between the total silicon and aluminum mass ratio of the fly ash-sodium carbonate-aluminum hydroxide solid mixture prepared before the fusion process and the Si / Al molar ratio obtained as a result of the fusion process was formulated. In this context, Si / Al mass ratio concept is defined in this thesis. This concept is frequently used in future sections. To confirm this approach, the same mixing ratio was repeated twice for each Si / Al molar ratio and a maximum deviation of 4% was determined.

The XRF results of the fusion products were shown in Table 3.4 and the repeatability of the formulation for fusion process, shown in Figure 3.7. To obtain desired Si/Al mol ratio, a sample calculation for one of the Si/Al mass ratio were shown below Equation 3.2, 3.3 and 3.4.

The rest of the other Si/Al mol ratio was determined based on the mass ratio of Si/Al in the solid mixture before the fusion process. According to desired mol ratio, the amount of fly ash could be changed according to chemical composition of fly ash, which means that the aluminum and silisium amount varied for the ash sources. The Si/Al mol ratio could be tuned by the adding aluminium hydroxide.

Table 3.4. Si/Al mass ratio and mol ratios of prepared fusion mixture in this study

Si/Al mass ratio	SiO ₂ (wt.%)	Al ₂ O ₃ (wt.%)	Na ₂ O(wt.%)	Si/Al (mol ratio)
0,99 0,99	33,74	18,15	30,41	1,58
	27,30	15,20	34,30	1,52
0,82 0,82	27,30	17,10	32,10	1,35
	31,54	19,43	31,61	1,38
0,72 0,72	27,60	20,00	31,10	1,17
	26,80	19,50	30,70	1,17
0,6 0,6	26,80	22,60	29,40	1,00
	26,80	21,20	30,70	1,04

$$\text{Amount of Si from FA (g)} = \text{FA (g)} \times \% \text{SiO}_2 \text{ content} \times \frac{1 \text{ mol SiO}_2}{60,08 \text{ g}} \times \frac{28 \text{ g Si}}{1 \text{ mol Si}} =$$

amount of Si from the FA Equation (3.2)

$$\text{Amount of Al from FA (g)} = \text{FA (g)} \times \% \text{Al}_2\text{O}_3 \text{ content} \times \frac{1 \text{ mol Al}_2\text{O}_3}{101,996 \text{ g}} \times \frac{2 \text{ mol Al}}{1 \text{ mol Al}_2\text{O}_3} \times \frac{27 \text{ g Si}}{1 \text{ mol Al}} =$$

amount of Al from the FA Equation (3.3)

$$\left(\frac{\text{Si}}{\text{Al}}\right) \text{ mass ratio in total mixture; } 0,7 = \frac{\text{amount of Si from the FA}}{\text{Al from FA (g)} + \text{required amount from Al(OH)}_3} \quad \text{Equation}$$

(3.4)

For these products, the reactions were carried out an aging temperature of 47 ° C, 16 hours aging and a crystallization time of 7 hours at 100 °C [21]. The mixture temperature was controlled by a water bath prepared at 60 °C. The desired temperature value was confirmed by measuring with a thermometer after the end of the aging time. Control experiments were then carried out under different alkalinity, aging time and aging temperature conditions for a gel with a molar ratio of 1,17 Si / Al and at a crystallization temperature of 90 °C. Aging temperature conditions were maintained without water bath for 25 °C. In contrast, for the aging temperature experiments at 37

° C and 47 ° C, it was provided with the help of a water bath prepared at 45 ° C and 60 ° C, respectively.

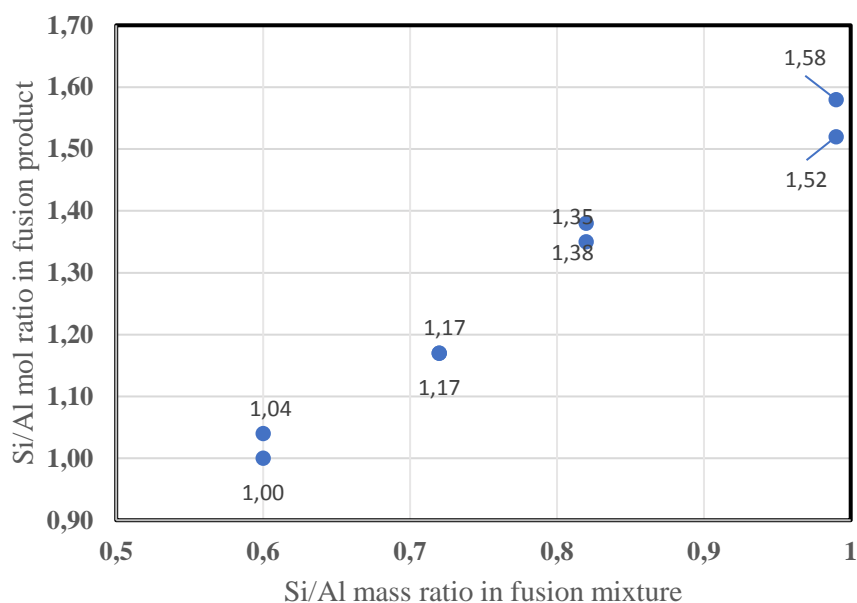


Figure 3.7. Influence of Si/Al mass ratio on the Si/Al mol ratio of fusion product

3.2.2. Optimization of Crystallization Conditions

In order to determine the quality and yield of zeolite and to obtain Zeolite 4A from the fusion product obtained from fly ashes, it is necessary to determine the optimal temperature and the optimal duration for the reaction step in which crystal growth occurs [13]. In this study, based on the conditions of the studies reported for the synthesis of zeolite 4A by alkali fusion method, experiments were carried out at crystallization temperature of 85, 90 °C, 100 °C for 4 hours and 7 hours[21],[22], [76]. In these experiments, mol ratio of the fusion products was selected as Si / Al 1,17 and 1,35. Moreover, the conditions was for the aging temperature was 47 °C, and the aging time 12 hours and 16 hours, respectively. The experimental matrix given on Table 3.5 and flowchart for the zeolite synthesis in Figure 3.8.

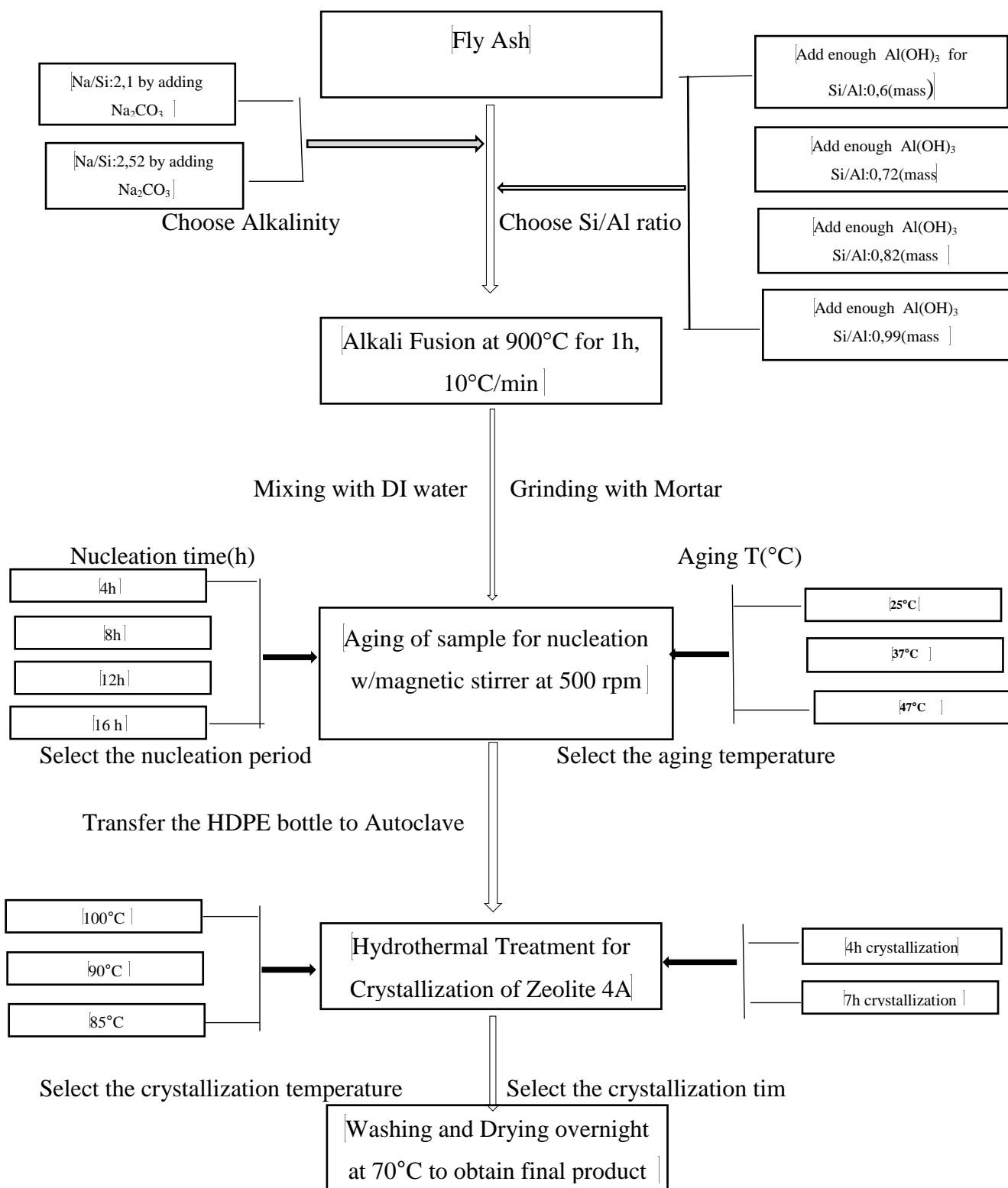


Figure 3.8. Process Flowchart for Zeolite 4A Synthesis from fly ash source

Table 3.5. Experimental Conditions of Optimization of Zeolite 4A Synthesis

Sample	Si/Al (mol ratio)	Alkalinity (weight)	Aging Time (hour)	Aging Temperature (°C)	Crys. Temp (°C)	Cry. Time (hour)
1	1,05	1,10	16	47	100	7
2	1,17	1,10	16	47	100	7
3	1,35	1,10	16	47	100	7
4	1,5	1,10	16	47	100	7
5	1,17	1,10	16	25	100	7
6	1,17	1,10	16	47	90	7
7	1,17	1,10	16	47	85	7
8	1,35	1,10	16	47	90	7
9	1,17	1,35	16	47	90	7
10	1,17	1,10	16	37	90	7
11	1,17	1,10	16	25	90	7
12	1,17	1,10	16	47	90	4
13	1,17	1,10	4	47	90	4
14	1,17	1,10	8	47	90	4
15	1,17	1,10	12	47	90	4
16	1,17	1,10	12	47	90	7
Optimal:	1,17	1,10	12	47	90	4

3.3. Zeolite 4A Synthesis Experiments with other Fly Ash Sources

One of the most important objectives of this study is to obtain a sustainable method for the synthesis of Zeolite 4A from fly ashes, independent of the fly ash source. In order to achieve this goal, ash resources with different characteristics were needed. Because, there are differences in the fusion product depending on the properties of the fly ash source and in this case affect the properties of the synthesis product [66]. In order to achieve a sustainable method, the impact of these differences needs to be determined. In this regards, Zeolite 4A synthesis experiments were carried out with Class F Tunçbilek ashes (including Thermal Power Plant ashes) obtained by applying different combustion parameters, as well as Soma 5-6 PP ash having different

chemical composition. For the synthesis experiments, the optimal conditions determined for Seyitömer thermal power plant ash were used as control experiments.

Fly ash contains different amounts of Si / Al and therefore different amounts of SiO₂ and Al₂O₃ depending on the conditions from which they are obtained or the source from which they are obtained. Relative to this, the determined optimal Si / Al molar ratio of 1,17 must be maintained in the fusion process for all the other fly ashes. To achieve this, the ratio of total silicon mass to total aluminum mass in a triple solid mixture of fly ash, sodium carbonate and Al (OH)₃ was taken as 0,7 for all samples. The Na / Si mass ratio determined for the alkalinity was taken as 2,1. The calculation was done as described in Section 3.2.1.

In order to observe the effect of different combustion parameters on the synthesis product on the ash obtained from a single coal, the following procedure was followed. MF1000, DTF 1000 and Tunçbilek Thermal power plant ash were used. The triple solid mixture of those ashes were prepared based on the given optimal Si/ Al mass ratio for the fusion process. Zeolite 4A was then synthesized with these fusion products, following the experimental steps given in section 3.3, at a aging temperature of 47 ° C, aging for 12 hours and crystallization conditions for 4 hours at 90° C. In this way, synthesis conditions were validated for a Class F ash source obtained from a different source. In addition, the effect of the difference in iron oxide and mullite mineral content could be observed. In addition, zeolite 4A synthesis was carried out with fusion product of Soma 5-6 Thermal Power Plant Ash, which contains high levels of calcium impurity, at aging temperature of 47 ° C, 16 hours aging and for 7 hours crystallization at 90° C conditions.

3.4. Zeolite 4A Synthesis Experiments with Fly ashes from Combustion Blends

As a unique approach, the chemicals necessary for the synthesis of zeolite 4A, sodium carbonate and aluminum hydroxide, were mixed with Tunçbilek coal and a combustion experiments was carried out in the ash furnace at 1000 °C, as described

in Section 3.1. Zeolite 4A synthesis was carried out with the obtained ashes at aging temperature of 47 °C, 12 hours aging and 4 hours crystallization at 90 ° C conditions. In the experiments carried out for this purpose, 4 different mixing ratios were used. For the 4th trial, the blend was prepared based on the calculation for the alkali fusion, with a molar ratio of 1 which means based on the validated ash content of Tunçbilek coal (15 %) and the chemical content of the SiO₂ and Al₂O₃ in the MF1000 Tunçbilek ash. The required amount of inorganic materials was added to the coal. With the help of this approach, the possibility of eliminating the fusion process was studied for energy saving. The conducted experiments were summarized on Table 3.6.

Table 3.6. Combustion Experiments with Coal-inorganic Blends

Combustion Temperature (°C)	Amount of Coal(g)	Amount of Na ₂ CO ₃ (g)	Amount of Al(OH) ₃ (g)
1000	3	0,15	-
1000	3	0,30	-
1000	3	0,30	0,24
1000	2	0,35	0,28

3.5. Analysis Techniques

Fly ash samples and zeolite 4A synthesis products obtained from experimental studies were analyzed with X Ray Fluorescence Spectroscopy (XRF), X Ray Diffraction (XRD) and Scanning Electron Microscopy (SEM). Information and analysis conditions related to the analysis methods are given in 3.5.1, 3.5.2 and 3.5.3.

3.5.1. X Ray Fluorescence (XRF)

The XRF method is a widely used analysis method to quantitatively determine the chemical content of solid samples. In this method, the sample placed in the sample holder is exposed to intense X-ray waves [85]. While some of the emitted electromagnetic wave is absorbed by the material, the rest is emitted as a secondary X-ray beam by fluorescence. The energy arising from this energy difference occurs at

different energy levels for each atom. Accordingly, the chemical content of the sample used is quantitatively determined.

The fly ash samples and the chemical content of the alkali fusion products were determined by Rigaku ZSX Primus II XRF instrument in METU Central Laboratory. Samples prepared as pellets were scanned in the boron-uranium range and the chemical composition as reported in oxide form.

3.5.2. X Ray Diffraction (XRD)

X Ray Diffraction is an analysis method that allows to determine the crystal structure and mineral content of solid materials. The X-Ray bombardment scattered at certain angles depending on its crystal structure and the placement of its atoms in crystal lattice and forms a distinct diffraction pattern. The spacing of the crystal structure is determined by Bragg's law, so that the mineral content and crystal phases of the respective sample are determined.

Fly ash, alkali fusion products and zeolite 4A samples were analyzed with Rigaku Ultima-IV XRD instrument in METU Central Laboratory. For the analysis, the mineral composition and crystal phases of the samples were determined by scanning with $0,02^\circ$ step size at a speed of $1^\circ / \text{min}$ in the range of $5-55^\circ$.

3.5.3. Scanning Electron Microscopy (SEM)

Scanning Electron Microscopy is a frequently used analysis method that allows to determine the morphology, topography and size of samples with the help of high resolution images. SEM, using a highly energised focused electron beam to scan the surface of a sample, generates a variety of signals. These are collected, amplified, and displayed on a cathode ray tube.

In this study, the fly ash samples and some of the zeolite samples were analyzed by FEI Quanta 400 F Scanning Electron Microscope at Central Laboratory at METU and TESCAN GAIA 3 Scanning Electron Microscope at HUNITEK in Hacettepe University.

CHAPTER 4

RESULTS AND DISCUSSION

The results of the experimental studies which were carried out in line with the defined objectives of the thesis are presented under five main subsections. In order to observe the effects of ash characteristics on zeolite 4A synthesis, properties of fly ash as a raw material were determined in subsections 4.1 and 4.2. Ashes obtained from different thermal power plants as well as ashes produced in the laboratory were compared in terms of morphology, chemical composition and mineral content. In subsection 4.3, the nucleation and crystallization behaviour of Class F fly ash, which is the source of silicon and aluminum for zeolite synthesis, was investigated in order to optimize the synthesis procedure. Afterwards, in Section 4.4, the effect of ash characteristics under the determined optimal conditions are investigated. In subsection 4.5 synthesis results of ashes obtained from combustion experiments carried out in order to eliminate the alkali fusion step were presented.

4.1. Effect of the Fuel Type on Fly Ash Characteristics

Primarily, the ash obtained from Seyitömer, Tunçbilek and Soma Thermal Power Plants were compared in terms of chemical composition, mineral content.

4.1.1. Chemical Composition

Particularly for zeolite synthesis, fly ash from Turkish lignites was used as a source material. It was therefore determined the content of fly ash, alumina and silica as well as the impurity content. Three different fly ash sources were chosen, all of which originated from pulverized coal combustion in power plants currently in operation.

Herein, the composition of the ash was determined using XRF, and is presented in Table 4.1.

Table 4.1. Chemical Composition of Power Plant Ashes

Fly Ash Sources	%SiO ₂	%Al ₂ O ₃	%impurity	
Seyitömer PP	47,8	19,2	%Fe ₂ O ₃	11,9
Tunçbilek PP	50,8	21,2	%Fe ₂ O ₃	8,35
Soma 5-6 PP	21,4	12,6	%CaO	43,1

As can be seen in Table 4.1, Seyitömer and Tunçbilek Thermal Power Plant ashes are of Class F in terms of chemical composition, in line with the studies previously reported in the literature . In addition, according to Vassilev's classification approach, Seyitömer is more prone to be ferrisialic, Tunçbilek ash has sialic characteristics [31]. In Soma 5-6 Thermal Power Plant Class C ash, the calcium purity is very high, and in fact this ash has a calcsialic character [31]. An impurity of 43,1% CaO was observed for fly ash from Soma 5-6 Power Plant. Moreover, 8,35% and 11,9% Fe₂O₃ impurities for Tunçbilek and Seyitömer fly ashes, respectively, were registered.

4.1.2. Mineral Content

The mineral content of the ash sources were determined by XRD analysis. The XRD patterns of power plant fly ashes were given in Figure 4.1 and 4.2.

According to XRD results, the main phases present were quartz (SiO₂) and mullite (3Al₂O₃:2SiO₂) for both Tunçbilek and Seyitömer power plant fly ash. Differences comprised lime (CaO), anhydrite (CaSO₄) melilite (Ca₂SiO₇), anorthite Ca(Al₂Si₂O₈) phases were observed for Soma 5-6 PP fly ash, in addition to quartz phases, whereas hematite (Fe₂O₃) and magnetite (Fe₃O₄) phases were observed for the remaining ashes.

Mullite intensities were highest in Tunçbilek PP fly ashes. The ash crystallinity was reported as 34 and 47% for Seyitömer and Tunçbilek PP ash, respectively. The higher crystallinity and higher mullite fraction of the Tunçbilek PP fly ash can be related to the low cooling rate or high combustion temperature in the boiler [38], [37]. In particular, mullite phase is the most stable mineral phase observed in the 1200-1600°C range [37]. For Tunçbilek PP fly ash, as a consequence of its high iron content, the hematite mineral observed can interfere with mullite in the diffraction pattern. In order to distinguish this, considering the presence of mullite peak observed at 2 θ angle 16,47, it can be said that the dominant phase is mullite. Furthermore, since Tunçbilek ash is a silicic ash, compared to Seyitömer, the mullite phase, which is an aluminosilicate phase, is observed at a higher intensity than the hematite [31]. However, in Seyitömer, in terms of relative crystallinity, the density of the quartz peak is quite low. Depending on this situation, it can be said that the primary quartz phase, which is a source of silica, might be converted to glassy aluminosilicate and ferrisilicate compounds, especially around 1200-1600 °C. Higher content of iron decrease the melting temperature of fly ash so, in Seyitömer fly ash yields lower crystallinity [28].

4.2. Effect of Combustion Parameters on Fly Ash Characteristics

Three different lab-scale setups are used herein to assess the effect of the combustion parameters on the characteristics of fly ash. Namely, Muffle Furnace, Drop Tube Furnace and Wire Mesh Reactor. These reactors are used to obtain ash from a single fuel (Tunçbilek lignite) which is further characterized using XRD. Moreover, these ashes generated in laboratory are compared with the fly ash from Tunçbilek PP. The samples are named by the abbreviation of the reactor name and the combustion temperature (e.g. MF1000 stands for Muffle Furnace ash obtained at 1000 °C).

The chemical composition of MF1000, DTF1000 and Tunçbilek PP ashes were determined using XRF and are presented in Table 4.2. Loss on ignition (LOI) values were 4, 1, and 2,4%, respectively. Due to high residence time in Muffle Furnace, the

unburned carbon content was expected the lowest level. In case of Power Plant conditions, the higher level of combustion temperature than Drop Tube Furnace(1000°C) provided lower unburned carbon content for Tunçbilek PP ashes.

Table 4.2. Main Components of Tunçbilek Fly Ashes

Fly Ash Sources	%SiO ₂	%Al ₂ O ₃	Impurity%
DTF1000	48,9	20,6	8,9(Fe ₂ O ₃)
MF1000	54,8	22,9	9,22 (Fe ₂ O ₃)
Tunçbilek PP	50,8	21,2	8,35 (Fe ₂ O ₃)

4.2.1. Effect of Combustion Temperature

Ash samples were obtained at three distinct temperatures (800, 900, and 1000 ° C) from all three setups and analyzed using XRD. The results are shown in Figures 4.3 for MF, in Figure and 4.4 for the WMR, and in Figure 4.5 for the DTF. According to the results, the main phases determined in the nine ash samples in the specified temperature range were quartz, mullite, hematite, and magnetite.

The hematite and mullite are the secondary mineral phases which starts to form from 800 °C, and tends to increase up to 1200 °C [37]. Tunçbilek ash has Class F characteristics, but it also contains a very high percentage of iron. In addition, in terms of hematite and mullite mineral diffraction pattern (Appendix Table B.1), it has very close peaks at 33°, 35°, 39°, 41°, 54° angles [86]. Therefore, it can be said that it interferes with the diffraction pattern in relation to the high iron content. However, it is evident that the aluminosilicate phases should be observed as amorphous because of the higher aluminum content [38].

In order to explain the relationship between combustion temperature and mineral transformations, MF ashes are a suitable reference point. In Figure 4.3, XRD patterns of MF ashes were given and the arrows were used to show the changing of the peak intensity. In line with the study of Vassilev (2006), in the range 800-1000 °C, the decomposition of kaolinite resulted in the increase of mullite [37]. It should be noted that the formation of mullite reaches its highest rate with the melting of quartz between

1200-1600 °C, beyond the temperatures used herein. The hematite phase also increased with increasing temperature, and the corundum (Al₂O₃) phase observed 800 °C almost disappeared when the temperature was raised to 1000 °C (see Figure 4.3) [14], [44]. The other source for silica and alumina from the coal was muscovite ((KF)₂(Al₂O₃)₃(SiO₂).6(H₂O)) and it was also disappeared after 800°C.

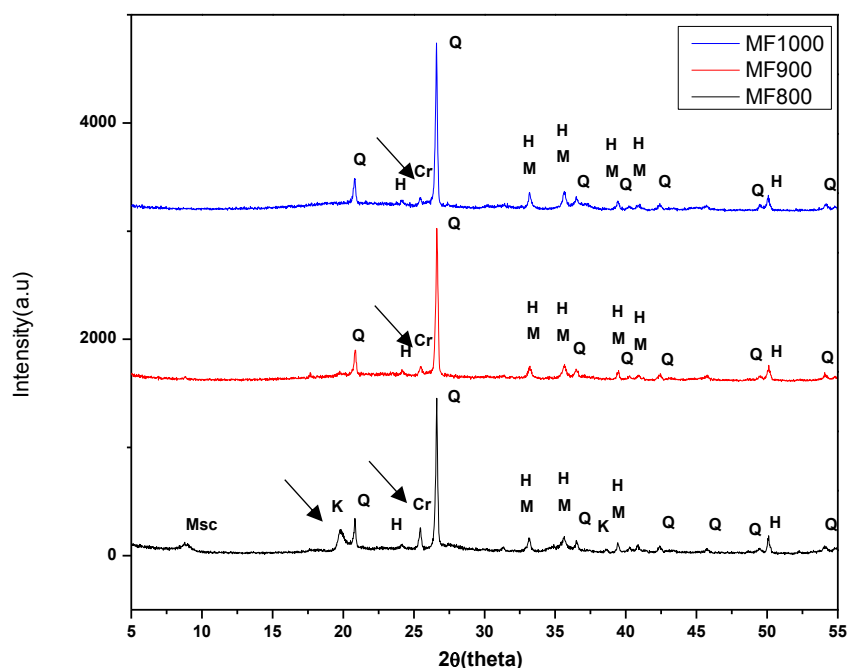


Figure 4.3. XRD patterns of Tunçbilek Fly Ashes at 800, 900 and 1000 °C from MF experiments Q: Quartz; M; Mullite; K: Kaolinite; H: Hematite, Cr: Corundum, Msc: Muscovite

Figure 4.4 represented the XRD patterns of WMR ashes. In WMR ashes, a trend similar to MF ashes was observed in terms of kaolinite and corundum minerals in the studied temperature range. However, there was no trend parallel to the increase in temperature in the ash crystallinity and mullite and hematite phases. As shown in Table 4.3, total hematite mullite mineral content increased from 800 °C to 900 °C, but decreased from 900 °C to 1000 °C. Based on this result, it can be considered that other combustion parameters (cooling rate) might have an effect especially on the mullite and hematite mineral composition. Compared to other reactor ashes, magnetite phase was observed in WMR ashes. Magnetite mineral occurs during combustion as

a result of reduction of hematite mineral [37]. This has been reported to occur due to diffusion limits, particularly at high flame temperatures [37]. Although experiments have been conducted at lower combustion temperatures than thermal power plant conditions, it is known that the reactor has diffusion limitation during combustion due to its design. Therefore, it can be said that the magnetite phase which was not observed in the ashes obtained from other reactors was observed for this reason.

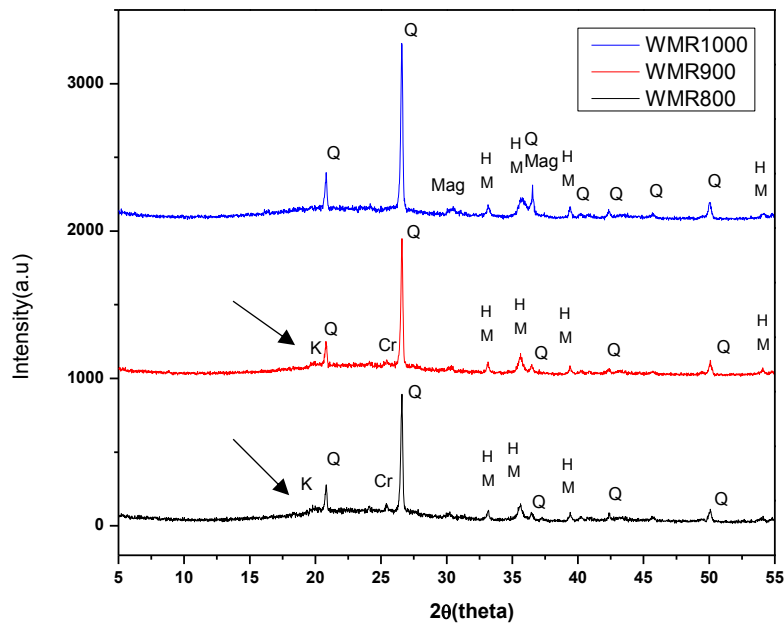


Figure 4.4. XRD patterns of Tunçbilek Fly Ashes at at 800, 900 and 1000 °C from Wire Mesh Reactor combustion experiments, Q: Quartz; M; Mullite; K: Kaolinite; H: Hematite, Mag: Magnetite, Cr: Corundum

In the following Figure 4.5, XRD patterns of DTF ashes were given. In terms of DTF ashes, the peak intensity of the kaolinite phase decreases with increasing temperature from 800 to 1000 ° C. As a result of this, the mullite phase, which is the secondary aluminosilicate phase, becomes apparent as a result of the decomposition of a clay mineral of kaolinite [37]. The corundum (Al_2O_3) phase, which can be observed in the 800-1000 ° C range, almost disappears at 1000 ° C [37]

Although there was no significant difference in ash crystallinity between DTF800, DTF900 and DTF1000 samples, the proportion of secondary phases such as mullite and hematite increased with the rise in temperature.

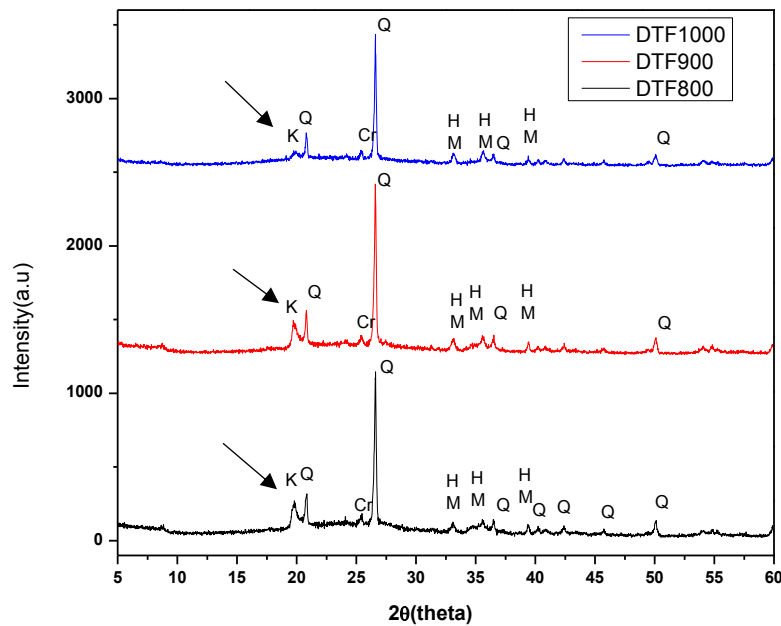


Figure 4.5. XRD Patterns of Tunçbilek Fly Ashes at 800, 900 and 1000 °C from DTF experiments
 Q: Quartz; M; Mullite; K: Kaolinite; H: Hematite, Cr: Corundum

Along with all these findings, it is observed that there are different tendencies in terms of mineral transformation in the ash obtained from combustion experiments carried out at the same temperature and for the same fuel. In this context, the effect of factors such as heating rate and cooling rate should be considered.

4.2.2. Effect of Heating Rate

In the previous section, samples of ash obtained from the reactors are considered for the respective experimental setup only in terms of combustion temperature. As mentioned in Section 2.3, one of the other factors that strongly affects mineral transformations is the heating rate [47]. Accordingly, the results from MF (low heating

rate, $< 1 \text{ C s}^{-1}$), WMR (high heating rate, $\sim 10^3 \text{ }^\circ\text{C s}^{-1}$), and DTF (very high heating rate, $\sim 10^4 \text{ }^\circ\text{C s}^{-1}$) are discussed herein. In Table 4.3, ash crystallinity and mineral ratios are given for all of the three reactors and also for the other Class F fly ashes that obtained from Tunçbilek Power Plant and Seyitömer Power Plant.

The most significant difference is the change in peak intensity of the kaolinite phase with respect to heating rate. Kaolinite phase was observed up to $1000 \text{ }^\circ\text{C}$ due to the high heating rate and very short residence time in the drop tube furnace. In MF and DTF ashes an upward trend was observed in mullite and hematite phases in parallel with temperature rise [44]. Within all three temperature values, the ash crystallinity was decreased by increasing heating rate. Within this temperature range, it can be said that the crystallization of aluminosilicate minerals has not yet been completed, and this is particularly noticeable for the DTF due to its very high heating rates [14],[47]. Experimental setups differ in both the heating rate and the cooling rate, so it can be said that the ash furnace samples with the lowest cooling rate have the highest crystallinity. In the previous figures, the XRD patterns were given on the same graph, so the changing in the mineral content might not observed clearly. Due to this, the mineral content and ash crystallinity of Class F ashes in this study was represented in Table 4.3.

Table 4.3. Mineral Content and Crystallinity of Class F Fly Ashes in this study

Reactor	Combustion Temperature	ash crystallinity, %	hematite+mullite, %	quartz, %
MF($10^\circ\text{C}/\text{min}$)	800	40	11	22
	900	41	12	26
	1000	43	14.2	26
WMR($10^3 \text{ }^\circ\text{C}/\text{s}$)	800	28	8	16
	900	37	12	19
	1000	35	8,75	22
DTF($10^4 \text{ }^\circ\text{C}/\text{s}$)	800	30	6	17
	900	33	8	19
	1000	31	8	19
Tunçbilek PP	1400-1600	48	18	24,8
Seyitömer PP	1400-1600	34	10,3	14

4.2.3. Effect of Cooling Rate

In addition to the heating rate, another determining factor for ash crystallinity is the cooling rate. Since the three reactors have different heating rates, a different set of experiments was applied to one of the setups, the WMR, to observe the change in ash crystallinity depending on the cooling rate [38]. From the three reactors, the WMR was chosen due to its ability to easily control the cooling rate. It should be noted that at 1200 °C, especially with the melting of quartz, mullite formation is observed by melt crystallization and mullite phase is the most stable phase [37]. For this reason the present trials were done at 1200 °C. The effect of cooling rate on mullite crystallinity and ash crystallinity was presented in Figure 4.6. As described in methods part, the cooling rate was provided by nitrogen flow but not recorded as °C/s, because the main aim was just to observe the changing of mullite content. The crystallinity, mineral phase distributions of the ashes obtained are given in Table 4.4. As expected, a decrease in ash crystallinity and in particular mullite and hematite phases was observed in parallel with the increase of cooling rate. In contrast, samples obtained at 1200 °C have a higher crystallinity compared to ashes at 800-1000 °C in WMR.

Table 4.4. Effect of Cooling Rate on mineral composition and crystallinity of WMR Ashes at 1200°C

Reactor	N2 Quench(L/min)	ash crystallinity, %	hematite+mullite, %	quartz, %
WMR	-	43	15	21,9
	4	39	11,8	24,1
	8	38	10,7	23,8

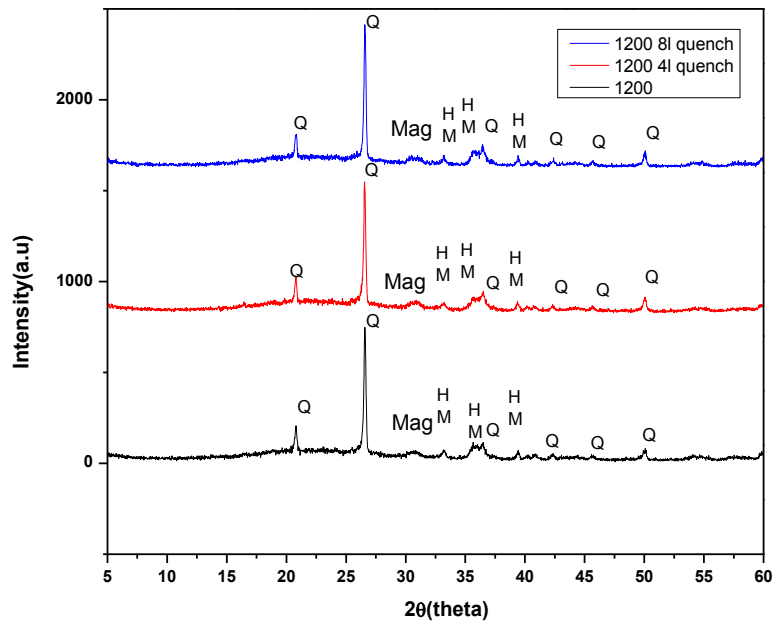


Figure 4.6. XRD Patterns of effect of cooling rate on Tunçbilek Ash from WMR combustion experiments at 1200 ° C, Q: Quartz; M; Mullite; , H: Hematite, Mag: Magnetite

Combining all these findings, it can be said that the mullite phase has a predominant effect on ash crystallinity. Similarly, the ash crystallinity of the Thermal Power Plant ashes resulting from higher heating rate and higher temperature combustion is higher than the DTF1000 ash sample, and the most significant difference when comparing the two ashes is the mullite mineral ratio. The same applies to the MF1000 and DTF1000 ashes and WMR1200 ashes [26].

4.3. Optimization of Zeolite 4A synthesis

The optimum synthesis conditions for zeolite 4A synthesis with alkali fusion step were determined using Class F fly ash (Seyitömer PP). Specifically, the influence of parameters such as the Si / Al mol ratio, the crystallization time and temperature, the aging time and temperature, and the alkalinity(Na_2CO_3 /fly ash ratio by mass) were investigated. The occurrence of zeolite formation depends on many parameters as described in Section 2.6. While conducting synthesis experiments, the effect of a

single parameter could be observed by selecting the result obtained from the previous trial as the control experiment. The abbreviation of S with number referred to Table 3.5(i.e S6) and this abbreviation was used in the XRD patterns for the respected samples.

The SEM images of Zeolite 4A was given in Figure 4.7. The validation of the presence of Zeolite 4A was done by detecting cubic morphology of Zeolite 4A, which is seen in Figure 4.7. The XRD pattern of commercial Zeolite 4A was also represented in Figure 4.8. The XRD pattern of commercial Zeolite 4A was taken as reference sample in respect of crystallinity by %100 and the crystallinity of fly ash synthesized zeolite 4A were calculated as a relative crystallinity by applying Equation 3.1.

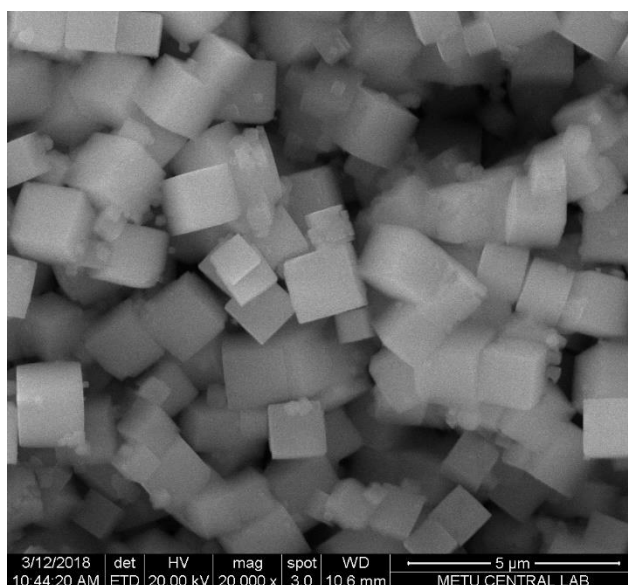


Figure 4.7. SEM Images of synthesized Zeolite 4A with sodium aluminate and sodium silicate in Nanodev Research Lab

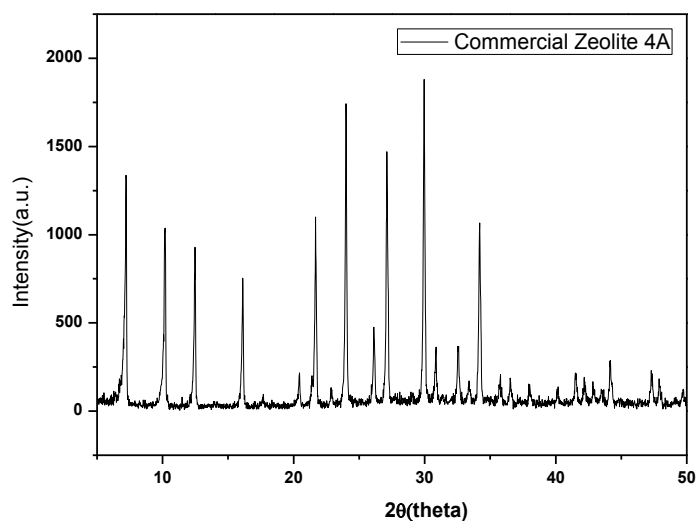


Figure 4.8. XRD pattern of commercial Zeolite 4A

4.3.1. Optimization of Si/Al ratio

In order to achieve the synthesis of Zeolite 4A from fly ashes, the optimal Si / Al molar ratio must be determined first. In the literature, the optimal Si / Al molar ratio for Zeolite A has been reported as 1-1,5 [84]. Accordingly, 4 different gels were prepared with 4% error in the range of 1-1,5 based on the sample calculation shown in Section 3.3. The results of XRF analysis of the fusion products obtained are shown in Table 4.5.

Table 4.5. Chemical Composition of Fusion Product with different Si/Al mixing ratio

Si/Al(mass)for Fusion Mixture	%SiO ₂	%Al ₂ O ₃	%Na ₂ O	Si/Al (mol basis)
0,6	27,30	15,20	34,30	1,52
0,72	27,30	17,10	32,10	1,35
0,82	26,80	19,50	30,70	1,17
0,99	26,80	21,20	30,70	1,04

As a starting point, the synthesis time and crystallization temperature were selected as 16 h aging and 7 h crystallization at 100 °C, based on the study of Izidoro(2013) except for the aging temperature [21]. As shown in Table 4.1, because of the high iron content of Seyitömer ash, aging was performed at 47 ° C, which is the optimal temperature for zeolite 4A instead of the room temperature condition reported in the literature [87]. The results of XRD analysis of synthesized products are given in Figure 4.9.

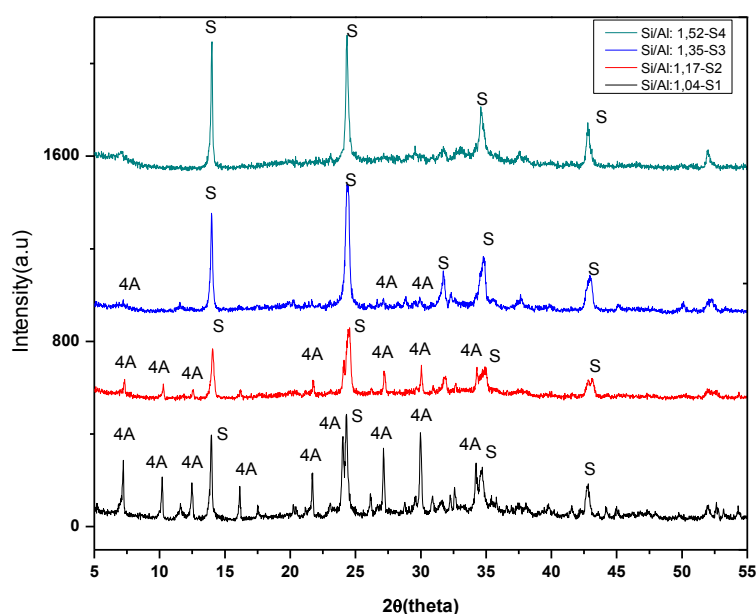


Figure 4.9. XRD patterns of zeolite 4A synthesized with different Si / Al ratios using Seyitömer Fly ash aged during 16 h at 47 ° C and crystallized during 7 h at 100 ° C, S: sodalite, 4A: zeolite 4A

As expected, the zeolite crystallinity increased as the Si / Al molar ratio of the fusion product decreased [67], [19] ,[66]. Studies in the literature have found that Al is the critical element especially for the formation of zeolite from fly ashes. In fact, it has been observed that the formation of zeolite also ceased when Al was consumed in the solution [17], [77].

Herein, the highest crystallinity of Zeolite 4A was achieved with the fusion product with a 1,04 Si/Al mol ratio, but the SEM analysis (See Figure 4.10) shows that morphology of the respected sample didn't have the chamfered edge and cubic

structure of the Zeolite 4A which were shown in Figure 4.7. Moreover, the filament like morphology is a evidence of the presence of sodalite.

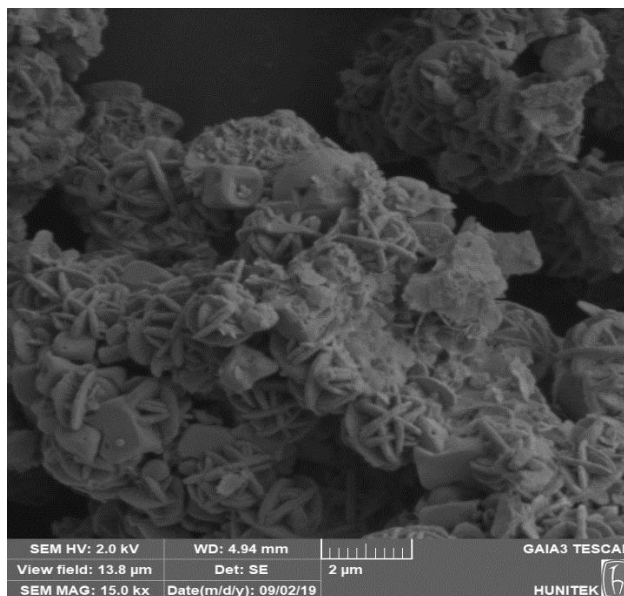


Figure 4.10. SEM Analysis of Zeolite 4A obtained from the gel with Si/Al mol ratio 1,04

It is practically preferable to use as few laboratory chemicals as possible. Although, it has lower zeolite 4A crystallinity, a gel with a molar ratio of 1,17 was used to observe the effects of other parameters. Relatively, the gel with 1,35 Si / Al mol ratio has the closest Si/Al mol ratio to the respected gel, so it was selected to check sensitivitiy of the respected parameters on the fusion product at the same synthesis condition.

4.3.2. Optimization of Crystallization Temperature

The effect of the crystallization temperature was investigated based on the synthesis conditions mentioned in Section 4.3.1. For the fusion product having Si / Al mol ratios of 1,17 and 1,35, the crystallization temperature was altered and the XRD results of the obtained samples are given comparatively in Figure 4.11 and Figure 4.12.

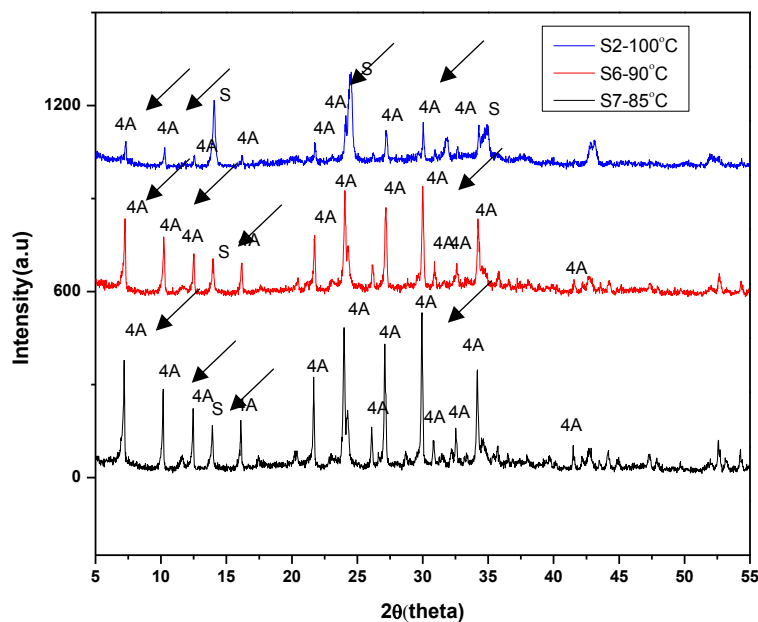


Figure 4.11. XRD pattern of zeolite 4A synthesized with different crystallization temperatures (85, 90, and 100 °C) for 7 h , and 16 h aging at 47 °C for a gel with Si/Al ratio of 1,17 S: sodalite, 4A: zeolite 4A

The results showed that the sodalite phase impurity was substantially lost as the crystallization temperature was reduced to 90 °C and 85 °C. It is known that the sodalite phase is a thermodynamically more stable than the zeolite 4A, thereby reducing the temperature to enable the less stable zeolite 4A phase to be obtained [19], [13], [82], [66], [22]. Although they used two different alkali agents, namely sodium hydroxide and sodium carbonate, Guozhi et al. (2019) and Liyun Yang et al. (2017) observed that the resulting zeolite phase transformed to a more thermodynamically stable phase at 100°C. This is theoretically explained by the Ostwald rule [13], [22], [66].

Zeolite 4A has a high crystal growth rate and is a metastable crystal structure [13], [66]. Correspondingly, the synthesis process of zeolite 4A is highly sensitive to parameters affecting the thermodynamic behavior of the system, such as temperature. In order to observe this effect, synthesis experiments were carried out at 90°C crystallization temperature for two fusion products having the closest mixing ratio by

mass (0,7 for 1,17 mol ratio, 0,8 for 1,35 mol ratio). The XRD results of the synthesis products are shown in Figure 4.12 and Figure 4.13.

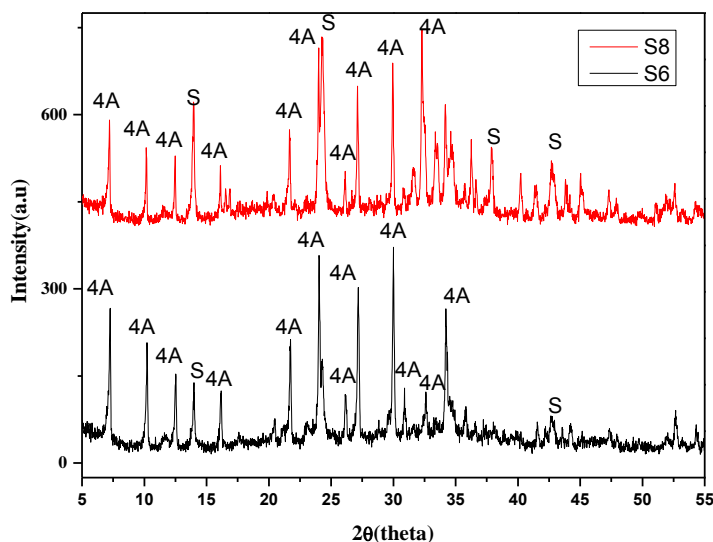


Figure 4.12. XRD pattern of zeolite 4A synthesized with different Si/Al mol ratio of 1,17(S6) and 1,35(S8) for 16 h aging at 47 °C and 7 h crystallization at 90°C , S: sodalite, 4A: zeolite 4A

As seen in Section 4.3.1, the sodalite phase increased as the Si / Al ratio increased. However, even with the fusion product having a higher Si / Al molar ratio, the peak intensity of Zeolite 4A increased significantly with the reduction of the crystallization temperature.

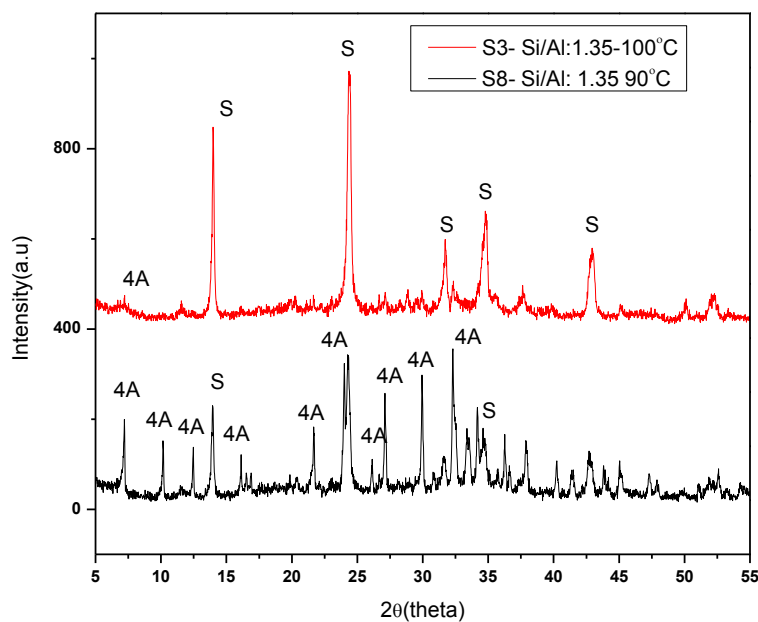


Figure 4.13. XRD pattern of zeolite 4A Synthesized with different crystallization temperatures (90 and 100 °C) for 7 h , and 16 h aging at 47 °C for a gel with Si/Al mol ratio of 1,35, S: sodalite, 4A: zeolite 4A

The SEM images of the Sample 6 and Sample 8 (See Table 3.5) were presented below in Figure 4.14. According to the respected images, the cubic structure of Zeolite 4A was observed in 4.14(b) which has the Si/Al mol ratio of 1,17. In Figure 4.14(a) it was observed similar morphology with the Figure 4.10, but as a difference, the rectangular elongated shape was detected and it could be the reason for the phase impurities around the range of 2θ angle of 34° in XRD pattern of Sample 8.

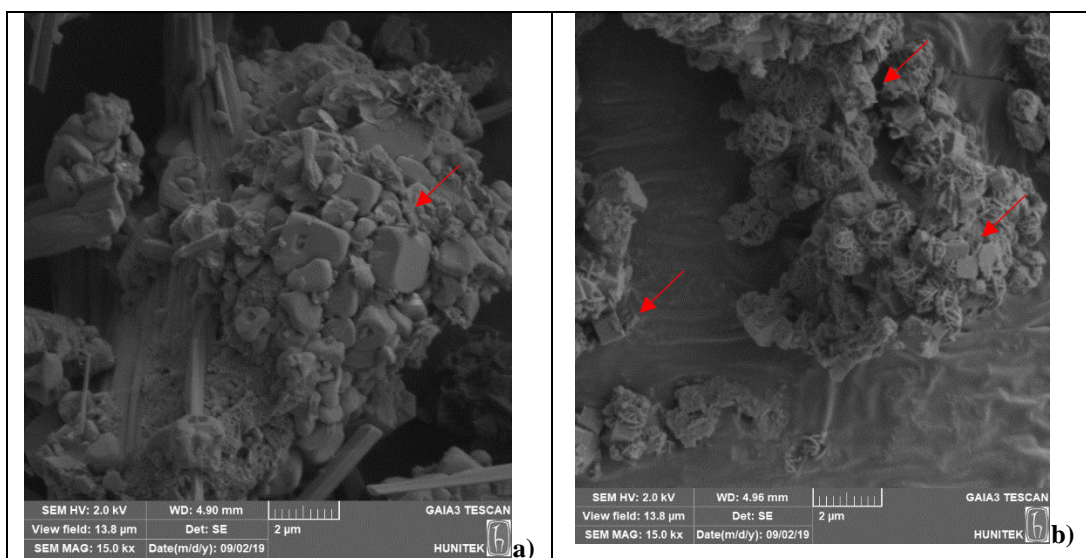


Figure 4.14. SEM Analysis of Zeolite 4A obtained from the gel with Si/Al mol ratio a) 1,35 and b) 1,17 for crystallization at 90°C

4.3.3. Optimization of the Aging Temperature

As mentioned in subsections 2.6 and 3.6.1, the nucleation behavior of the fusion product directly affects properties such as the phase impurity and the crystal size of the zeolite product [13]. In this context, the aging temperature is an effective parameter to observe nucleation behavior. In this subsection, starting with the synthesis conditions applied in the previous section, synthesis experiments were carried out at 3 different aging temperatures, 25, 37, and 47 °C, and the XRD patterns were represented in Figure 4.15.

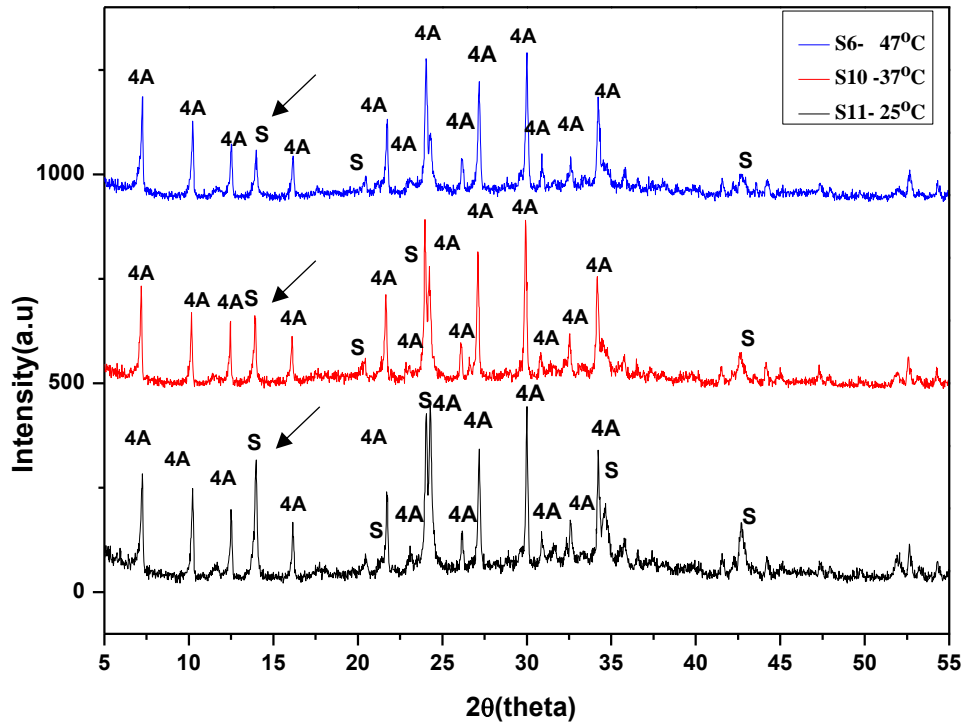


Figure 4.15. XRD pattern of Zeolite 4A synthesized with different aging temperatures (25, 37, and 47 °C), crystallized at 90 °C during 16 h for Si/Al: 1,17 S: sodalite, 4A: zeolite 4A

In contrast to the crystallization temperature, the rate of nucleation in zeolite formation is inversely proportional to temperature [68]. However, the high iron content prevents nucleation since it competes with alumina content in the aqueous solution medium [9]. For this reason, the nucleation rate was controlled by performing aging at more elevated temperatures (37 and 47 °C), along with 25 °C, since this is the temperature used in almost every study in the literature [17],[21],[66],[82].

It was observed that as the aging temperature increased, the amount of sodalite, a phase impurity for zeolite 4A, decreased significantly. Furthermore, it can be stated that thermodynamic hysteresis occurs in the system due to the increase in the difference between the aging and crystallization temperatures, and accordingly the system tends to form the more stable sodalite phase or the high level of iron oxide content [13],[66],[82]. To be specific, it has been detected that for the fusion product

obtained from Seyitomer ash, it is critical to determine the appropriate temperature to control the nucleation rate, even if it is inversely proportional to temperature.

4.3.4. Optimization of the Alkalinity

For the synthesis of Zeolite 4A containing alkali fusion step, NaOH was used in many studies in the literature. In addition, even in studies employing sodium carbonate for the fusion step, the alkaline solution in the aging step is frequently encountered [76]. In particular for the synthesis of zeolite 4A, the level of alkalinity is crucial point. However, in the reported studies, the use of high amount of alkali agents and high amounts of distilled water is noteworthy. It can also be asserted that a high level of alkalinity can be achieved by exerting reduced amounts of water. In this study, the pH of the aging step was roughly controlled by the sodium carbonate / fly ash mass ratio and a quite low water / gel mass ratio of 1,6. A comparison of the synthesis experiments obtained with the alkali mass ratio of 1.35 with reference to the synthesis conditions of Sample 6 is given in Figure 4.16.

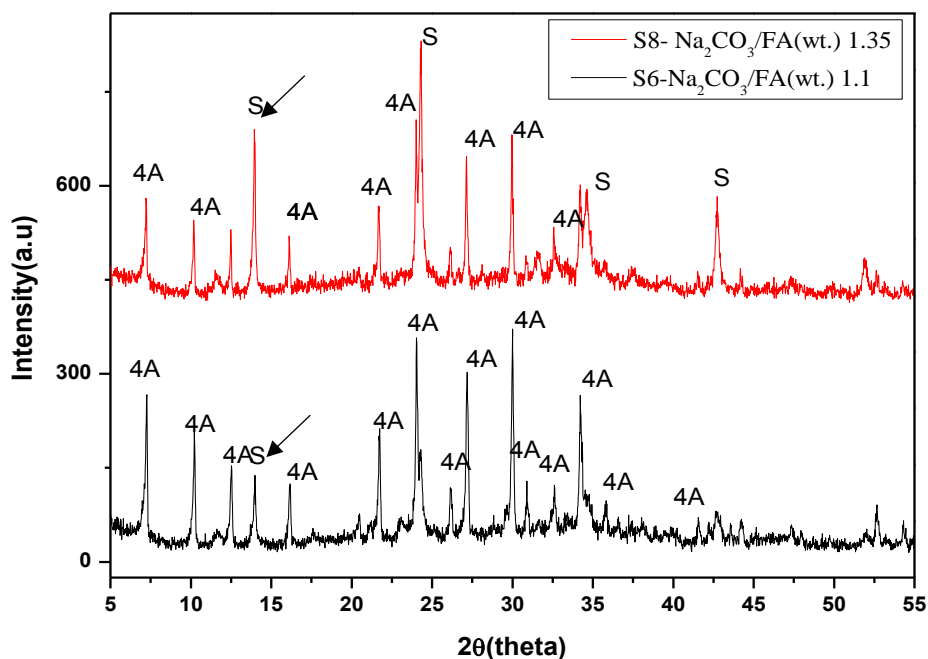


Figure 4.16. XRD pattern of Zeolite 4A synthesized with different alkalinity ratios (1,35 and 1,10), aged at 47 °C during 16 h, crystallized at 90 °C during 7 h for mol ratio of Si/Al, 1.17, S: sodalite, 4A: zeolite 4A

In terms of experimental conditions, the alkalinity value selected as the starting point (1,1 by mass) was found to be more suitable for phase purity. Although sodium carbonate does not have a basic effect as sodium hydroxide, it has a beneficial effect on nucleation and crystallization as it provides more cation release into the solution medium. The presence of high alkalinity increases the rate of nucleation, but in relation to this situation, following Ostwald Rule dictates the formation of vaster amounts of sodalite in the end product [13].

4.3.5. Optimization of Crystallization Time and Aging Time

Crystallization time

Apart from the effects of chemical composition including Si / Al mol ratio and alkalinity, and especially parameters affecting kinetics, i.e temperature, another critical parameter for zeolite formation is the crystallization time. In comparison with the studies in the literature, the crystallization time proposed by Izidoro (2013) [21] in

her study can be considered as short. For this study, the fusion product obtained from Seyitömer ash displayed a contrary tendency in terms of temperature values, although the suggested synthesis time was fit incredibly practical in terms of applicability in synthesis time. Soe et al. (2016) suggested the crystallization time of 4 h at 100 °C [76]. Based on this information, the crystallization time herein was reduced to 4 h. XRD patterns of synthesis products obtained for 4 and 7 h are presented in Figure 4.17.

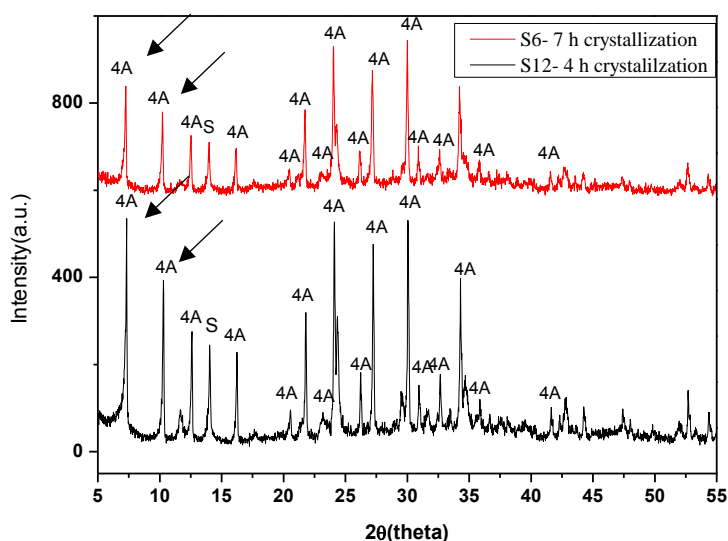


Figure 4.17. XRD Pattern of Zeolite 4A Synthesized with different crystallization times (4 and 7 h), aged at 47 °C during 16 h, crystallized at 90 °C, for Si/Al of 1.17 S: sodalite, 4A: zeolite 4A

The crystallization rate of zeolite 4A is known to be relatively high. Although vastly different crystallization times have been reported in various studies , the general consideration from the studies is that the zeolite 4A phase is converted to sodalite if the crystallization time is extended [20] , [22], [66], [82]. It was also observed that, the intensity of zeolite 4A peaks increased significantly. It can be said that the ideal crystallization time for fusion product obtained from Seyitömer ash is 4 h.

Aging time

In particular, in subsections 4.3.3 and 4.3.4, conditions for reducing the nucleation rate have been found to be more favorable to reduce phase impurity. However, to determine the optimal aging time, synthesis studies were carried out at 4, 8 and 12 h and compared with the case of 16 h aging. XRD results of aging time optimization were given in Figure 4.18.

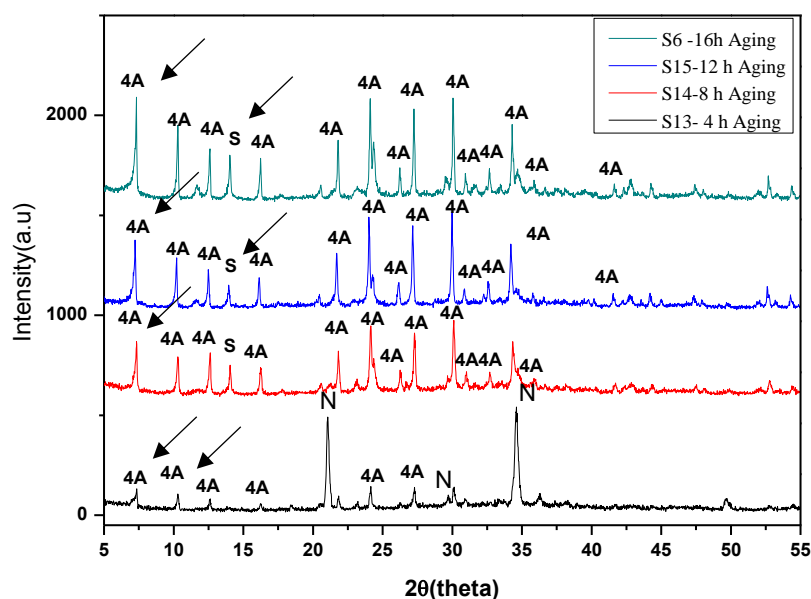


Figure 4.18. XRD Pattern of Zeolite 4A Synthesized with different aging times(4,8,12 and 16 h) aged at 47 °C , crystallized at 90 °C for 4 h, for Si/Al of 1.17 S: sodalite, 4A: zeolite 4A, N: Nepheline

According to Figure 4.16, minimal sodalite impurity was achieved in 12 h aging. In the literature, nucleation induction period parameter is defined for ideal nucleation time [13]. Herein, nepheline, an undissolved sodium aluminosilicate mineral, was detected in the synthesis product obtained with an aging time of 4 h. In addition, although sodalite impurity is not observed, the intensity of the zeolite A peaks is considerably low. Based on these findings, it is clear that 4 hours is insufficient for t_n and t_g duration. Moreover, even though the zeolite crystallinity increases during the 16 h aging period, it contains a intenser amount of sodalite impurity as compared with the 12 h period and is thus undesirable.

Finally, to determine the ideal combination of aging and crystallization time, a synthesis experiment was carried out in comparison to Sample 15 under conditions of 12 hours aging and 7 hours crystallization. XRD results of time optimization were given in Figure 4.19.

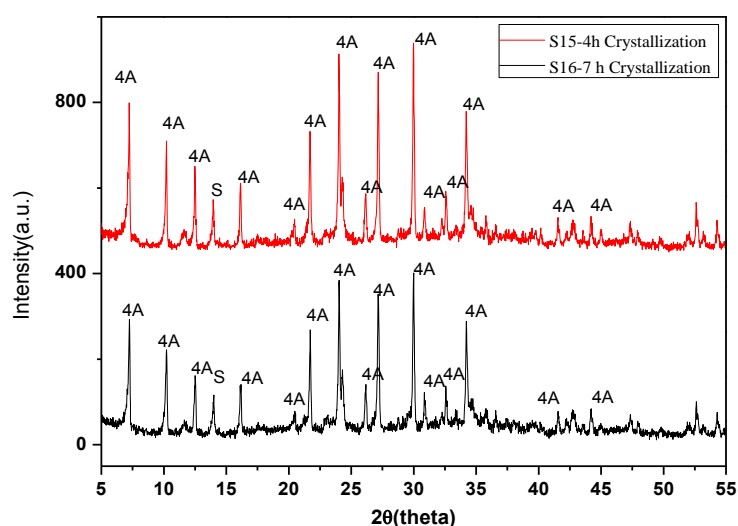


Figure 4.19. XRD pattern of Zeolite 4A synthesis of Seyitömer Fly Ashes at 90°C crystallization , for 47°C aging for 12 h for 4h and 7 h crystallization S: sodalite, 4A: zeolite 4A

The result showed the crystallization time had no significant effect under 12 hour aging conditions. Thus, in the light of the data obtained, it was observed that the ideal aging conditions were 12 hours and 47 °C to avoid thermodynamic hysteresis. In terms of time optimization, total synthesis time was determined as 16 hours with 12 h aging and 4 h crystallization which was achieved with Sample 15 for 47 °C aging and 90° C crystallization.

4.4. Zeolite 4A Synthesis for Different Fly Ashes with the Optimized Parameters

In subsections 4.1 and 4.2, fly ash properties were discussed in detail, as a function of the type of coal and combustion conditions. In Section 4.3, the nucleation and crystallization behavior of the fusion product obtained from fly ash, was discussed with the help of an expanded experimental matrix and optimal synthesis conditions were determined. In this subsection, by combining these findings, the effect of ash

properties on the end product was investigated. The synthesis conditions applied are the optimal conditions defined in subsection 4.3.

4.4.1. Effect of Chemical Composition on the Zeolite 4A

In this study, except the alkali fusion, the obtained fly ash was used without any pretreatment. Under the optimal conditions determined in Section 4.2, the effects of the level of impurity contained in the ash on the Zeolite 4A product were examined. Emphasis was given to understanding the effects on nucleation and crystallization. As seen in Table 4.6, the formulization of the mixing ratio was validated with different fly ash sources by maximum %6,8 deviation which was observed on Soma fusion product.

Table 4.6. Chemical Composition of Fusion Product from different fly ash sources with mixing ratio of Si/Al:0,72

Fly Ash Source For Fusion	%SiO ₂	%Al ₂ O ₃	%Na ₂ O	% impurity	Si/Al (mol basis)
Soma 5-6	17,70	12,00	15,30	37,3(CaO)	1,25
Seyitömer	27,6	20	31,1	6,22(Fe ₂ O ₃)	1,17
Tunçbilek	27,90	19,80	33,60	4,48(Fe ₂ O ₃)	1,20

Comparison of iron and calcium impurities:

Firstly, the synthesized zeolite (Sample 6) using high iron ash (Seyitömer) was compared with that of high calcium ash (Soma). Results of XRD patterns are presented in Figure 4.20.

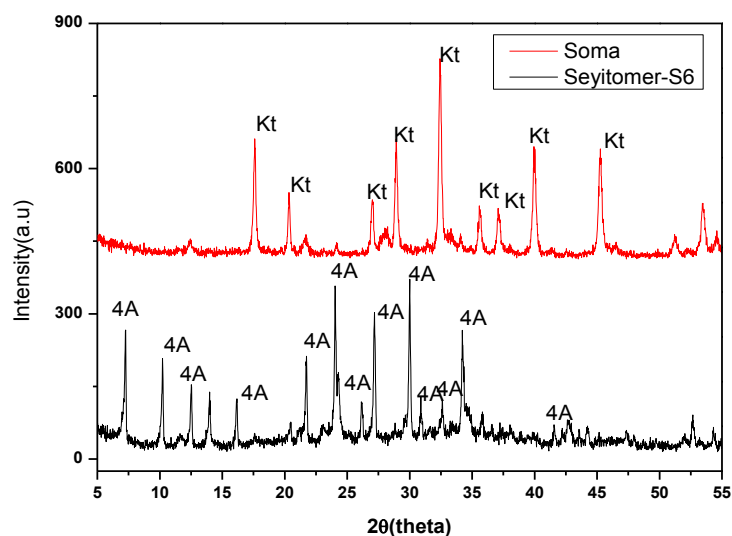


Figure 4.20. XRD Pattern of Zeolite 4A Synthesis of Seyitömer and Soma Fly Ashes at 90°C crystallization , for 47 °C aging for 16 h and 7 h crystallization, Kt: Katoite ($\text{Ca}_3\text{Al}_2(\text{SiO}_4)_{1.5}(\text{OH})_6$, 4A: Zeolite 4A

According to the results, it can be said that iron behaves inertly in the synthesis steps as compared to calcium [88]. However, since calcium is an alkali element such as sodium, calcium solid state reactions are in competition with those involving sodium, and differences in the resulting mineral phases were observed. Furthermore, in terms of zeolite synthesis, it has an inhibitory effect in the crystallization step, and consequently it has been found that even though the Si / Al mol ratio and the alkalinity values of sodium were similar in the fusion product, the phase product is dominated by a calciumaluminum silicate hydrate mineral, katoite [88].

Effect of iron impurity level

Possible effects of iron impurity on zeolite synthesis were analyzed by comparison of Seyitömer and Tunçbilek fly ashes, since these fly ashes present different iron content. In Figure 4.21 was presented the XRD analysis of fusion products of those ashes with same Si/Al mixing ratio.

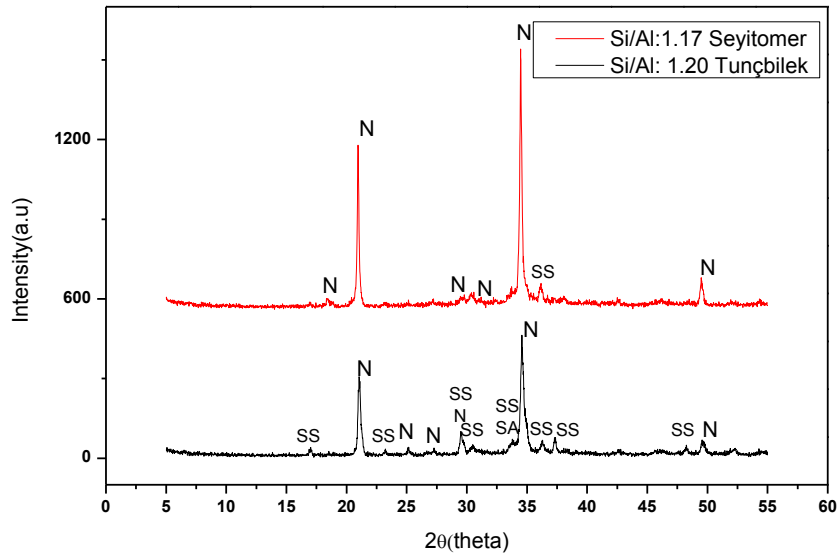


Figure 4.21. XRD Pattern of Alkali Fusion of Tunçbilek PP, Seyitömer PP ashes for same Si/Al mass ratio (0,72), N: nepheline (NaAlSiO_4), SS: Sodium disilicate (NaSi_2O_5), SA: sodium aluminate(NaAlO_2)

A grander proportion of sodium aluminosilicate (nepheline) phase was obtained in the fusion product of the Seyitömer fly ash as compared to Tunçbilek fly ash. This could be related with the higher content of glassy aluminosilicate ($3\text{Al}_2\text{O}_3:2\text{SiO}_2$). In fact, it has been affirmed that the high glassy phase ratio, i.e. the excessive number of defects, facilitates the interaction with sodium carbonate with aluminum hydroxide and liberated aluminum from the coarser crystalline mullite [18].

Tunçbilek fly ash presents a higher proportion of mullite as compared to Seyitömer fly ash. Herein, alkali fusion was done at 900°C , and at this temperature mullite might remain stable [18]. Consequently, even though sodium silicate is formed at around 850°C , its conversion to the sodium aluminosilicate phase is achieved with a lower yield. In addition, it should be noted that differences in iron content may affect the minerals and percentage of crystallinity that will occur during the fusion reaction.

As discussed above, significant differences were observed in the fusion product depending on the mineral composition and crystallinity of the ash. As a result, these minerals (sodium aluminate, sodium silicate, and sodium aluminosilicate) with

different water solubility are likely to affect the nucleation behavior [13]. Further discussion on the effect of iron impurity on the synthesis will be given at the end of the following subsection.

4.4.2. Effect of Combustion Parameters on Zeolite 4A

Another important factor for the fusion product, except for its chemical composition, is the combustion conditions under which ash formation takes place. To observe the relative effect of combustion parameters on the fusion product were examined by comparison of mineral distribution of Tunçbilek Power Plant ashes and laboratory ashes of MF1000 and DTF1000 and in Figure 4.22 was represented the XRD results of fusion products of respected ashes.

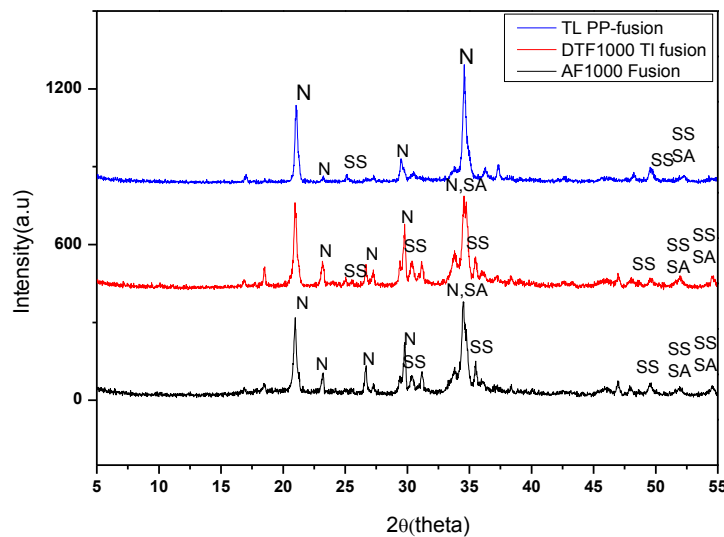


Figure 4.22. XRD Pattern of Alkali Fusion of Tunçbilek PP, DTF1000 and MF1000 ashes for same Si/Al mass ratio (0,72), N: nepheline ($\text{NaAlSi}_3\text{O}_8$), SS: Sodium disilicate ($\text{Na}_2\text{Si}_2\text{O}_7$), SA: sodium aluminate(NaAlO_2)

For thermal power plants and lab ashes of Tunçbilek lignite, it can be said that, regardless of the heating rate, the preponderant factor is the combustion temperature. Laboratory ashes were obtained at 1000 °C. Therefore, considering that the aluminum oxide content and especially silica content in ash is largely free and does not convert to mullite, the sodium aluminosilicate, sodium silicate, and sodium aluminate were

formed [18]. It was concluded that the lower temperature (1000 °C) enables the co-existence of these three phases. Furthermore, even though the temperature has a strong effect on the ash crystallinity, a correlation between the crystallinity of the fusion product and the ash crystallinity could not be found.

It was found that the ash characteristic caused significant differences on the crystallinity and mineral composition of the fusion product obtained. In the next step, zeolite 4A synthesis experiments were conducted with Tunçbilek ashes under optimal conditions to compare with synthesis product of Sample 15 (Zeolite 4A at optimal condition See Table 3.5.)

In general, the XRD pattern is similar for the zeolites generated from all ashes (see Figure 4.23). Herein it was assumed that hematite and mullite phases concurrently affect nucleation and crystallization, since there was no inference as to which one is the most dominant. Accordingly, the influence of the combustion parameters will be analyzed always taking both hematite and mullite into account. In addition, the sodalite phase was used to identify the effect of the combustion parameters on the nucleation and crystallization.

Specifically, the characteristic sodalite peak intensity at an angle of $13,9^\circ$ is lower than the zeolite peak at $16,2^\circ$. (See Appendix Table B.2) Accordingly, it can be said that the determined optimal Si / Al mol ratio and the synthesis conditions are successful in terms of applicability for all ashes. The first noticeable difference between laboratory generated ashes and PP fly ashes is that there are albite phases in laboratory ashes that have not been converted to zeolites (see Figure 4.23). The fly ash synthesized zeolite 4A crystallinity was compared with the commercial Zeolite 4A crystallinity which was taken as reference sample (See Figure 4.8). It should be mentioned that the relative crystallinity to commercial zeolite 4A of the zeolite obtained from all four ashes is in the range of 57% to 68 % (See Table 4.7) and the reason(s) for this difference were discussed below.

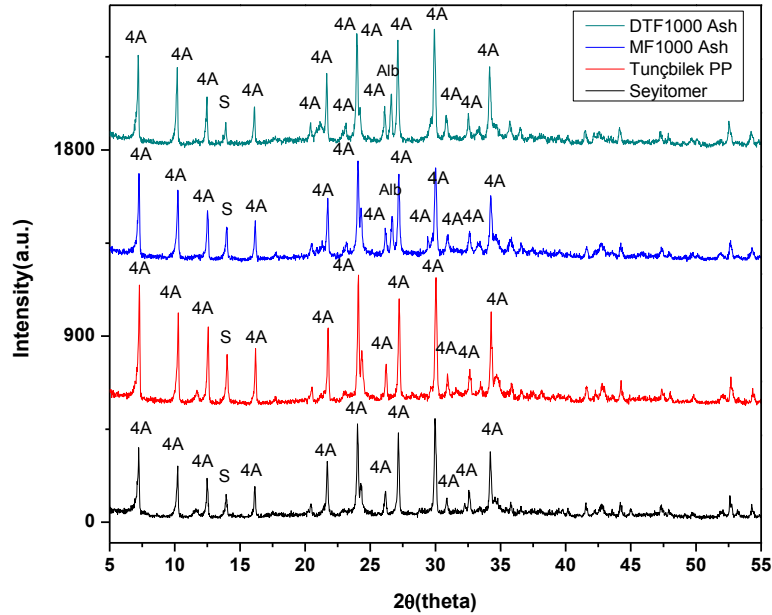


Figure 4.23. XRD Pattern of Synthesized Zeolites from different Class F Ashes at optimal conditions, S: Sodalite, 4A: Zeolite 4A

Although not seen in the crystalline phase of the fusion product, the samples contain varying amounts of iron. In this manner, the presence of ash-borne iron minerals could be decisive factor on which type of sodium minerals to be formed (sodium silicate, sodium aluminate or sodialuminosilicate) Furthermore, iron compounds may also interfere with the nucleation and crystallization steps [9].

The crystallinity of hematite, magnetite and mullite phases also affects the nucleation behavior and results in higher sodalite phase impurity. This is observed for the synthesis products of Tunçbilek thermal PP ash and MF1000 ashes (see Table 4.7). Especially this effect was dominant for Tunçbilek PP ash which has the richest for mullite and the mullite is the only aluminosilicate mineral form due to higher combustion temperature on the PCC boiler, so the effect was mostly depend on mullite presence. For Seyitömer ash, even though it contains high iron content, the nucleation is not significantly affected, likely due to the absence of large amount of mullite, and the ash consists mostly of glassy phases. In a similar fashion, DTF1000 ash has the lowest ash crystallinity among these four samples, and hence a lower percentage of

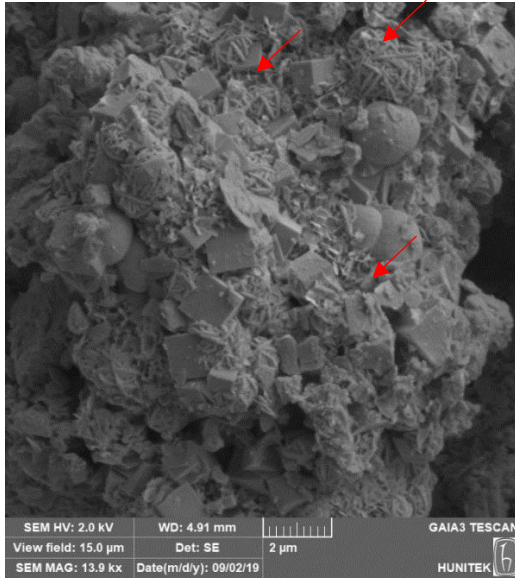
iron oxide (magnetite, hematite) and mullite phases. In these two ashes, a low amount of sodalite phase impurity in relation to the crystallinity values is present.

The alkalinity of the fusion product also plays a minor role. Zeolite 4A synthesized using Tunçbilek PP ash has the highest zeolite crystallinity among the products obtained, but also the highest sodalite phase impurity. From this point, the Tunçbilek fusion product has a higher alkalinity which will enable a higher nucleation rate, as mentioned in subsection 4.3.4.

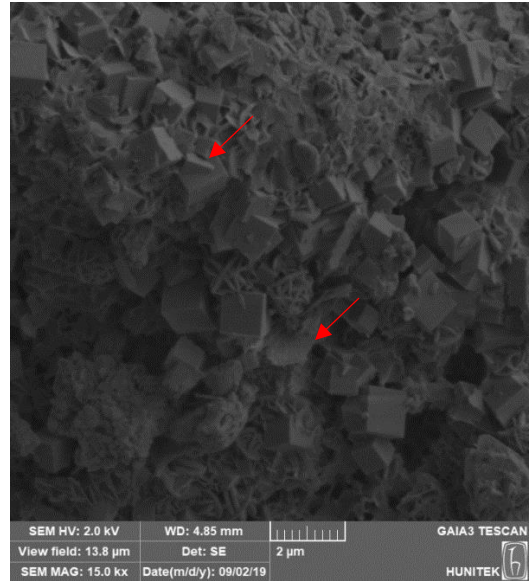
Table 4.7. Relation of Mineral Composition and Ash Crystallinity on Zeolite Crystallinity

Fusion Product	Relative Zeolite 4A Crystallinity,%	ash crystallinity %	hematite+mullite, %	sodalite%
Tunçbilek	68	48	18	8,8
MF1000	57	43	14,2	4,5
DTF1000	64,1	31	8	1,6
Seyitömer	65	34	10,3	4,3

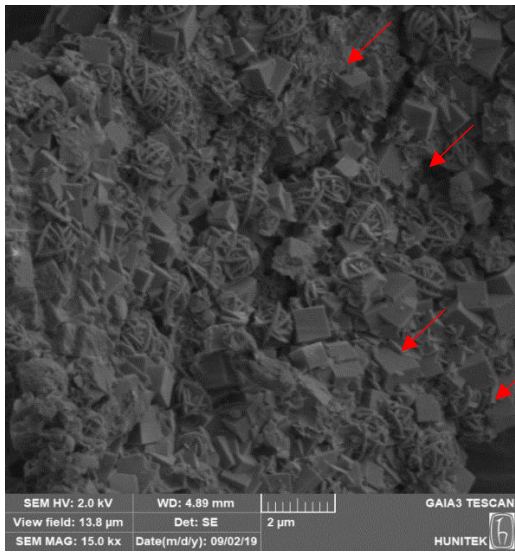
To validate the arguments, the SEM analysis were conducted to detect the perfect morphology that matches the industrial Zeolite 4A samples (See Figure 4.8). As seen in Figure 4.24, the cubic structure and chamfered edge were detected on the SEM images for all of the 4 samples. It should be considered the details on the images, which is the distribution of sodalites which was detected by filament like structures. In Figure 4.24(d), (DTF1000 4A), the crystals distributed smoothly and the heterogeneity of topography was the least for this sample. The sodalite crystals were more distinguishable for MF1000 and Tunçbilek PP synthesis product.



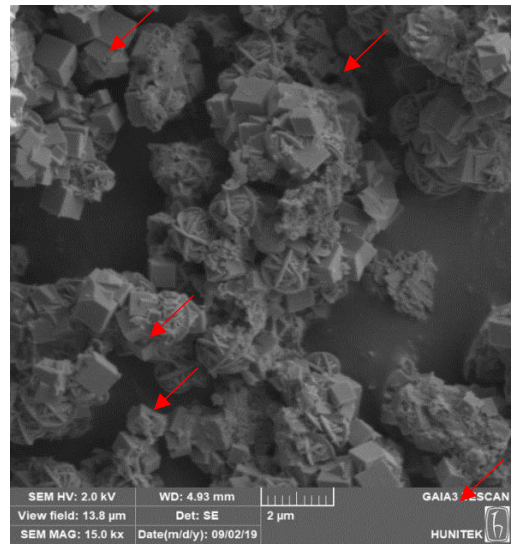
a) Seyitömer 4A



b) Tunçbilek PP 4A



c) MF1000 4A



d) DTF1000 4A

Figure 4.24. SEM Analysis of Zeolite 4A obtained from the fusion product of a) Seyitömer PP b) Tunçbilek PP, c) MF100 d) DTF1000, ashes

4.5. Zeolite 4A Synthesis with Fly Ashes from Combustion Blends

The alkaline fusion process, including in this study, provides the water-soluble phases necessary for zeolite synthesis, allowing zeolite in high yields. However, as mentioned in Section 2.7.1, the alkali fusion step is an energy-intensive process [1], and is therefore undesirable in terms of production cost. Based on this information, it has been considered that the addition of aluminum and silicon sources prior to combustion may allow the elimination of the fusion step and was investigated in detail in this subsection.

The XRD diffraction pattern of the ash sample obtained in the muffle furnace at 1000 °C as a result of the addition of aluminum hydroxide and sodium carbonate was presented in Figure 4.25. In parallel with the studies in the literature, sodium sulfate phases were also determined. The vital point is that nepheline phases, which are sodium aluminosilicate phases, are in line with those represented in Figure 4.22. In this context, it can undoubtedly be stated that the high amount of aluminum and quartz minerals formed by decomposition of clay minerals such as kaolinite present in coal occurs directly in the sodium aluminosilicate phase. This finding is thought to be the cause of the high amount of sodium aluminosilicate detected in the alkali fusion product diffraction patterns of other ash samples. This is due to the fact that the alkali agent, aluminum and silicon source in the coal, which are present during combustion, occur directly in the sodium aluminosilicate(nepheline) phase without the possibility of mullite phases being formed.

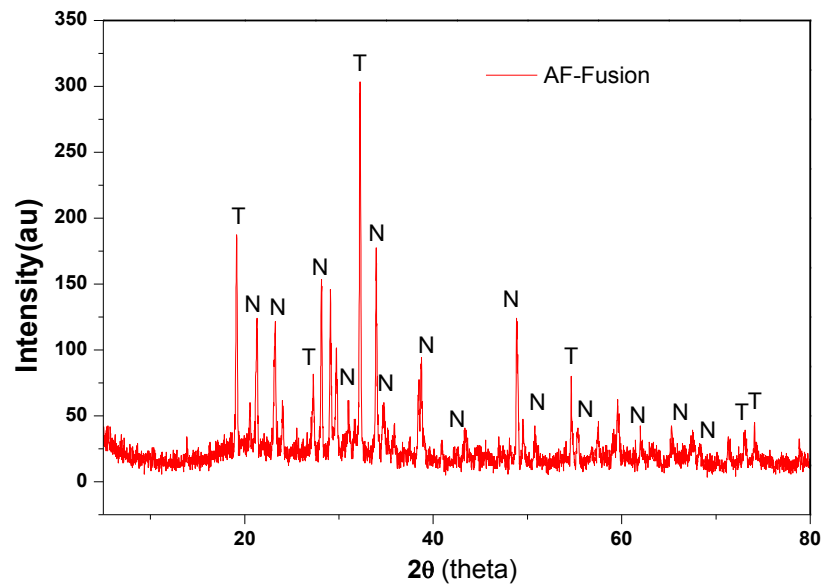


Figure 4.25. XRD Patterns of Tunçbilek Fly Ashes ;from combustion experiments with sodium carbonate in Ashing Furnace at 1000 °C
 N:Nepheline, NaAlSiO_4 ; T:Thenardite (sodium sulfate)

After determining the desired sodium aluminosilicate phases in the fusion product, Zeolite 4A synthesis was carried out under the optimized conditions specified in Section 4.3. Despite the possibility of slagging and fouling, Zeolite 4A is obtained by the formation of partial sodium aluminosilicate phases as described in Section 3.5.

XRD analysis of synthesis products of ashes from combustion blends were given in Figure 4.26. In Figure 4.26, it was observed that the sodium sulphate peaks in the ash sample from the fuel mixture disappeared, and the scattering angles of the phases also differ from the positions in other alkali fusion products. Based on this information, it can be asserted that zeolitic phases were formed. However, it can be mentioned that the presence of impurities and sulphate mineral phases in the products obtained adversely affect the nucleation rate [62] in the aging step. It is also important to note that the crystallinity in terms of zeolitic phases is very low when compared with the reference sample from MF1000 synthesis (see Figure 4.22).

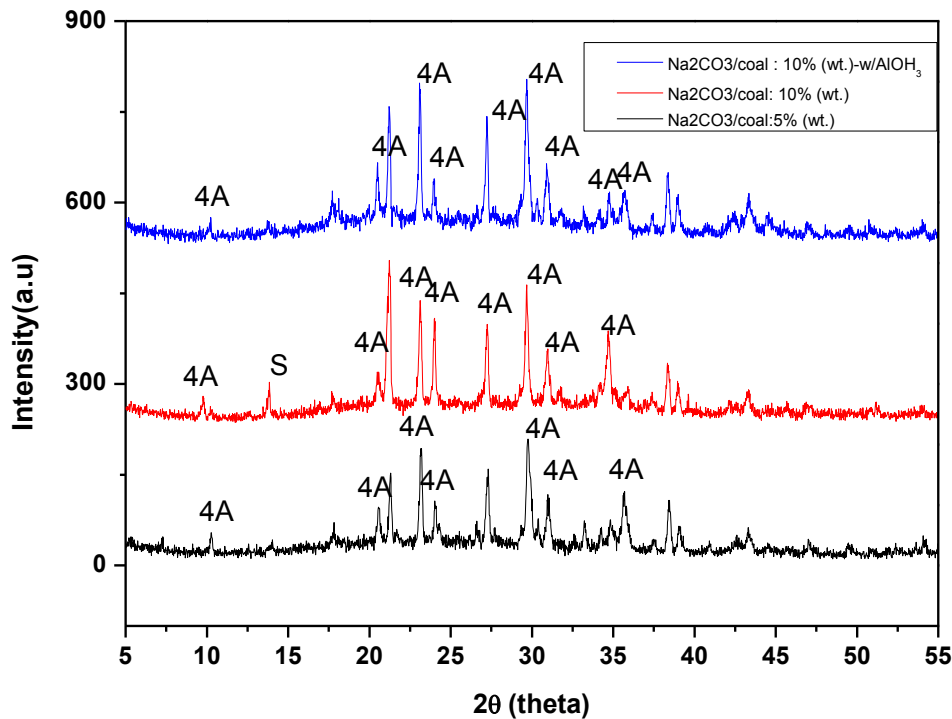


Figure 4.26. XRD Patterns of Zeolite 4A Synthesis Tunçbilek Fly Ashes from combustion experiments with sodium carbonate in Ashing Furnace at 1000 °C with 12 h Aging at 47°C and 4 h crystallization at 90°C, 4A: Zeolite 4A, S: Sodalite

After observing that the formation of zeolitic phases is possible, based on the mass mixing ratio of the fusion product having a Si / Al ratio of 1.04 where zeolite 4A crystal phases can be achieved even at 100 °C, (15% ash yield of the coal), and considering the ash content of Tunçbilek coal, fuel mixture was prepared. The synthesis of ashes was carried out under optimal conditions. XRD analysis of the obtained synthesis product is given in Figure 4.27.

Since the low crystallinity content was observed, many of the characteristic Zeolite 4A peaks were detected after the obtained diffraction pattern was smoothed. Furthermore, the presence of the sodalite phase proves that nucleation occurs at least.

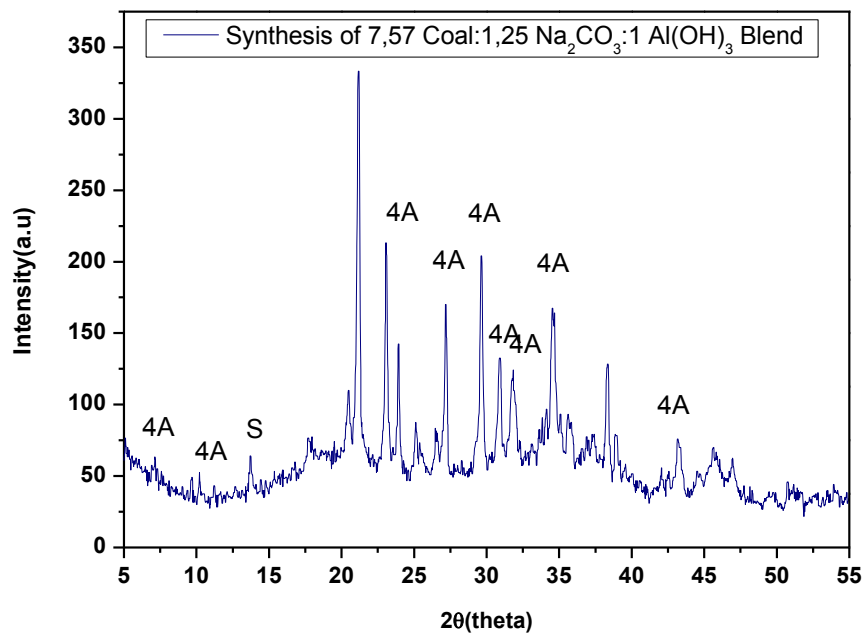


Figure 4.27. Smoothed XRD Patterns of Zeolite 4A synthesis from the combustion blends with mass ratio 7,57 Coal: 1,25 Na₂CO₃:1 Al(OH)₃ in Ashing Furnace at 1000 °C with 12 h Aging at 47°C and 4 h crystallization at 90°C

| CHAPTER 5

CONCLUSION AND FUTURE RESEARCH

5.1. Conclusion

In this study, zeolite synthesis using fly ash from Turkish lignites was investigated. A comprehensive characterization study was carried out, with the thermal power plant Tunçbilek, Soma and Seyitömer fly ashes, and also with Tunçbilek ashes obtained under different conditions in laboratory controlled experiments. When considering the results, as a difference from the literature, instead of a merely ash characterization, this study was focused on explaining the relationship between the raw material - fly ash, and the final product - zeolite 4A. Moreover, the effect of different combustion conditions on the fly ash characteristics was considered with the help of drop tube furnace and wire mesh reactor with high heating rate, which closely reflects the pulverized combustion conditions. There were no study investigating the effect of combustion parameters on the characteristics of zeolites, using ash obtained from industrial and lab-scale equipment. In particular, the novelty of this thesis is the fact that it considers both the effect of the combustion parameters on the characteristics of fly ash, and the suitability of the characterized fly ash for zeolite synthesis.

As a result of the experimental studies that were defined and carried out for the research questions put forward, the findings obtained from the thesis in relation to the questions sought were answered as follows;

As a result of the experimental studies, ‘**what is the effect of the proposed coal source on the mineral composition?**’ in response to the question;

- In the ash obtained from Soma Thermal Power Plant 5-6 units, phases of minerals such as anorthite, anhydrite, mellite and lime ,containing very high levels of calcium, were observed. However, quartz, mullite and hematite were determined as major phases in Tunçbilek and Seyitömer Thermal Power Plant

ashes (Class F). For Seyitömer ash the magnetite phase, another iron oxide mineral, was also present.

Based on the findings, the presence of calcium or iron minerals in relation to the chemical content of coal, which should be considered as impurity in terms of zeolite synthesis, was determined as the effect of geographic source. It was also observed that Seyitömer fly ash had a lower percentage of crystallinity due to its high iron content.

As a raw material for zeolite synthesis, determination of the change of the fly ash's mineral content depending on the combustion parameters expected to provide a better understanding of the effect of ash crystallinity and minerals such as mullite and hematite in the alkali fusion and hydrothermal process steps, ‘**What is the effect of the combustion conditions on fly ash characteristics?**’ the question put forward and the findings obtained as a result of experimental studies conducted in this view;

Effect of Combustion Parameters on Fly Ash Characteristics

- For the MF ashes obtained as a result of combustion experiments, it was observed that the peak intensity of mullite and hematite-related phases increased in parallel with a temperature increase from 800 to 1000 ° C.
- Compared to Tunçbilek thermal power plant ashes, due to the lower combustion temperature, in laboratory ashes there are mineral phases such as corundum and kaolinite which are alumina phases.
- Kaolinite phase was observed in DTF ashes due to low residence time and high heating rate, along with the 800-1000 ° C temperature. Likewise, the presence of kaolinite phase in the ash obtained at 800 and 900 ° C from WMR, reinforces the previous statement.
- In the 800-1000 ° C range, MF ash was found to have the highest crystallinity and mullite phase, since the cooling rate was lowest among all reactors.

- As a significant discovery, despite the experiments were carried out at low temperatures, it was clear that for MF ashes conditions such as long residence time and low heating rates were also decisive factors, in the formation of the mullite phase.
- It was observed that as the cooling rate increases, the ash crystallinity decreases. Both mullite and hematite phases became amorphous depending on the cooling rate and it was validated with WMR1200 ashes.

As a result, in controlled experiments carried out considering the heating rate, temperature and cooling rate of Tunçbilek lignite, it was determined that the aluminosilicate mineral which is important for zeolite synthesis, mullite and also the impurity hematite mineral content showed significant differences. As the most important finding, the effect of geographic resource could be eliminated thanks to the ash samples obtained from a single coal, in thermal power plant conditions and laboratory conditions.

In order to understand the mechanism of zeolite synthesis from fly ash and to obtain a reproducible synthesis method, using Class F Seyitömer ash, ‘‘**What is the nucleation behavior of fusion product for Zeolite 4A synthesis?**’’, ‘‘**Which condition is optimal for the crystal growth of Zeolite 4A?**’’ these questions were put forward, the findings;

Optimization of Zeolite 4A synthesis

The optimal synthesis conditions are as follows: The optimal Si/Al mol ratio was optimized as 1,17 and the most crystalline Zeolite 4A with the least sodalite impurity obtained for 12 h aging and 4 h crystallization at 47°C and 90°C, respectively. Specifically, the following was concluded;

- Aluminum hydroxide $\text{Al}(\text{OH})_3$ was used herein before the alkali fusion step for the first time to synthesize zeolite using fly ash. The addition of $\text{Al}(\text{OH})_3$ enables the elimination of further processing steps such as acid leaching,

desilification, separation of the supernatant solution, treatment with alkali solution, addition of sodium aluminate solution.

- Increasing amounts of Al (OH)₃ were added to the fly ash-sodium carbonate mixture and fusion products of the same molar ratio could be obtained in the range of 1-1,5 Si / Al molar ratio with a maximum error value of 4%. With the help of this information, the relationship between Si / Al and Na / Si mass mixture ratio and molar ratio was formulated and applied independently to the source of ash (eg Tunçbilek Thermal Power Plant Ash) for the synthesis of zeolite ratio. As a result, for the fusion product, the Si / Al mass mixture ratio was 0,72 and the corresponding Si / Al molar ratio was found to be 1,17.
- One of the most important findings was that the solid / liquid ratio was kept high in the aging step instead of using high amounts of alkali agent and thus aqueous solution. In addition, a small amount of DI water was used. Thus, it has been proved that the synthesis of Zeolite 4A is achieved both in terms of crystal structure and morphology.
- The crucial findings from the optimization experiments, the nucleation should be controlled by increasing aging temperature and providing lower alkalinity. Also, the crystallization time and temperature shouldn't be extended, especially for high iron impurity ash.

Zeolite 4A Synthesis for different Fly Ashes using the Optimized Parameters

The key point of the study was to understand the effect of fly ash characteristics on Zeolite 4A synthesis and to validate the reproducibility of the optimized conditions and to determine the tolerance of the changing characteristics of fly ash during the synthesis process. The answers of the respected questions,

“how do the combustion parameters effect the fusion product?”

“Is there a direct realation between combustion conditions and Zeolite 4A synthesis?”

‘What is the effect of impurities of fly ash on the zeolite synthesis? ‘

were given as follows,

- The mineral composition of the fly ash could be tuned by changing conditions such as heating rate, cooling rate, combustion temperature. Especially, the mullite and hematite content of the ash was asserted as the decisive factor on the mineral composition of fusion product and the sodalite content on the Zeolite 4A. Relatively, the key parameter was determined as the mineral composition of the fly ash for the zeolite synthesis.
- The Zeolite 4A samples from the MF1000, DTF1000, TL PP and Seyitömer ashes almost matched the crystallinity and structure of commercial Zeolite 4A at the optimized conditions. With DTF1000 ashes, the least sodalite impurity (%1,6) and less heterogeneity on the morphology were observed in the synthesis product with %64,1 relative crystallinity of commercial Zeolite 4A.
- Even in the fusion products prepared at the same mixing ratio, differences in the ratio of sodium silicate and sodium aluminosilicate and crystallinity of the fusion product were observed, depending on the mineral composition in the ash. Therefore, the mineral composition of the ash source to be used for the fusion process should be a factor to be considered.

Zeolite 4A Synthesis with Fly ashes from combustion blends

The question of the possibility of the elimination of alkali fusion by helping of combustion process was the innovative part of the study and it was found that;

- The synthesis of zeolite 4A was performed with the ashes obtained from the combustion of the fuel mixture of coal - sodium carbonate and aluminum hydroxide. As a result, it has been shown that synthesis of zeolite 4A is possible without the need for an alkali fusion step. However, loss of crystallinity of the final product was observed.

5.2. Future Research

Although the findings give various ideas in order to understand the effect of combustion parameters on ash characteristics and thus on zeolite formation, there are various recommendations that need to be addressed in order to broaden the scope of the study. Also, by considering the research questions that are not fully answered with defined objectives. These can be listed as follows;

- Selecting a combustion temperature range of 800-1000 ° C caused the iron oxide phase hematite to interfere with the mullite in the diffraction pattern. To overcome this, the temperature range must be extended to 1500 ° C.
- As another approach, the Rietveld method should be used to overcome this situation, especially in order to determine the chemical composition and crystallinity ratio of minerals.
- Depending on the mineral content of the ash source used, even if it is from the same fuel, the nucleation and crystallization behavior of the resulting fusion product may be affected. In order to be able to observe and interpret these effects more clearly, the alkali fusion product should be obtained in different conditions in terms of time, heating rate and temperature, and the changing mineral composition and fusion chemistry should be examined in more detail from the theoretical point of view.
- As an alternative, in order to eliminate hematite and mullite phase interferences, the iron content should be removed from the ash source by acid leaching procedure. Therefore, it should be clearly established whether the predominant factor affecting zeolite formation is the impurity content or the crystallinity value of the aluminosilicate phase.
- With the minimum number of experimental studies, the nucleation and crystallization behavior of the fusion product obtained from Class F fly ash was tried to be understood. However, for fusion products having different Si / Al molar ratios, synthesis products should be obtained under different aging

and crystallization conditions and the effects of each parameter should be demonstrated.

- Likewise, using an ash source rich in Si / Al but with a relatively low iron content, synthesis studies should be carried out with the formulated mixture ratio and the reproducibility of the optimized method should be tested.
- Sodium carbonate and Al (OH)₃ used in the thesis are inorganic additives which are frequently used for different purposes in terms of combustion science. However, the coal-inorganic mixture is considered only for zeolite synthesis. To determine the applicability of the proposed approach, the optimal mixing ratio of the respective fuel mixtures should be determined. In addition, the factors such as slag and fouling formation in the boiler as well as their effects on combustion kinetics and calorific value should be examined in detail in terms of science of combustion with test devices such as TGA, DTF and WMR.
- Since sulphate phases are also present in ash samples from fuel mixtures, the synthesis steps for the combustion blends should be redesigned for experimental conditions.
- Finally, the experimental studies in this thesis have been shaped to understand the formation mechanisms of fly ash and zeolites and examine scientifically the raw material-end product relationship in detail. On the other hand, Zeolite 4A product was predominantly obtained in many synthesis products. Therefore, in terms of usability of these products in industrial applications, according to the required functional properties (surface area, pore size, pore distribution, distribution of Si/Al tetrahedra in the framework), it must be characterized by analysis methods such as FTIR, BET and tested in these applications.

REFERENCES

- [1] C. Belviso, “State-of-the-art applications of fly ash from coal and biomass: A focus on zeolite synthesis processes and issues,” *Prog. Energy Combust. Sci.*, vol. 65, pp. 109–135, 2018.
- [2] L. Bartoňová, “Unburned carbon from coal combustion ash: An overview,” *Fuel Process. Technol.*, vol. 134, pp. 136–158, 2015.
- [3] R. S. Blissett and N. A. Rowson, “A review of the multi-component utilisation of coal fly ash,” *Fuel*, vol. 97, pp. 1–23, 2012.
- [4] G. Görhan, E. Kahraman, Ar, M. . S. , Başpınar, and İ. Demir, “Uçucu Kül Bölüm I: Oluşumu, Sınıflandırılması ve Kullanım Alanları,” *Yapı Teknol. Elektron. Derg.*, vol. 4, no. 2, pp. 85–94, 2008.
- [5] M. Ahmaruzzaman, “A review on the utilization of fly ash,” *Prog. Energy Combust. Sci.*, vol. 36, no. 3, pp. 327–363, 2010.
- [6] O. Bayat, “Characterisation of Turkish fly ashes,” *Fuel*, vol. 77, no. 9–10, pp. 1059–1066, 1998.
- [7] “Waste materials - Catalytic opportunities: An overview of the application of large scale waste materials as resources for catalytic applications,” *Green Chem.*, vol. 13, no. 1, pp. 16–24, 2011.
- [8] N. Moreno, X. Querol, F. Plana, J. M. Andres, M. Janssen, and H. Nugteren, “Pure zeolite synthesis from silica extracted from coal fly ashes,” *J. Chem. Technol. Biotechnol.*, vol. 77, no. 3, pp. 274–279, 2002.
- [9] Y. R. Lee, J. T. Soe, S. Zhang, J. W. Ahn, M. B. Park, and W. S. Ahn, “Synthesis of nanoporous materials via recycling coal fly ash and other solid

- wastes: A mini review,” *Chem. Eng. J.*, vol. 317, pp. 821–843, 2017.
- [10] C. Zhang and S. Li, “Utilization of iron ore tailing for the synthesis of zeolite A by hydrothermal method,” *J. Mater. Cycles Waste Manag.*, vol. 20, no. 3, pp. 1605–1614, 2018.
- [11] X. Ni, Z. Zheng, X. Wang, S. Zhang, and M. Zhao, “Fabrication of hierarchical zeolite 4A microspheres with improved adsorption capacity to bromofluoropropene and their fire suppression performance,” *J. Alloys Compd.*, vol. 592, pp. 135–139, 2014.
- [12] İ. Ustabaş and A. Kaya, “Comparing the pozzolanic activity properties of obsidian to those of fly ash and blast furnace slag,” *Constr. Build. Mater.*, vol. 164, pp. 297–307, 2018.
- [13] C. S. Cundy and P. A. Cox, “The hydrothermal synthesis of zeolites: Precursors, intermediates and reaction mechanism,” *Microporous Mesoporous Mater.*, vol. 82, no. 1–2, pp. 1–78, 2005.
- [14] F. Meng, J. Yu, A. Tahmasebi, and Y. Han, “Pyrolysis and combustion behavior of coal gangue in O₂/CO₂ and O₂/N₂ mixtures using thermogravimetric analysis and a drop tube furnace,” *Energy and Fuels*, vol. 27, no. 6, pp. 2923–2932, 2013.
- [15] W. Sujanti and D. K. Zhang, “Investigation into the role of inherent inorganic matter and additives in low-temperature oxidation of a Victorian brown coal,” *Combust. Sci. Technol.*, vol. 152, no. 1, pp. 99–114, 2000.
- [16] S. V. Vassilev and C. G. Vassileva, “Methods for characterization of composition of fly ashes from coal-fired power stations: A critical overview,” *Energy and Fuels*, vol. 19, no. 3, pp. 1084–1098, 2005.
- [17] H. L. Chang and W. H. Shih, “Synthesis of zeolites A and X from fly ashes and

- their ion-exchange behavior with cobalt ions,” *Ind. Eng. Chem. Res.*, vol. 39, no. 11, pp. 4185–4191, 2000.
- [18] J. J. BROWN, *The Use of Phase Diagrams to Predict Alkali Oxide Corrosion of Ceramics*. ACADEMIC PRESS, INC., 2007.
- [19] A. E. Ameh, O. O. Fatoba, N. M. Musyoka, and L. F. Petrik, “Influence of aluminium source on the crystal structure and framework coordination of Al and Si in fly ash-based zeolite NaA,” *Powder Technol.*, vol. 306, pp. 17–25, 2017.
- [20] X. Ren *et al.*, “Synthesis and characterization of a single phase zeolite A using coal fly ash,” *RSC Adv.*, vol. 8, no. 73, pp. 42200–42209, 2018.
- [21] J. D. C. Izidoro, D. A. Fungaro, J. E. Abbott, and S. Wang, “Synthesis of zeolites X and A from fly ashes for cadmium and zinc removal from aqueous solutions in single and binary ion systems,” *Fuel*, vol. 103, pp. 827–834, 2013.
- [22] L. Yang *et al.*, “Green synthesis of zeolite 4A using fly ash fused with synergism of NaOH and Na₂CO₃,” *J. Clean. Prod.*, vol. 212, pp. 250–260, 2019.
- [23] E. Rokni, H. Hsein Chi, and Y. A. Levendis, “In-Furnace Sulfur Capture by Cofiring Coal With Alkali-Based Sorbents,” *J. Energy Resour. Technol.*, vol. 139, no. 4, p. 042204, 2017.
- [24] A. Molina, J. J. Murphy, C. R. Shaddix, and L. G. Blevins, “The effect of potassium bromide and sodium carbonate on coal char combustion reactivity,” *Proc. Combust. Inst.*, 2005.
- [25] Q. Huang, Y. Zhang, Q. Yao, and S. Li, “Mineral manipulation of Zhundong lignite towards fouling mitigation in a down-fired combustor,” *Fuel*, vol. 232, no. June, pp. 519–529, 2018.

- [26] B. Wei, X. Wang, H. Tan, L. Zhang, Y. Wang, and Z. Wang, "Effect of silicon–aluminum additives on ash fusion and ash mineral conversion of Xinjiang high-sodium coal," *Fuel*, vol. 181, pp. 1224–1229, 2016.
- [27] J. Si *et al.*, "Effect of kaolin additive on PM_{2.5} reduction during pulverized coal combustion: Importance of sodium and its occurrence in coal," *Appl. Energy*, vol. 114, pp. 434–444, 2014.
- [28] A. R. McLennan, G. W. Bryant, C. W. Bailey, B. R. Stanmore, and T. F. Wall, "An experimental comparison of the ash formed from coals containing pyrite and siderite mineral in oxidizing and reducing conditions," *Energy and Fuels*, 2000.
- [29] T. Babcock and W. Company, "Steam: its generation and use," *Nucl. Energy*, 2007.
- [30] K. S. Vorres, "Chemistry of Mineral Matter and Ash in Coal: An Overview," 2009.
- [31] S. V. Vassilev and C. G. Vassileva, "A new approach for the classification of coal fly ashes based on their origin, composition, properties, and behaviour," *Fuel*, vol. 86, no. 10–11, pp. 1490–1512, 2007.
- [32] A. I. Karayigit, R. A. Gayer, X. Querol, and T. Onacak, "Contents of major and trace elements in feed coals from Turkish coal-fired power plants," *Int. J. Coal Geol.*, 2000.
- [33] A. I. Karayigit and Y. Celik, "Mineral matter and trace elements in miocene coals of the Tuncbilek-Domanic basin, Kutahya, Turkey," *Energy Sources*, 2003.
- [34] S. V. Vassilev, C. G. Vassileva, A. I. Karayigit, Y. Bulut, A. Alastuey, and X. Querol, "Phase-mineral and chemical composition of composite samples from

- feed coals, bottom ashes and fly ashes at the Soma power station, Turkey,” *Int. J. Coal Geol.*, 2005.
- [35] A. C618-05, “Standard Specification for Coal Fly Ash and Raw or Calcined Natural Pozzolan for Use in Concrete,” *AIP Conf. Proc.*, 2012.
- [36] İ. Görhan, G. Kahraman, E. Başpınar, M. S., Demir, “Uçucu Kül Bölüm II: Kimyasal, Mineralojik ve Morfolojik Özellikler,” *Yapı Teknol. Elektron. Derg.*, vol. 5, no. 2, pp. 33–42, 2009.
- [37] C. G. Vassileva and S. V. Vassilev, “Behaviour of inorganic matter during heating of Bulgarian coals. 2. Subbituminous and bituminous coals,” *Fuel Process. Technol.*, vol. 87, no. 12, pp. 1095–1116, 2006.
- [38] C. R. Ward and D. French, “Determination of glass content and estimation of glass composition in fly ash using quantitative X-ray diffractometry,” *Fuel*, vol. 85, no. 16 SPEC. ISS., pp. 2268–2277, 2006.
- [39] N. Koukouzas, C. R. Ward, D. Papanikolaou, Z. Li, and C. Ketikidis, “Quantitative evaluation of minerals in fly ashes of biomass, coal and biomass-coal mixture derived from circulating fluidised bed combustion technology,” *J. Hazard. Mater.*, vol. 169, no. 1–3, pp. 100–107, 2009.
- [40] D. Zhu, H. Yang, Y. Chen, Z. Li, X. Wang, and H. Chen, “Fouling and slagging characteristics during co-combustion of coal and biomass,” *BioResources*, vol. 12, no. 3, pp. 6322–6341, 2017.
- [41] J. Tomeczek and H. Palugniok, “Kinetics of mineral matter transformation during coal combustion,” *Fuel*, vol. 81, no. 10, pp. 1251–1258, 2002.
- [42] J. C. Hower *et al.*, “Coal-derived unburned carbons in fly ash: A review,” *Int. J. Coal Geol.*, vol. 179, no. March, pp. 11–27, 2017.

- [43] G. P. Huffman and F. E. Huggins, "Reactions and Transformations of Coal Mineral Matter At Elevated Temperatures.," *ACS Div. Fuel Chem. Prepr.*, vol. 29, no. 4, pp. 56–67, 1984.
- [44] C. G. Vassileva and S. V. Vassilev, "Behaviour of inorganic matter during heating of Bulgarian coals: 1. Lignites," *Fuel Process. Technol.*, vol. 86, no. 12–13, pp. 1297–1333, 2005.
- [45] J. J. Helble, S. Srinivasachar, and A. A. Boni, "Factors influencing the transformation of minerals during pulverized coal combustion," *Progress in Energy and Combustion Science*. 1990.
- [46] ASTM, "ASTM: Standard Test Method for Ash in the Analysis Sample of Coal and Coke from Coal 1," *ASTM Int.*, 2002.
- [47] Y. Zhao, J. Zhang, and C. Zheng, "Transformation of aluminum-rich minerals during combustion of a bauxite-bearing Chinese coal," *Int. J. Coal Geol.*, vol. 94, pp. 182–190, 2012.
- [48] D. Yu, L. Zhao, Z. Zhang, C. Wen, M. Xu, and H. Yao, "Iron transformation and ash fusibility during coal combustion in air and O₂/CO₂ medium," *Energy and Fuels*, vol. 26, no. 6, pp. 3150–3155, 2012.
- [49] D. Dermatas and X. Meng, "Utilization of fly ash for stabilization/solidification of heavy metal contaminated soils," *Eng. Geol.*, 2003.
- [50] V. C. Pandey and N. Singh, "Impact of fly ash incorporation in soil systems," *Agriculture, Ecosystems and Environment*. 2010.
- [51] R. Siddique, "Performance characteristics of high-volume Class F fly ash concrete," *Cem. Concr. Res.*, 2004.
- [52] O. M. Dunens, K. J. Mackenzie, and A. T. Harris, "Synthesis of multiwalled

- carbon nanotubes on fly ash derived catalysts,” *Environ. Sci. Technol.*, 2009.
- [53] P. Bankowski, L. Zou, and R. Hodges, “Reduction of metal leaching in brown coal fly ash using geopolymers,” *J. Hazard. Mater.*, 2004.
- [54] X. Y. Zhuang *et al.*, “Fly ash-based geopolymer: Clean production, properties and applications,” *Journal of Cleaner Production*. 2016.
- [55] W. R. Roy, R. G. Thiery, R. M. Schuller, and J. L. Suloway, “Coal fly ash: a review of the literature and proposed classification system with emphasis on environmental impacts.,” *Illinois State Geol. Surv. Environ. Geol. Notes*, 1981.
- [56] J. C. Hower and M. Mastalerz, “An approach toward a combined scheme for the petrographic classification of fly ash,” *Energy and Fuels*, 2001.
- [57] “Zeolite Molecular Sieves: Structure, Chemistry, and Use D. W. Breck (Union Carbide Corporation, Tarrytown, New York) John Wiley and Sons, New York, London, Sydney, and Toronto. 1974. 771 pp. \$11.95,” *J. Chromatogr. Sci.*, 1975.
- [58] J. Weitkamp and L. Puppe, *Catalysis and Zeolites: Fundamentals and Applications*. 1999.
- [59] A. Elliot and D.-K. Zhang, “Controlled Release Zeolite Fertilisers: A Value Added Product Produced from Fly Ash,” *World Coal Ash*, 2005.
- [60] R. M. Barrer, “Zeolites and their synthesis,” *Zeolites*. 1981.
- [61] C. Baerlocher and L. B. McCusker, “Database of Zeolite Structures,” Available at: <http://www.iza-structure.org/databases/>, 2014. .
- [62] R. M. Mohamed, A. A. Ismail, G. Kini, I. A. Ibrahim, and B. Koopman, “Synthesis of highly ordered cubic zeolite A and its ion-exchange behavior,” *Colloids Surfaces A Physicochem. Eng. Asp.*, vol. 348, no. 1–3, pp. 87–92,

- 2009.
- [63] A. Pfenninger, "Manufacture and Use of Zeolites for Adsorption Processes," 1999.
- [64] J. C. Jansen, D. Kashchiev, and A. Erdem-Senatalar, "Preparation of Coatings of Molecular Sieve Crystals for Catalysis and Separation," in *Studies in Surface Science and Catalysis*, 1994.
- [65] K. Byrappa and M. Yoshimura, "Hydrothermal Technology—Principles and Applications," in *Handbook of Hydrothermal Technology*, 2001.
- [66] L. Guozhi *et al.*, "Zeolite a preparation from high alumina fly ash of china using alkali fusion and hydrothermal synthesis method," *Mater. Res. Express*, vol. 6, no. 6, p. 65049, 2019.
- [67] P. Panitchakarn, N. Laosiripojana, N. Viriya-umpikul, and P. Pavasant, "Synthesis of high-purity Na-A and Na-X zeolite from coal fly ash," *J. Air Waste Manag. Assoc.*, vol. 64, no. 5, pp. 586–596, 2014.
- [68] D. Georgiev, B. Bogdanov, K. Angelova, I. Markovska, and Y. Hristov, "Synthetic zeolites—structure, classification, current trends in zeolite synthesis: Review. International Science conference, 4th - 5th June 2009, Stara Zagora, BULGARIA," *Proc. Int. Sci. Conf.* ..., 2009.
- [69] K. S. Hui and C. Y. H. Chao, "Pure, single phase, high crystalline, chamfered-edge zeolite 4A synthesized from coal fly ash for use as a builder in detergents," *J. Hazard. Mater.*, vol. 137, no. 1, pp. 401–409, 2006.
- [70] J. Bronić and B. Subotić, "Role of homogeneous nucleation in the formation of primary zeolite particles," *Microporous Mater.*, 1995.
- [71] B. Subotić and L. Sekovanić, "Transformation of zeolite A into

hydroxysodalite,” *J. Cryst. Growth*, 1986.

- [72] C. Belviso, F. Cavalcante, and S. Fiore, “Synthesis of zeolite from Italian coal fly ash: Differences in crystallization temperature using seawater instead of distilled water,” *Waste Manag.*, vol. 30, no. 5, pp. 839–847, 2010.
- [73] N. Shigemoto, H. Hayashi, and K. Miyaura, “Selective formation of Na-X zeolite from coal fly ash by fusion with sodium hydroxide prior to hydrothermal reaction,” *J. Mater. Sci.*, 1993.
- [74] Y. Yaping, Z. Xiaoqiang, Q. Weilan, and W. Mingwen, “Synthesis of pure zeolites from supersaturated silicon and aluminum alkali extracts from fused coal fly ash,” *Fuel*, vol. 87, no. 10–11, pp. 1880–1886, 2008.
- [75] V. Berkgaut and A. Singer, “High capacity cation exchanger by hydrothermal zeolitization of coal fly ash,” *Appl. Clay Sci.*, 1996.
- [76] J. T. Soe, S. S. Kim, Y. R. Lee, J. W. Ahn, and W. S. Ahn, “CO₂ capture and Ca²⁺ exchange using zeolite A and 13X prepared from power plant fly ash,” *Bull. Korean Chem. Soc.*, vol. 37, no. 4, pp. 490–493, 2016.
- [77] H. L. Chang and W. H. Shih, “A General Method for the Conversion of Fly Ash into Zeolites as Ion Exchangers for Cesium,” *Ind. Eng. Chem. Res.*, vol. 37, no. 1, pp. 71–78, 1998.
- [78] N. M. Musyoka, L. Petrik, and E. Hums, “Synthesis of Zeolite A, X and P from a South African Coal Fly Ash,” *Adv. Mater. Res.*, 2012.
- [79] P. Kunecki, R. Panek, M. Wdowin, and W. Franus, “Synthesis of faujasite (FAU) and tschernichite (LTA) type zeolites as a potential direction of the development of lime Class C fly ash,” *Int. J. Miner. Process.*, vol. 166, pp. 69–78, 2017.

- [80] Z. Jiang, J. Yang, H. Ma, X. Ma, and J. Yuan, "Synthesis of pure NaA zeolites from coal fly ashes for ammonium removal from aqueous solutions," *Clean Technol. Environ. Policy*, vol. 18, no. 3, pp. 629–637, 2016.
- [81] J. D. Monzón, A. M. Pereyra, M. S. Conconi, and E. I. Basaldella, "Phase transformations during the zeolitization of fly ashes," *J. Environ. Chem. Eng.*, vol. 5, no. 2, pp. 1548–1553, 2017.
- [82] T. Hu, W. Gao, X. Liu, Y. Zhang, and C. Meng, "Synthesis of zeolites Na-A and Na-X from tablet compressed and calcinated coal fly ash," *R. Soc. Open Sci.*, vol. 4, no. 10, 2017.
- [83] D. Magalhães, F. Kazanç, J. Riaza, S. Erensoy, Ö. Kabaklı, and H. Chalmers, "Combustion of Turkish lignites and olive residue: Experiments and kinetic modelling," *Fuel*, 2017.
- [84] E. M. Flanigen, "Chapter 2 Zeolites and Molecular Sieves an Historical Perspective," *Stud. Surf. Sci. Catal.*, 1991.
- [85] M. Mantler and M. Schreiner, "X-ray Fluorescence Spectrometry in Art and Archaeology," *X-Ray Spectrom.*, 2000.
- [86] B. Lafuente, R. T. Downs, H. Yang, and N. Stone, "The power of databases: The RRUFF project," in *Highlights in Mineralogical Crystallography*, 2016.
- [87] P. W. Du Plessis, T. V. Ojumu, O. O. Fatoba, R. O. Akinyeye, and L. F. Petrik, "Distributional fate of elements during the synthesis of zeolites from South African coal fly ash," *Materials (Basel)*, 2014.
- [88] A. Moutsatsou, E. Stamatakis, K. Hatzitzotzia, and V. Protonotarios, "The utilization of Ca-rich and Ca-Si-rich fly ashes in zeolites production," *Fuel*, 2006.

APPENDICES

A. SEM Images of Fly Ashes and Zeolite 4A Samples

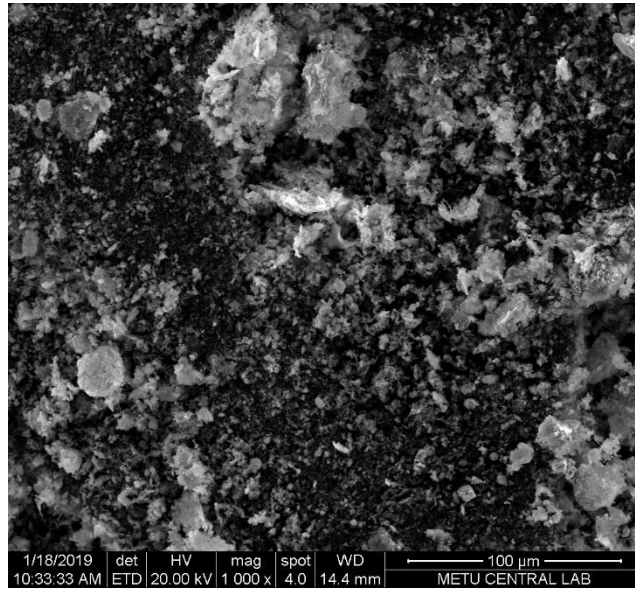


Figure A.1. WMR1000 Ashes

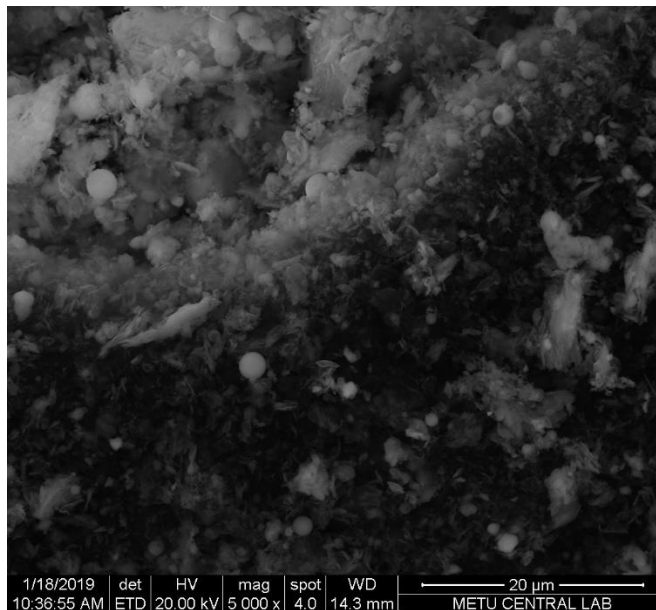


Figure A.2. SEM Images of DTF1000 Ashes

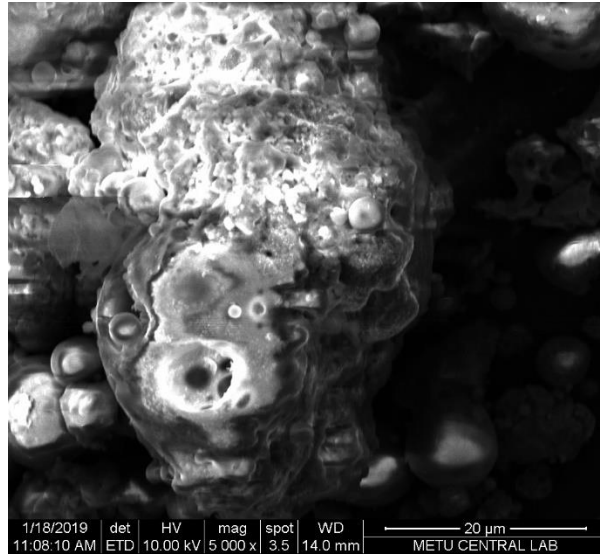


Figure A.3. SEM Images of Tunçbilek PP Ashes

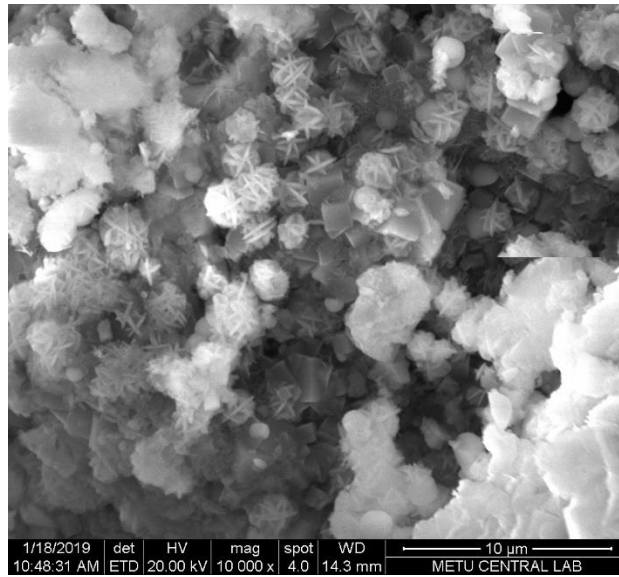


Figure A.4. SEM Images of Zeolite 4A from Seyitömer Fly Ash 16 h Aging at 47 °C and 7 h Crystallization at 85°C of with Fusion Product Si/Al : 1,17

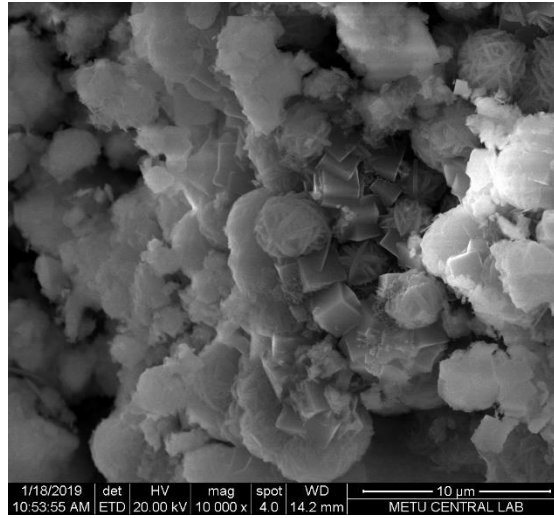


Figure A.5. SEM Images of Zeolite 4A from Seyitömer Fly Ash 12 h Aging at 47 °C and 7 h Crystallization at 90°C of with Fusion Product Si/Al : 1,17

B. 2θ Angles of Minerals of Fly Ashes and Zeolite 4A Crystal

Table B.1. 2θ Angles of Hematite, Mullite and Quartz [86]

quartz	mullite	hematite
2θ	2θ	2θ
20,77	16,4	24,2
26,66	31,15	33,15
36,37	33,3	35,72
39,61	35,5	39,3
40,13	37	40,87
42,17	39,3	43,46
45,55	41	49,49
50,14	42,6	54,09
54,6	48,2	57,63
55,26	49,72	
59,85	53,62	
	54,1	
	57,8	
	58,6	

Table B.2: 2 θ Angles of Zeolite 4A Crystal [84]

2θ	2θ
7,2	36,4
10,3	38
12,6	39,6
16,2	40
17,5	41,5
20,6	42,2
21,8	42,8
23	43,2
24	44,2
26,2	47,4
27,2	48
29	49,9
29,9	
30,9	
32,6	
33,4	
34,3	
35,7	